
[All ETDs from UAB](#)

[UAB Theses & Dissertations](#)

2011

Bone Morphogenetic Protein Signaling Pathways during Mouse Heart Development: Roles for CHD7 and MYCN

Cristina Harmelink
University of Alabama at Birmingham

Follow this and additional works at: <https://digitalcommons.library.uab.edu/etd-collection>

Recommended Citation

Harmelink, Cristina, "Bone Morphogenetic Protein Signaling Pathways during Mouse Heart Development: Roles for CHD7 and MYCN" (2011). *All ETDs from UAB*. 1873.
<https://digitalcommons.library.uab.edu/etd-collection/1873>

This content has been accepted for inclusion by an authorized administrator of the UAB Digital Commons, and is provided as a free open access item. All inquiries regarding this item or the UAB Digital Commons should be directed to the [UAB Libraries Office of Scholarly Communication](#).

BONE MORPHOGENETIC PROTEIN SIGNALING PATHWAYS DURING MOUSE
HEART DEVELOPMENT: ROLES FOR CHD7 AND MYCN

by

CRISTINA M. HARMELINK

DANIEL BULLARD, COMMITTEE CHAIR

KAI JIAO

JIANBO WANG

QIN WANG

BRADLEY YODER

A DISSERTATION

Submitted to the graduate faculty of The University of Alabama at Birmingham,
in partial fulfillment of the requirements for the degree of
Doctor of Philosophy

BIRMINGHAM, ALABAMA

2011

BONE MORPHOGENETIC PROTEIN SIGNALING PATHWAYS DURING MOUSE HEART DEVELOPMENT: ROLES FOR CHD7 AND MYCN

CRISTINA M. HARMELINK

GENETICS

ABSTRACT

Bone Morphogenetic Protein (BMP) signaling pathways are imperative for proper heart development. BMP ligands bind serine threonine kinase receptors, which activate intracellular receptor-regulated SMAD proteins. SMAD1, SMAD5, and SMAD8 transduce BMP signals from the cytoplasm to the nucleus, where they regulate transcription. We have investigated two aspects of BMP signaling during mouse cardiogenesis: identifying SMAD1-interacting proteins and exploring the roles of a known BMP target, *Mycn*, in the developing myocardium.

Chromodomain helicase DNA binding protein 7 (CHD7) is a highly conserved transcription factor that promotes protein synthesis, proliferation, and differentiation. Haploinsufficiency for *CHD7* causes CHARGE syndrome, a developmental disorder characterized by diverse heart defects. CHD7 was identified as a SMAD1-interacting protein in a yeast two-hybrid screen. The interaction was confirmed with glutathione S-transferase (GST) pull-down assays in mammalian cells and *in vitro*. Future studies are needed to verify the functional significance of the SMAD1-CHD7 interaction and to delineate *Chd7*'s roles during mouse heart development with conditional gene inactivation.

MYCN is a conserved transcription factor with roles in development and disease. Mutations in *MYCN* are associated with Feingold syndrome, a disorder associated with

congenital heart defects. To uncover the roles of *Mycn* in the developing mouse myocardium, we used a novel transgenic mouse model with *Mycn* deleted from the myocardium. Conditional deletion of *Mycn* from the myocardium resulted in embryonic lethality at E12.5. Histological examination of mutant embryos revealed a thin ventricular myocardial wall defect, which likely reduced contractility and resulted in cardioinsufficiency. Mutants had hypocellular myocardial walls with significantly decreased cardiomyocyte proliferation within the ventricles, but no detectable changes in apoptosis. Expression of cell cycle regulators and MYCN targets, CCND1, CCND2, and ID2 was reduced within the mutant ventricles. Depletion of MYCN from the myocardium also caused a significant reduction in ventricular cardiomyocyte size along with reduced expression of p70(S6K), a key regulator of ribosome biogenesis and protein synthesis. MYCN was also necessary for the proper expression of a subset of myofilament proteins that are important for cardiomyocyte structure and function. These results reveal that *Mycn* is a critical mediator of cardiomyocyte proliferation, size, and gene expression.

DEDICATION

To my parents who unfailingly provide love, support, and perspective.

ACKNOWLEDGEMENTS

Foremost, I would like to thank my mentor, Kai Jiao, for the opportunity to work in his lab. Kai has been a very enthusiastic and supportive mentor who is always available for discussions. He has provided me with many opportunities to present data at scientific conferences throughout the United States. Kai's experience, knowledge, insight, and mentorship have provided me with a strong foundation that I will rely on in my future career.

I would like to thank the Jiao lab members, past and present. I would also like to thank our close collaborators in Qin Wang's lab, especially Yunjia Chen and Chris Cottingham. It has been a joy to work and learn with all of you.

I am grateful for my committee members, past and present. Thanks to Daniel Bullard, Jianbo Wang, Qin Wang, Bradley Yoder, and Guillermo Marques for your time, guidance, and support over the years.

I would like to thank my family members for their love and support. Special heartfelt thanks to Rebecca and Larry Harmelink, Laura and Wes Harmelink, Irene Enright, Nancy and Bud Harmelink, Marilyn Paplow, and Kristine, Larry, Matthew and Angela Reiners. Thank you for your encouragement and for believing in me.

I am very thankful for my "Birmingham family". A big thanks to my friends in the Genetics program for many great memories, especially Becky Smith, Tyesha Farmer,

Louisa Pyle, Wenyi Luo, Brandon Shaw, Jingyu Guo, Svetlana Masyukova, and Arindam Ghosh. I have been very fortunate to have the friendship and support of Paige DeBenedittis, Emily Spencer, Jacob Watts, Michelle McClure, and Mozella Kerley in my day-to-day life. Thank you, Taffi, Dave, Sandi, Pepper, O.C., and Skitter Bailey, for making me feel at home in the South. Love and thanks to Jason Bailey, for six years of laughter, good food, late nights, and many wonderful memories. Lastly, I extend my love and gratitude to my dear friend, kindred spirit, and comrade-in-arms, Paige DeBenedittis.

TABLE OF CONTENTS

	<i>Page</i>
ABSTRACT	ii
DEDICATION	iv
ACKNOWLEDGEMENTS	v
LIST OF TABLES	ix
LIST OF FIGURES	x
LIST OF ABBREVIATIONS	xii
INTRODUCTION	1
Heart Development	1
BMP Signaling Pathways	4
Cardiac Specification and Heart Tube Formation	7
BMP ligands.....	7
BMP receptors	8
SMADs	9
BMP inhibitors.....	9
Cardiogenesis after Heart Tube Formation.....	11
Myocardial wall morphogenesis	11
Conduction system development	12
Development of the septal-valvulo structures.....	13
Epicardium formation	17
Significance: BMP Signaling Pathways and Human CHDs.....	18
INTERACTION BETWEEN THE BMP SIGNAL TRANSDUCTION MOLECULE SMAD1 AND THE CHROMODOMAIN HELICASE DNA BINDING PROTEIN 7 (CHD7)	19
MYOCARDIAL MYCN IS ESSENTIAL FOR MOUSE VENTRICULAR WALL MORPHOGENESIS	50

SUMMARY AND FUTURE DIRECTIONS	86
Chromodomain Helicase DNA Binding Protein 7 (CHD7) Interacts with SMAD1	86
Future Directions: Roles of CHD7 during Heart Development.....	87
Roles of MYCN in the Developing Mouse Myocardium.....	89
Myocardial wall morphogenesis: E7.5-E9.5.....	90
Myocardial wall morphogenesis: E9.5-E11.5.....	91
Cardiomyocyte maturation and ventricle chamber formation	92
Future Directions: MYCN and Epigenetic Regulation.....	94
Acetylation and methylation	94
microRNA.....	95
Future Directions: MYCN in Other Cardiogenic Processes	96
Future Directions: MYCN in Adult Heart Disease.....	97
Summary and Significance	98
LIST OF GENERAL REFERENCES	100
APPENDIX: IACUC APPROVAL FORM.....	120

LIST OF TABLES

<i>Table</i>		<i>Page</i>
	INTERACTION BETWEEN THE BMP SIGNAL TRANSDUCTION MOLECULE, SMAD1, AND THE CHROMODOMAIN HELICASE DNA BINDING PROTEIN 7 (CHD7)	
1	Candidates isolated from the yeast two-hybrid screen	45
	MYOCARDIAL MYCN IS ESSENTIAL FOR MOUSE VENTRICULAR WALL MORPHOGENESIS	
S1	Recovery of living mutant embryos	85

LIST OF FIGURES

<i>Figure</i>		<i>Page</i>
INTRODUCTION		
1	Overview of heart development.....	3
2	BMP signaling pathways	5
INTERACTION BETWEEN THE BMP SIGNAL TRANSDUCTION MOLECULE, SMAD1, AND THE CHROMODOMAIN HELICASE DNA BINDING PROTEIN 7 (CHD7)		
1	Analyses of candidates.....	41
2	Confirming the SMAD1 interaction in yeast	41
3	CHD7 interacts with SMAD1 in yeast.....	42
4	<i>Chd7</i> clone	43
5	CHD7-SMAD1 interaction in mammalian cells and <i>in vitro</i>	44
MYOCARDIAL MYCN IS ESSENTIAL FOR MOUSE VENTRICULAR WALL MORPHOGENESIS		
1	Conditional deletion of <i>Mycn</i> from the myocardium caused embryonic lethality	76
2	Histological analyses of <i>cTnt-Cre;Mycn^{loxp/loxp}</i> hearts revealed thin myocardial walls	77
3	Analyses of cardiomyocyte number and proliferation at E9.5	78
4	Mutant ventricular myocardium had reduced expression of CCND1, CCND2, and ID2	79
5	Measurement of cardiomyocyte size	80

6	Examination of myofilament proteins	81
S1	Myocardial wall formation	82
S2	The mouse MYCN protein	83
S3	Breeding strategy	84
S4	<i>Mycn</i> allele and primer design	84
S5	Representative image of TUNEL staining on sagittal sections of control and mutant embryos at E11.5	85

LIST OF ABBREVIATIONS

ASD	atrial septal defect
AVC	atrioventricular canal
AVN	atrioventricular node
BMP	bone morphogenetic protein
CHD	congenital heart disease
CHD7	chromodomain helicase DNA binding protein 7
CNCC	cardiac neural crest cells
DORV	double outlet right ventricle
ECM	extracellular matrix
EMT	epithelial to mesenchymal transition
FHF	first heart field
FS	Feingold syndrome
IFT	inflow tract
HAT	histone acetyltransferases
PE	proepicardium
OFT	outflow tract
R-SMAD	receptor-regulated SMAD protein
SHF	second heart field
TGF β	transforming growth factor beta
VSD	ventricular septal defect

INTRODUCTION

The heart is the first organ to develop and, as form follows function, its proper formation is requisite for survival of the embryo. Heart development relies on exquisitely controlled signaling cascades that together weave the temporal and spatial cardiac gene expression patterns required for normal morphogenesis and function. Aberrations in cardiogenic signaling pathways or in cardiac gene expression patterns can result in congenital heart defects (CHDs), the most common type of birth defect worldwide and the leading noninfectious cause of infant morbidity and mortality in the Western world.¹⁻

⁵ This review provides evidence from multiple experimental models that demonstrates the conserved, critical roles of Bone Morphogenetic Protein (BMP) signaling pathways throughout heart development, from induction of the cardiac mesoderm to the formation of the four-chambered heart.

Heart Development

During gastrulation, cardiac progenitors within the lateral plate mesoderm migrate in bilateral sheets of cells to the anterior of the embryo. There are two populations of mesodermal cells that contribute to the developing heart in distinct temporal-spatial manners: the first and second heart fields (FHF and SHF, respectively). At embryonic day 7.5 (E7.5) in mice, the cells of the FHF connect at the midline to form the cardiac

crescent (Figure 1). The initial stages of cardiac differentiation occur in the cells of the cardiac crescent, with expression of genes encoding cardiac transcription factors and structural proteins. The second population of cardiac cells, the SHF, is medial and anterior to the FHF. As the embryo folds, at mouse E8.0, the cardiac crescent fuses along the midline and forms the heart tube while the SHF moves dorsally. The heart tube consists of an outer myocardial layer and an inner endocardial layer, separated by an extracellular matrix (ECM) called the cardiac jelly. SHF cells migrate through the pharyngeal mesoderm to populate the anterior and posterior regions of the heart tube. Starting from E8.5 in the mouse, the heart undergoes rightward looping to position the atria above the ventricles. Regional proliferation along the myocardium of the outer curvature of the heart tube demarcates the future atrial and ventricular chambers. The myocardium of the inflow tract (IFT), outflow tract (OFT), atrioventricular canal (AVC), and inner curvature of the heart tube is characteristically non-proliferative. The FHF contributes primarily to the left ventricle as well as to part of the atria, and the SHF contributes to the right ventricle, atria, and OFT. The endocardial cells, meanwhile, respond to signals from the myocardium and undergo epithelial to mesenchymal transition (EMT) to form the cushions, the primordial valve structures. Cushions form at the atrioventricular junction at about E9.5, and in the OFT slightly later. Around E10.0, another population of cells called the cardiac neural crest cells (CNCC) migrates from dorsal neural tube and contributes to the developing OFT. By E11.5, the proepicardial cells have migrated around and enveloped the heart, forming the epicardium. Finally, development of the septa and valves results in the four-chambered heart with right, pulmonary, and left, systemic, halves by mouse E14.5. ⁶⁻¹⁹

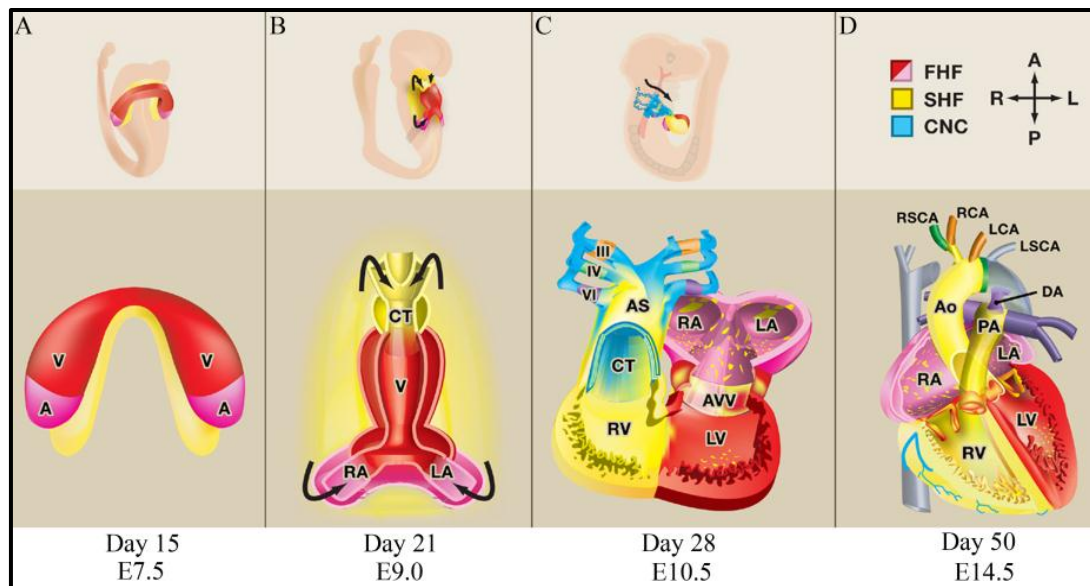


Figure 1. Overview of heart development. (Top) Oblique views of embryos, (middle) frontal views of cardiac development, and (bottom) human and mouse developmental stages. A. The first heart field (FHF) forms the cardiac crescent in the anterior of the embryo. The second heart field (SHF) is anterior and medial to the FHF. B. The cardiac crescent coalesces, forming the linear heart tube. The SHF migrates into the heart tube (arrows) and contributes to the right ventricle, conotruncus (the common outflow tract), and the atria. C. After looping, the cardiac neural crest cells contribute to the outflow tract. D. Septation results in the formation of the four-chambered heart. A, atria; RA, right atria; LA, left atria; V, ventricle; RV, right ventricle; LV, left ventricle; CT, conotruncus; AVV, atrioventricular valves; VI, IV, and VI are aortic arches; AS, aortic sac; Ao, aorta; PA, pulmonary artery; RSCA, right subclavian artery; LSCA, left subclavian artery; RCA, right carotid artery; LCA, left carotid artery; DA, ductus arteriosus.

NOTE: Adapted from “Making or Breaking the Heart: From Lineage Determination to Morphogenesis” by D. Srivastava, 2006, *Cell*, 126(6), p. 1037. Copyright 2006 by Elsevier. Adapted with permission.

BMP Signaling Pathways

BMP ligands are conserved growth factors that belong in the Transforming Growth Factor- β (TGF β) superfamily. More than twenty BMPs have been identified that have a myriad of functions during development. BMP precursor proteins are activated via endoproteolytic cleavage, glycosylated, and secreted as homo- or hetero-dimers.^{20, 21} Once processed and secreted, BMP ligands relay their signal to the nucleus through signaling cascades that utilize unique combinations of serine threonine kinase receptors which respond to specific ligand combinations (Figure 2). There are three type I receptors (out of seven) and three type II receptors (out of five) that transduce the BMP signals. The type I receptors are ALK2 (ACVRI, ACTRI), ALK3 (BMPRIA/BRK-1), and ALK6 (BMPRIIB, BRK-2).²²⁻²⁴ The type II receptors are BMPR2 (BMPRII, BRK-3), ACVR2A (ACTRIIA), and ACVR2B (ACTRIIB).²⁵⁻²⁸ The BMP dimer binds a type II receptor, which recruits and phosphorylates a type I receptor in its intracellular kinase domain.²⁵ The type I receptor then phosphorylates an intracellular receptor-regulated SMAD protein (R-SMAD). SMAD1, SMAD5, and SMAD8 are regulated specifically by BMP signals.²⁹⁻³³ After phosphorylation, activated R-Smads form a heterotrimeric complex with another R-SMAD and the common SMAD, SMAD4.³⁴ The R-SMAD-SMAD4 complex translocates to the nucleus, where it cooperates with other cofactors to regulate gene transcription.^{20, 35} BMP signaling can occur in non-canonical pathways, independent of SMAD proteins. For instance, BMP signaling can activate MAP kinase pathways, resulting in activation of p38 MAPK, PIK3, ERK and JNK with downstream effects on cell proliferation and differentiation.³⁵⁻⁴¹

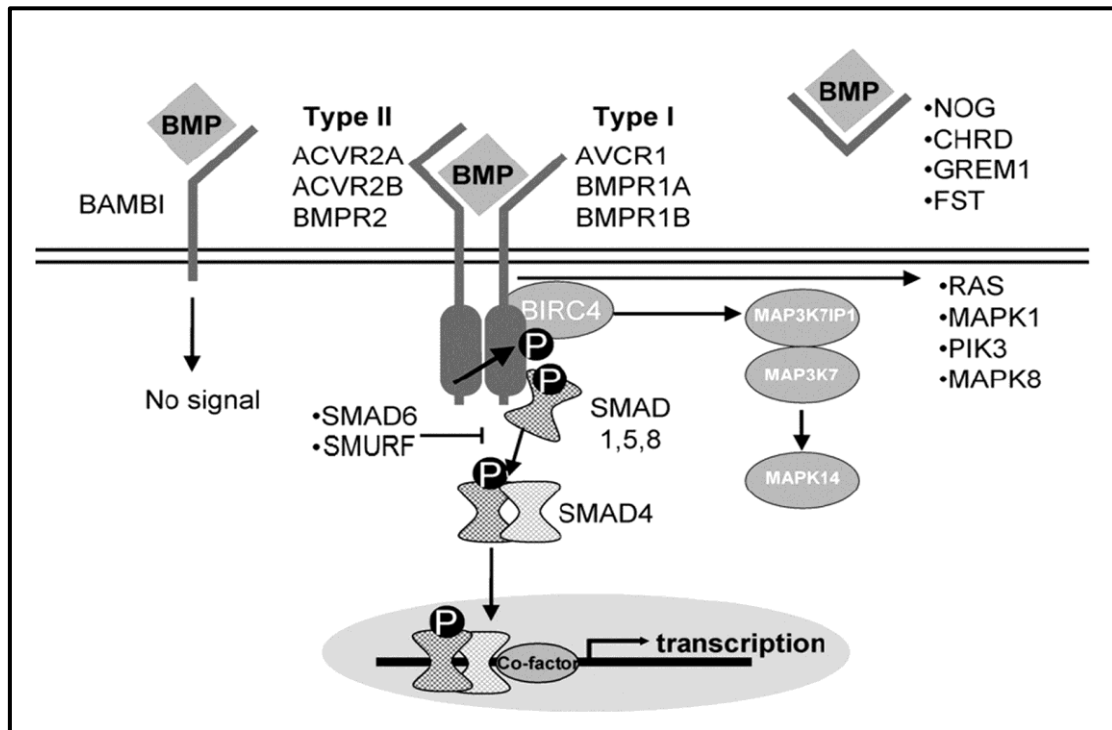


Figure 2. BMP signaling pathways. BMP ligands bind type I and type II BMP receptors. The type II receptor phosphorylates the Type I receptor, which activates SMAD1, SMAD5, or SMAD8. The activated SMAD forms a complex with the common SMAD4 and translocates to the nucleus where it interacts with cofactors to regulate gene transcription. Noncanonical BMP signaling occurs independently of SMAD proteins. BMP cytokines can signal through RAS, MAPK, and PIK3 pathways. BMP signaling can be regulated extracellularly by secreted inhibitors such as NOG (noggin), CHRDR (chordin), GREM (gremlin), and FST (follistatin). BAMBI inhibits BMP signaling at the membrane by binding to the BMP receptor and disrupting the downstream signaling, as it lacks the intracellular domain needed to propagate the BMP signal. Intracellularly, BMP signaling is inhibited by SMAD6 or SMURF.

NOTE: Reprinted from “Role of bone morphogenetic proteins in cardiac differentiation” by Bram van Wijk, et al., 2007, *Cardiovascular Research*, 74(2), p. 244. Copyright 2006 by European Society of Cardiology and published by Elsevier. Reprinted with permission.

It has recently been demonstrated that BMP signaling can regulate microRNA (miRNA). miRNA are short non-coding RNA that target messenger RNA (mRNA) in a sequence-specific manner for post-transcriptional degradation. miRNA are transcribed as primary miRNA (pri-miRNA), which are processed by the Drosha complex within the nucleus. pri-miRNA processing results in a shorter product called pre-miRNA, which is exported from the nucleus to the cytoplasm where it is cleaved into its mature miRNA structure by Dicer.⁴²⁻⁴⁴ One example is the upregulation of *miR-21* by BMP signaling in damaged cardiovascular tissue.⁴⁵ BMP signaling increases the processing of pri-miRNA to pre-miRNA through an interaction between an activated R-SMAD and a subunit of microprocessor Drosha complex, the RNA helicase p68.⁴⁶⁻⁴⁸ R-SMADs can also directly bind *pri-miR-21* through a RNA SMAD-binding-sequence, which is necessary and sufficient for pri-miRNA processing.⁴⁹ The direct interaction between the R-SMAD and pri-miRNA may enhance miRNA processing and/or it may recruit the Drosha complex to the pri-miRNA.⁴⁹

The timing, duration, and gradient of BMP ligands affect the outcomes and add to the complexity of BMP signaling pathways. After BMP processing and secretion, access to the BMP receptors and retention in the ECM are inhibited by extracellular factors such as noggin, chordin, gremlin, and follistatin.⁵⁰⁻⁵⁵ These inhibitors bind BMP ligands and interfere with ligand-receptor interaction. An example of a BMP inhibitor that acts at the membrane level is the pseudo-receptor BAMBI (BMP and activin membrane bound inhibitor). BAMBI lacks the intracellular domain needed for signal transduction and, upon binding BMP receptors, it inhibits the formation of an active BMP receptor complex.^{21, 56, 57} Transmembrane tyrosine kinases and cytoplasmic serine-threonine

kinases such as TRKC and ROR2 also bind to BMP receptors and inhibit downstream signaling.^{58,59} Alternatively, BMP signaling can be enhanced at the membrane level by modulators such as DRAGON, which acts as a co-receptor and presents BMPs to the receptors.⁶⁰ Another example is endoglin, a transmembrane protein that binds to BMP ligands and enhances BMP signaling.^{61,62} Intracellularly, BMP signaling can be downregulated by SMURF, an E3 ubiquitin ligase that promotes R-SMAD degradation, receptor turnover, and inhibition by the inhibitory SMADs, SMAD6 and SMAD7.⁶³⁻⁶⁵ SMAD6 and SMAD7 inhibit BMP signaling cascades through binding active type I receptors and preventing R-SMAD activation, and by competing with SMAD4 for R-SMADs.⁶⁶⁻⁶⁸ Lastly, cross-talk between signaling pathways affects R-SMAD phosphorylation, activity, turnover, and nuclear accumulation⁶⁹⁻⁷²

Cardiac Specification and Heart Tube Formation

BMP ligands. Initial insight into the roles of BMP signaling pathways in cardiac specification came from studying the *BMP2/4* ortholog, *Dpp*, in *D. melanogaster*. *Dpp*-deficient larva did not form the precursor cells for the heart organ, the dorsal vessel, while ectopic *Dpp* protein caused ectopic formation of the dorsal vessel precursor cells.⁷³⁻⁷⁵ In chicken embryos, the endoderm expresses BMP2 and 5, and the ectoderm expresses BMP4 and BMP7.^{76,77} *In vivo* and *in vitro* experiments using chicken embryos reveal that both the FHF and the SHF pre-cardiac mesodermal cells differentiate in response to BMP signals.^{78,79} In mice, BMP2, BMP4, BMP5, and BMP7 are expressed in the anterior mesoderm.⁸⁰⁻⁸² Regardless of the differences in BMP expression patterns

between species; it has been well-established that BMP signaling pathways induce precardiac mesoderm to undergo cardiac differentiation.⁸³⁻⁸⁵ *Bmp2* deletion in mice causes embryonic lethality between E7.5-E9.0.⁸⁰ Some mutant embryos lack hearts altogether and others develop ectopic heart tubes in the exocoelomic cavity.⁸⁰ *Bmp4* deletion in mice results in embryonic death from E6.5-E9.5 due to aberrant gastrulation and mesodermal differentiation.⁸⁶ These data suggest critical roles for BMP signaling pathways in gastrulation, mesoderm formation, and subsequent heart development.

BMP signaling pathways induce cardiac differentiation through upregulation of cardiogenic genes. Expression of the transcription factors *Nkx2.5* and *Gata4* is initiated by BMP signaling.^{74, 76, 87-94} The *Nkx2.5* promoter region contains evolutionary conserved BMP-response elements that are required for its expression in the cardiac crescent.^{90, 92, 95} BMP signaling also activates the expression of myocardin, a transcriptional cofactor for a regulator of cardiac differentiation called serum response factor (SRF).⁹⁶⁻⁹⁸ SMAD1, a BMP R-SMAD, is also a cofactor for myocardin.⁹⁸ Autoregulatory mechanisms in BMP signaling pathways have roles in cardiac differentiation as well. The promoters of *Bmp* genes and the BMP inhibitor *Smad6* have BMP-responsive elements.^{92, 99} Ectopic delivery of BMP initiates heart development and increases the expression domain of *Smad6*, as well as *Nkx2.5* and *Gata4-6*.^{76, 100}

BMP receptors. The BMP type I receptor ALK3 is widely expressed in mouse embryos and *Alk3* deletion causes embryonic lethality at E8.0 with no mesoderm formation.^{101, 102} ALK2, another type I receptor, is expressed in Hensen's node and in the primitive streak. Deleting *Alk2* in mouse embryos results in embryonic lethality by E9.5 with gastrulation defects.^{103, 104} The third type I receptor, ALK6, is not expressed during

early heart development and disrupting its function does not affect mouse cardiogenesis or viability.^{102, 105} Knockout of the type II receptor, *BMPR2*, which is widely expressed in chicken embryos and during mouse cardiomyogenesis, causes embryonic lethality at gastrulation.¹⁰⁶⁻¹⁰⁹ In mice, *ACVR2A* is expressed after cardiomyocyte formation at E9.5 and *ACVR2B* is ubiquitously expressed during cardiomyogenesis.^{108, 109} Disruption of *Acvr2a* alone does not cause heart defects and disruption of *Acvr2b* causes defects later in development.^{110, 111} However, deletion of both *Acvr2a* and *Acvr2b* results in embryonic death at gastrulation, suggesting functional redundancy of these type II receptors.¹¹²

SMADs. In chicken embryos, *SMAD1*, *SMAD5*, and *SMAD8*, are enriched in the heart forming region.¹¹³ In mice, *Smad1* and *Smad5* mRNA are expressed in the mesoderm during cardiomyocyte formation.¹¹⁴ *Smad1* disruption in mice results in embryonic lethality at E10.5 from failure of umbilical-placental connections to form.¹¹⁴ Germline deletion of *Smad5* results in defective left-right symmetry with a heart looping abnormality and defective angiogenesis.^{115, 116} Deletion of *Smad4*, the gene encoding the common SMAD, causes death before E7.5 with reduced size and failure to gastrulate.¹¹⁷ Conditional deletion of *Smad4* from the epiblast causes embryonic lethality by E8.5, but the heart tube forms and *Nkx2.5* is expressed.¹¹⁸ Heart tube formation and cardiac gene expression may occur in these mice because the *Cre* did not completely remove *Smad4* from the epiblast, or because canonical BMP signaling occurs before *Cre*-mediated recombination.

BMP inhibitors. Inhibition of BMP during gastrulation restricts the heart forming fields to discrete territories. BMP inhibitors are downregulated in the anterior of the embryo to allow for BMP induction of lateral plate mesoderm. Due to the location of the

SHF dorsal and medial to the FHF, it is effectively hidden from high levels of ventral BMP signaling and is exposed to inhibitory signals from the neural tube. The cells of the SHF therefore undergo differentiation later than the cells of the FHF.^{11, 119}

Pre-cardiac mesoderm is initially exposed to canonical WNT signaling from the primitive streak and then from the neural tube. In the anterior region of the embryo, WNT signaling is antagonized by *crested*, allowing BMP induction of the cardiac gene program.^{76, 120-123} Non-canonical WNT signaling by WNT11 has positive roles in cardiac induction, in part by suppressing canonical WNT signaling.^{124, 125} In chickens and mice, *Wnt11* mRNA is detected in the mesoderm and endoderm.^{126, 127} The *Xenopus* and zebrafish *Wnt11* ortholog is able to induce cardiomyocyte formation even though it is normally expressed after myocardial differentiation and is not necessary for cardiac specification during development.^{124, 128-130}

Noggin, chordin, and follistatin are secreted from the notochord and bind BMP ligands to prevent receptor activation. The responsiveness of pre-cardiac mesoderm to inhibitory signals from the notochord is developmentally regulated. Ectopic application of noggin to stage 4 chick mesendoderm prevents the initiation of the cardiac gene expression and development of the contracting cardiomyocytes.^{76, 88} If noggin is applied to explants a stage later, the cardiac gene expression is initiated without spontaneous contraction of myocytes. If noggin is applied at stage 6, differentiation occurs normally.¹³¹ In mice, deletion of noggin or follistatin individually does not cause heart defects, but deletion of both reverses heart looping.⁵¹⁻⁵³ Deleting chordin causes defects phenocopying those in DiGeorge syndrome.^{51, 53, 132}

Cardiogenesis after Heart Tube Formation

Myocardial wall morphogenesis. During early heart development, myocardial walls expand through cardiomyocyte proliferation and differentiation. The chamber myocardium develops a latticework of muscular projections on the subendocardial surface called trabeculae. Trabecular myocardium generates contractile force, coordinates intraventricular conduction, and helps diffuse nutrients to the cardiomyocytes within the expanding heart wall prior to vascularization. Later in heart development, the trabecular myocardium undergoes remodeling and is incorporated into the compact myocardium, the interventricular septum, and the papillary muscles of the atrioventricular valves.^{133,}
¹³⁴ Proper formation of the myocardial walls is essential for embryo viability and adult cardiac function. For instance, abnormalities in myocardial wall morphogenesis can result in left ventricular noncompaction, an adult cardiomyopathy.^{135, 136}

BMP10 is initially expressed in the looping mouse heart within regions destined to be the atrial and ventricular chambers, and its expression is maintained in the chamber myocardium during heart development.¹³⁷⁻¹³⁹ Also, *Bmp10* is upregulated in mouse models of hypertrabeculation.¹³⁹ Myocardial expression of BMP10 during chamber formation relies on endocardial expression of notch.¹⁴⁰ Deleting *Bmp10* in mice causes embryonic lethality at E9.0 with decreased cardiomyocyte proliferation, downregulation of cardiac genes *Nkx2.5* and *Mef2c*, and loss of trabecular myocardium.¹³⁹ Removing both *Bmp6* and *Bmp7* in mice causes embryonic lethality at midgestation with hypoplastic ventricles and reduced trabeculations.¹⁴¹ Mice with conditional deletion of the BMP receptor *Alk3* from the myocardium die during embryogenesis and display underdeveloped myocardial walls and ventricle septal defects (VSD).¹⁴² Specific

inactivation of the common Smad, *Smad4*, from the myocardium likewise causes embryonic lethality at midgestation and disrupts myocardial wall formation and ventricle septation.¹⁴³⁻¹⁴⁶ Myocardial deletion of *Smad4* causes downregulation of genes encoding cell cycle regulators, cardiac structural proteins, and transcription factors.¹⁴³⁻¹⁴⁶ Together, these studies provide multiple lines of evidence that show BMP signaling is required for ventricular myocardial wall morphogenesis through regulation of cardiomyocyte proliferation, differentiation, and gene expression.

Conduction system development. In vertebrates, regional differentiation of the myocardium allows for development of slow-conducting, nonchamber myocardium (IFT, AVC, and OFT) and fast-conducting chamber myocardium (atria and ventricles).^{147, 148} Proper formation of the AVC is important for establishment of the primary conduction system. The primary conduction system includes the atrioventricular node (AVN) and its associated structures. In mice, AVN precursor cells are observed in the AVC at E9.5.¹⁴⁹⁻¹⁵¹ The AVN subsequently extends into the left ventricle and connects with the trabecular myocardium and the interventricular septum.¹⁵⁰ It carries the electrical impulse from the atria, across the AVC to the ventricles.¹⁵²⁻¹⁵⁴ Having a slower conduction rate than the atria, the AVC delays the atrial-ventricular electrical impulse.¹⁵²

BMP2 is necessary for AVC specification and expression of *Tbx2*.^{155, 156} TBX2 is a transcriptional repressor of chamber-specific genes and is specifically expressed in nonchamber myocardium of the IFT and the AVC.^{155, 157-160} In the AVC, BMP2 activates *Tbx2* transcription to suppress proliferation and inhibit the expression of chamber-specific genes *Nppa*, *Cx40*, *Cx43*, and *Chisel*.^{156, 159, 161} BMP2 can directly regulate *Tbx2* through a SMAD-dependent enhancer upstream of its transcription start site.¹⁶² BMP

signaling also indirectly promotes *Tbx2* transcription through SMAD1 inhibition of TBX20, a *Tbx2* repressor.¹⁶² The BMP2-TBX2 pathway is restricted to the AVC region by notch/HEY signaling in the developing heart chambers.^{163, 164}

Deletion of *Bmp2* from mouse myocardium decreases *Tbx2* expression and results in the expansion of chamber myocardium into the AVC region.¹⁵⁶ Inactivation of the BMP receptor *Alk3* specifically in the AVC myocardium disrupts AV valve development and AVN morphogenesis, resulting in ventricular pre-excitation.^{165, 166} Lastly, removal of myocardial *Tbx2* results in abnormal AVC patterning and ventricular pre-excitation.¹⁶⁷ Taken together, these data suggest that BMP2 regulation of *Tbx2* expression and AVC myocardial patterning is important for development of the AVN and proper atrial-ventricular conduction. Indeed, the phenotype resulting from AVC-depletion of *Alk3* in mice resembles Wolff-Parkinson-White syndrome (WPWS, OMIM 224700), a pre-excitation syndrome that can present as tachycardia due to an abnormal connection between the atria and ventricles.¹⁶⁵ A heterozygous microdeletion was recently identified in a chromosomal region encompassing *BMP2*, 20p12.3, that predisposes people to WPWS.¹⁶⁸

Development of the septal-valvulo structures. Atrial and ventricular septa are formed by myocardial outgrowth and fusion. The AVC and OFT are septated by endocardial cushion maturation into valvulo-septal structures. Primordial valve structures called cushions develop in the AVC and OFT through the expansion of the ECM. Induction of cushion formation occurs within the looped heart, when the myocardium signals through the cardiac jelly to the endocardium. Endocardial cells then delaminate and invade the cardiac jelly to form the mesenchymal cells of the endocardial cushions.

¹⁶⁹ Cell fate mapping in mouse studies have confirmed the endocardial origin of the mesenchymal cells within the AVC and proximal OFT cushions. ¹⁷⁰ The morphogenesis of the AVC and OFT cushions are not identical. The AVC cushions form earlier and are invaded by epicardial cells. ¹⁷¹ They develop into the mitral (left) and tricuspid (right) valves at the junction of the atria and ventricles. The OFT cushions, but not the AVC cushions, have a CNCC contribution. ¹⁷²⁻¹⁷⁵ The cushions in the OFT develop into the semilunar valves in the aorta (left) and pulmonary artery (right). Congenital defects in valve formation and septation comprise the most common CHDs, while defects involving the OFT are found in 4 per 10,000 live births and are often lethal. ^{1, 176} Pathological mutations in the BMP receptor *ALK2* have been found in patients with congenital defects in atrioventricular septum development, providing evidence for the importance of BMP signaling pathways in human heart development. ^{177, 178}

At E9.5 in mice, BMP2 has weak expression in OFT myocardium which disappears by E10.5. ¹⁷⁹ But, BMP2 is strongly and persistently expressed in AVC and atrial myocardium at E10.5. ^{179, 180} It is also expressed in the cushion mesenchyme during valve remodeling and in adult mouse valves. ¹⁸¹ In mice, BMP2 enhances cardiac jelly formation, endocardial EMT, and AVC myocardial patterning. ^{156, 181-183} BMP2 upregulates *Twist1*, an inducer of EMT, and *Has2*, a component of the cardiac jelly necessary for EMT. ^{156, 184, 185} Myocardial deletion of *Bmp2* decreases ECM in the AVC cushions, however the OFT cushions develop normally. ^{156, 182} This suggests a compensatory mechanism in the OFT such as BMP4 signaling. ^{156, 182} Data suggests that BMP2 signaling interacts with notch1 and TGF β signaling pathways to coordinate EMT.

BMP4 is expressed in AVC myocardium in mice at E9.5, but at E10.5 its expression is restricted to the myocardium of the OFT.^{180, 189} It is also expressed in the chicken OFT.⁷⁷ BMP4 is 92% identical in the C-terminus to BMP2, and they have overlapping functions.^{190, 191} Conditional deletion of *Bmp4* from mouse myocardium causes atrioventricular septation defects and double outlet right ventricle (DORV, both arteries are connected to the right ventricle), and aortic arch patterning anomalies.^{192, 193} Mouse models with myocardial-specific deletion of *Bmp4* or with hypomorphic *Bmp4* alleles have impaired AVC cushion mesenchymal cell proliferation.^{192, 194} Mice compound heterozygous for *Bmp2*-null and *Bmp4*-null or -hypomorphic alleles have VSD.¹⁹⁰ Decreased expression of myocardial BMP4 does not affect OFT development, but it increases BMP7 expression.¹⁹³ On a *Bmp7*-null background, decreased BMP4 causes a shortened OFT with hypoplastic cushions, revealing dose-dependence and functional redundancy of BMP signaling in OFT morphogenesis.¹⁹³

Despite being expressed during early heart development, single gene deletions of *Bmp5*, *Bmp6*, or *Bmp7* do not cause heart defects, likely due to redundancy of the BMP family members.^{81, 141, 195-198} BMP5 is expressed throughout the heart tube myocardium and later becomes restricted to the myocardium of the AVC and OFT in mouse and chicken embryos.^{77, 82, 199} In mice, BMP6 is expressed in OFT endocardium and myocardium, and within the OFT and AVC mesenchyme.^{82, 141, 189, 199} BMP6 is not expressed in the developing chicken heart.⁷⁷ BMP7 is robustly expressed throughout the myocardium of the developing hearts of mice and chickens.^{77, 82, 200} Combinations of gene deletions in mouse models reveal essential roles in chamber formation and septal-valvulogenesis. *Bmp5* and *Bmp7* double deletion causes embryonic lethality at

E10.5, with delayed heart development, no endocardial cushion formation or chamber septation, and abnormal pericardium.⁸² Removal of *Bmp6* and *Bmp7* results in defects in OFT cushion development, chamber septation, and myocardial wall formation.¹⁴¹ Deletion of *Bmp5* and *Bmp6* does not cause heart defects.¹⁹⁸

Deletion of *Alk3* from the myocardium or the endocardium disrupts endocardial cushion formation.^{142, 156, 201} Myocardial deletion of *Alk3* causes VSD and hypoplastic AVC cushions, with decreased TGF β in the AVC myocardium.¹⁴² Endocardial deletion of *Alk3* causes hypoplastic cushions with fewer mesenchymal cells.^{156, 182, 201, 202} Endocardial deletion of *Alk2* causes failure of EMT in AVC cushions along with decreased expression of EMT proteins MSX1 and SMAD2, an intracellular modulator of TGF β signaling.²⁰³ The role of ALK2 in cushion formation appears to be specific to the endocardium, as conditional deletion of *Alk2* from the myocardium has no effect on cushion development.²⁰³ Ectopic expression of active ALK2 in the chicken ventricle endocardium induces EMT.⁶² CNCC-depletion of *Alk3* or *Alk2* disrupts CNCC invasion, resulting in a shortened OFT with defective proximal septation.^{204, 205} Hypomorphic *Bmpr2* alleles cause defects in proximal OFT septation and loss of semilunar valve formation, while AVC cushions form normally.²⁰⁶ However, completely abrogating *Bmpr2* in mouse hearts causes an array of CHDs, such as DORV, VSD, and AVC cushion defects.²⁰⁷ Disruption of *Acvr2b* causes postnatal death with abnormal cardiac septation.¹¹¹ Deletion of *Smad4* from the myocardium affects OFT positioning, with a DORV phenotype.¹⁴³ Conditional deletion of *Smad4* in CNCC reduced the contribution of CNCC to OFT, causing defects in OFT cushion formation, septation, elongation, and

positioning.^{208, 209} Deletion of *Smad8* does not affect viability or heart development, but mice display defects in pulmonary vascular remodeling.²¹⁰

BMP signaling regulates SHF myocardialization and OFT morphogenesis in part by promoting *miR-17-92* cluster transcription.²¹¹ The *miR-17-92* cluster has roles in lung and heart development.^{212, 213} It is expressed as a primary transcript that encodes six miRNA (*miR-17*, *-18a*, *-19a*, *-20a*, *-19b-1*, and *-92a-1*). BMP regulates the transcription of *miR-17-92* through SMAD binding sites in the 5' region.²¹¹ In turn, *miR-17-92* targets *Isl1* and *Tbx1* transcripts for degradation.²¹¹ Deleting BMP reduces *miR-17-92*, causes misexpression of *Isl1* and *Tbx1*, and leads to defects in proximal OFT septation.²¹¹

Inhibition of BMP signaling is also critical for normal septal-valvulogenesis. For example, *Nkx2.5* is required for OFT development, in part by repressing BMP signaling. Deleting *Nkx2.5* results in expansion of SHF specification due to increased BMP expression, decreased proliferation, and failed OFT truncation. Disrupting the misregulated BMP signaling in the *Nkx2.5* mutants by deleting *Smad1* effectively rescues the proliferation and the OFT defects.²¹⁴ Mutations in the BMP-inhibitor *Smad6* cause hyperplasia of cardiac valves and OFT septation defects, due to unregulated BMP signaling.²¹⁵ Noggin blocks EMT in mouse explants and overexpression of noggin in chicken embryos causes OFT septation defects.^{181, 216} Mutations in chordin cause abnormal OFT septation, resembling syndromes associated with loss of CNCC and phenocopying DiGeorge syndrome.¹³²

Epicardium formation. The proepicardium (PE) is a transient structure derived from pericardial coelomic mesothelium at the venous pole of the heart.^{217, 218} BMP,

TBX5, and FGF activities are required for PE specification.²¹⁹⁻²²¹ PE cells migrate toward and attach to the looped heart, forming an epithelial cover called the epicardium that envelops the embryonic heart.²²² Some epicardial cells invade the heart and contribute to cardiac fibroblasts, coronary smooth muscle cells, myocardium, and AVC cushions.^{217, 220, 223-231} Myocardial BMP signaling promotes PE protrusion toward and attachment to the looping heart tube.²²⁶ Ectopic BMP induces ectopic attachment, while noggin decreases PE attachment in chickens.²²⁶

Significance: BMP Signaling Pathways and Human CHDs

CHDs are the most common type of birth defect worldwide, occurring in nearly 1% of live newborns and in over 5% of fetuses that do not survive to term in the Western world.¹⁻⁵ Furthermore, advances in medical care have resulted in a growing number of children and adults living with CHDs who require lifelong healthcare.⁵ BMP signaling pathways have evolutionarily conserved roles in cardiac specification from the mesoderm, myocardial wall formation, valve development, chamber septation, and OFT morphogenesis. Mutations in genes encoding components of the BMP signaling pathways have been identified in humans. Due to the conservation of BMP signaling pathways in heart development, information gleaned from a variety of model systems, from fruit flies to mice, provides valuable insight into human heart development and CHDs. In the future, this insight into the molecular mechanisms of heart development and the underlying causes of CHDs may help develop diagnostic tests and therapeutic options for people with CHDs.

INTERACTION BETWEEN THE BMP SIGNAL TRANSDUCTION MOLECULE,
SMAD1, AND THE CHROMODOMAIN HELICASE DNA BINDING PROTEIN 7
(CHD7)

by

CRISTINA M. HARMELINK, YUNJIA CHEN, PAIGE DEBENEDITTIS,
AND KAI JIAO.

In preparation for publication

Format adapted for dissertation

1. Introduction

Bone Morphogenetic Protein (BMP) signaling pathways are imperative for proper heart development. BMP ligand dimers bind serine threonine kinase receptors, which relay the signal intracellularly through activation of receptor-regulated SMAD proteins (R-SMADs). R-SMADs transduce the signals from the cytoplasm to the nucleus, where they cooperate with other cofactors to regulate gene expression.¹ The R-SMADs SMAD1, SMAD5, and SMAD8 relay BMP signals.²⁻⁴ The BMP signaling pathway can be regulated extracellularly, within the cytoplasm, and within the nucleus by a multitude of effectors that modulate the outcomes of the signaling cascade.⁵⁻⁹ Throughout heart development, BMP signaling pathways are thus fine-tuned in complex temporal-spatial manners to ensure proper cardiac gene expression. Aberrations in BMP signaling cascades result in congenital heart defects in humans and in animal models.^{10,11} Due to the complexity of BMP signaling regulation, the effectors have not been completely delineated. The goal of this project was to identify and characterize novel intracellular modulators of the BMP signaling pathway during mouse cardiogenesis.

In this study, Chromodomain helicase DNA binding protein 7 (CHD7) was identified as a SMAD1-interacting protein. CHD7 belongs to a family of nine conserved proteins (CHD1-9) that have roles in development and disease. They regulate transcription by altering nucleosome structure through ATP hydrolysis.¹²⁻¹⁸ CHD7 is a member of a subfamily of chromodomain helicase DNA binding proteins that includes CHD6-9. The members of this subfamily are characterized by the presence of three C-terminal domains: one SANT domain and two BRK domains.^{19,20} The molecular functions of CHD6-9 are not well-defined, but CHD7 can promote protein synthesis, proliferation,

and differentiation.²¹⁻²³ Haploinsufficiency for *CHD7* is the major cause of CHARGE syndrome, which is characterized by coloboma of the eye, hear defects, atresia of the choanae, retarded growth and development, genital abnormalities, and ear anomalies (OMIM 608892). It affects approximately 1 in 10,000 newborns in North America.^{24, 25} Approximately 77% of people with CHARGE syndrome have cardiovascular defects.²⁶ The heart defects are diverse and include Tetralogy of Fallot (characterized by defects in ventricle septation, narrowing of the pulmonary outflow tract, misalignment of the aorta, and right ventricle hypertrophy; OMIM 187500), interrupted aortic arch, double-outlet right ventricle (DORV, wherein both the pulmonary artery and the aorta arise from the right ventricle), truncus arteriosus (a single blood vessel arises from right and left ventricles due to outflow tract septation defects), atrioventricular canal (AVC) defects (poorly formed or absent chamber walls), atrial septal defects (ASD), and ventricle septal defects (VSD).^{27, 28}

CHD7 is evolutionarily conserved and animal models have provided insight into its cardiogenic functions. In mice, *Chd7* expression is strong in the embryonic stem cells and subsequently becomes restricted to the heart, brain, kidney, inner ear, eye, and olfactory epithelium.^{29, 30} Within the embryonic mouse heart, *Chd7* is expressed in the atrial and ventricular myocardium, and in the outflow tract.^{30, 31} Mice homozygous for a gene-targeted *Chd7* allele (*Chd7^{Gt/Gt}*) died between embryonic day (E) 10.5 and E11.5, with reduced embryo size.³⁰ The *Chd7^{Gt}* allele disrupted the N-terminal portion of the gene and transcripts contained only the last two exons, exons 37-38, which do not encode any known functional domains. Mice heterozygous for the gene-targeted *Chd7^{Gt}* allele (*Chd7^{Wt/Gt}*) had about half the survival rate and displayed abnormal behavior such as

head-bobbing and hyperactivity. Unfortunately the hearts of *Chd7^{Gt/Gt}* and *Chd7^{Wt/Gt}* mice were not characterized. In another study, a mutant mouse called *Whirligig* (*Chd7^{Whl}*) was generated with ENU mutagenesis.²⁹ The *Chd7^{Whl}* allele had a G>A mutation in exon 11 that was predicted to result in a truncated protein lacking the C-terminal SANT and BRK domains. *Chd7^{Whl/Whl}* homozygotes were developmentally delayed and did not survive past E11.5. The heart tube had formed and looped by E9.5, however later stages of heart development were not characterized. Heterozygosity for the *Whirligig* mutation (*Chd7^{Wt/Whl}*) resulted in early postnatal lethality, thought to be secondary to a VSD. A third mouse model demonstrated that haploinsufficiency for *Chd7* (*Chd7^{Wt/-}*) caused defective aortic arch morphogenesis at E10.5.³² Disruption of *Chd7* in *Xenopus* caused aberrant neural crest cell (NCC) gene expression and migration, resulting in abnormal outflow tract positioning.³³ While the molecular functions and tissue-specific requirements of CHD7 are not completely understood, it appears to have roles in multiple aspects of heart morphogenesis.

We first identified the SMAD1-CHD7 interaction in a yeast two-hybrid screen using a cDNA library isolated from embryonic mouse hearts.³⁴ The interaction was confirmed with glutathione S-transferase (GST) pull-down assays in mammalian cells and *in vitro*. Future studies will verify the functional significance of this interaction and conditional inactivation of *Chd7* in transgenic mouse models will help delineate its roles during heart development.

2. Materials and Methods

2.1 Yeast Two-Hybrid Screen

A yeast two-hybrid screening was performed using Matchmaker Yeast Two-Hybrid System (Clontech). Mouse *Smad1* and *Smad2* were cloned into GAL4 DNA binding domain (pGBD, leucine selection) vector to create the bait constructs (*Smad1*-pGBD and *Smad2*-pGBD, respectively). cDNA was previously isolated from E9.5-E11.5 mouse hearts and cloned into the GAL4 DNA activation domain (pGAD) vector to generate the prey constructs (prey-pGAD, tryptophan selection). Negative controls in the yeast two-hybrid experiments were AH109 haploid yeast cells transformed with (1) either *Smad1*-pGBD or *Smad2*-pGBD + pGAD vector, (2) prey-pGAD + pGBD vector, (3) pGAD vector + pGBD vector, (4) denatured carrier DNA, and (5) nothing. After transformation, AH109 cells were plated on plates lacking tryptophan and leucine (-TRP/-LEU) to select for proper transformation and incubated at 30 °C 2-3 days to allow growth. They were then replica-plated onto plates lacking tryptophan, leucine, adenine, and histidine (-TRP/-LEU/-ADE/-HIS) to select for protein-protein interaction through expression of reporter genes that express the essential amino acids ADE and HIS upon prey and bait interaction.

For transformation experiments, a lithium acetate yeast transformation protocol was followed. To culture AH109 cells, 100-300 ml of media was inoculated at 1:5 media:flask volume ratio and incubated overnight, 30 °C, shaking 200 rpm. Alternatively, a 5 ml starter culture of AH109 cells were incubated overnight in YPD media, shaking 200 rpm at 30 °C, and the following morning 1 ml of inoculated media was transferred to

50 ml YPD and incubated 4-6 hour, shaking 200 rpm at 30 °C. Inoculated media was divided between 15 ml conical tubes and centrifuged 5,000 rpm, 5 minutes at room temperature. YPD media was aspirated and cells were resuspended in 10 ml total volume of sterile water, and then spun down as before. The supernatant was aspirated and cells were resuspended in 5 ml 1XLiAcTE. Cells were centrifuged again, as before, and the supernatant was aspirated. Cells were resuspended in 2 ml 1XLiAcTE. The single stranded carrier DNA (salmon sperm) was denatured for 10 minutes at 95 °C and then placed on ice for 2 minutes. In a 1.5 ml eppendorf tube, 200 µl yeast cells in 1XLiAcTE suspension were combined with 5 µl denatured carrier DNA and X µl DNA (10 µl from Qiagen miniprep). The cells were transformed with 1.5 µg pGBD, 9 µg *Smad1*-pGBD, or 9 µg *Smad2*-pGBD. The solution was mixed and 1 ml PLATE (8 ml 50% PEG/1 ml 1MLiAC/ 1 ml 10XTE) was added. Cells were incubated at 30 °C for 30-60 minutes, followed by 42 °C incubation for 15 minutes. Then the cells were put on ice for 2 minutes, followed by centrifugation in short pulses, removing the supernatant, washing with 1 ml sterile water, and then aspirating most of the supernatant but leaving about 200 µl to plate. Plates were stored at 30 °C for 2 days.

For the initial yeast two-hybrid screen, AH109 cells were first transformed with *Smad1*-pGBD. Two 500 ml cultures of AH109[*Smad1*-pGBD] in -TRP media were incubated overnight, shaking 250 rpm at 30 °C. Subsequently, the two 500 ml volumes of AH109[*Smad1*-pGBD] cells were co-transformed with 2.5 µg prey-pGAD. The co-transformed AH109 cells were collected in PLATE, and serial dilutions were made in sterile water to a final dilution of 1/100,000. Cells were plated on -TRP/-LEU plates to select for efficient transformation of both vectors. Plates were incubated at 30 °C for 2-3

days to allow for growth, and subsequently replica-plated onto +4 mM 3AT (3-amino-1,2,4-triazole, to increase stringency of HIS reporter gene expression) -TRP/-LEU/-ADE/-HIS. Over 300 individual colonies were transferred with sterile toothpicks to 4 -TRP/-LEU/-ADE/-HIS master plates, grown two days at 30°C, and then sealed and stored at 4 °C.

2.2 Candidate DNA Isolation

To isolate DNA from yeast cells, a phenol:chloroform DNA extraction protocol was followed. 5 ml cultures were inoculated with a colony and grown to saturation overnight (~10⁹ cells total) in 15 ml conical tubes at 30 °C, shaking 200 rpm. Cultures were centrifuged for 5 minutes at room temperature in a fixed speed table top centrifuge. The supernatant was aspirated and the pellets were resuspended in 0.4 ml sterile water, and then transferred to 1.5 ml eppendorf tubes. Cells were spun briefly, for about 5 sec, and supernatant was decanted. Samples were vortexed briefly, 0.2 ml lysis solution (2% Triton/ 1%SDS/ 0.1M NaCl/ 1XTE) was added along with 0.3 g of acid washed, sterile glass beads (about 100 µl, baked for 2 hours at 180 °C). 0.2 ml phenol:chloroform was added and the solution was vortexed for 10 minutes at maximum speed. 0.2 ml 1XTE was added and the samples were centrifuged for 5 minutes at 13,000 rpm. The aqueous layer was transferred to a new tube. 1 ml ice-cold 95% ethanol was added and the sample was inverted to mix, then stored at -80 °C for at least 30 minutes. Then, the samples were centrifuged, 13,000 rpm at 4 °C, the ethanol was aspirated, the pellet was washed with cold 70% ethanol, and centrifuged again at 13,000 rpm for 5 minutes at 4 °C. The pellet was allowed to air dry, then resuspended in 100 µl elution buffer (Qiagen) with 10 µl 10X RNase. Samples were incubated at 37 °C for 15 minutes. DNA was

precipitated with an ice-cold solution of 40 μ l 3M NaAc in 1 ml cold 95% ethanol, mixed by inversion, and stored at -20 °C overnight. Samples were centrifuged for 10 minutes, 13,000 rpm, at 4 °C. The pellet was air-dried and resuspended in 50 μ l 1XTE. 10 μ l was used to determine concentration of DNA and 3 μ l was used for PCR analyses.

2.3 PCR Analyses of Candidates in pGAD vector

PCR was performed using Advantage 2 PCR System (Clontech). The PCR mixture was: 17 μ l H₂O, 2.5 μ l 10X Advantage 2 Buffer, 1 μ l 10 μ M primer mix, 1 μ l dNTP, 0.5 μ l Advantage 2 Taq, 3 μ l DNA, for a total volume of 25 μ l. The primers for the pGADT7 vector multiple cloning site were:

5'CTATTCGATGATGAAGATACCCACCAAACCC and

3', AGTGAACCTTGCGGGGTTTTTCAGTATCTACGAT. The PCR program was: 1) 94 °C, 5 min; 2) 94 °C, 30 sec; 3) 68 °C, 30 sec; 4) 72 °C, 45 sec; 5) Go to 2, 1X; 6) 94 °C, 30 sec; 7) 65 °C, 30 sec; 8) 72 °C, 45 sec; 9) Go to 6, 2X; 10) 94 °C, 30 sec; 11) 63 °C, 30 sec; 12) 72 °C, 45 sec; 13) Go to 10, 2X; 14) 94 °C, 30 sec; 15) 60 °C, 30 sec; 16) 72 °C, 45 sec; 17) Go to 14, 2X; 18) 94 °C, 30 sec; 19) 58 °C, 30 sec; 20) 72 °C, 45 sec; 21) Go to 18, 2X; 22) 94 °C, 30 sec; 23) 55 °C, 30 sec; 24) 72 °C, 45 sec; 25) Go to 22, 39X; 26) 72 °C, 4 min; 27) End. Results were run on 1.2% agarose gels at 100V.

2.4 Sequence Analyses of Candidates

Competent DH5 α *E.coli* cells were transformed with candidate DNA from yeast cells for DNA isolation and sequence analyses. 5 μ l yeast DNA (from the phenol-chloroform extraction described above) was added to the *E.coli* cells. Samples were gently tapped to mix and kept on ice for 30 minutes. Samples were incubated in a 42 °C water bath for 90

sec, and then placed on ice for 2 minutes. 1 ml LB media was added to the samples and they were incubated at 37 °C for 1 hour. Cells were plated on LB plates with selection and incubated at 37 °C overnight. Transformants were cultured in 2 ml LB with antibiotic selection overnight, shaking, 37 °C. DNA was isolated using Minipreps (Qiagen) according to the manufacturer's protocol. 2 µl of the Miniprep DNA was used to measure DNA concentration and 2 µl was analyzed on a 0.7% agarose gel, run at 100V. Sequencing was performed using T7 sequencing primer. Sequence alignment and verification of correct reading frame was performed using DNA Star sequence analysis software, BLASTN (http://www.ncbi.nlm.nih.gov/blast/Blast.cgi?CMD=Web&PAGE_TYPE=BlastHome), and CLUSTALW2 (<http://www.ebi.ac.uk/Tools/msa/clustalw2/>). The CHD7 protein schematic was created with Prosite MyDomains (<http://us.expasy.org/tools/mydomains/>).

2.5 GST Pull-down Experiments

The *Chd7* clone was inserted into the GST vector to create a GST-CHD7 fusion construct. COSM6 cells were transfected with 1 µg constitutively active ALK6 BMP receptor, 1 µg HA-SMAD1, 1.4 µg GST or 6 µg GST-CHD7 using Lipofectamine 2000 (Invitrogen) per manufacturer's protocol. The afternoon before transfection, 1.2×10^6 cells were plated in 100 mm cell culture dishes in 0.2M HEPES DMEM media without antibiotic. The media was refreshed the morning of the experiment, again without antibiotic. DNA and Lipofectamine 2000 were combined at a ratio of 1 µg DNA: 2 µl Lipofectamine 2000 in Opti-MEM (Invitrogen). The media was refreshed 4-6 hours after the transfection and again the next morning, without antibiotic.

For the GST pull-down assay, glutathione sepharose beads were hydrated in autoclaved water rotating at room temperature for 30 minutes, or overnight at 4 °C. For 8 samples, 10 mg beads were hydrated in 15 ml water. Beads were centrifuged in a fixed speed centrifuge for 1 minute at room temperature, the water was aspirated off, and hydrated beads were resuspended in 5 ml Lysis Solution (0.05 M TrisHCl, pH 7.4/ 0.5% TritonX/ 0.5% NP40/ 0.004 M EDTA/ 10.4% glycerol, no salt, no protease inhibitor). Beads were spun again, as before, and the Lysis Solution was aspirated. 10 mg of hydrated beads resulted in about 200 µl volume. An equal volume of Lysis Solution (200 µl) was added to the beads (no salt, no protease inhibitor), and stored at 4 °C for up to 2 weeks.

Blocking: 50 µl beads were aliquoted for each pull-down sample, using a large tip pipette, and blocked with 0.5% BSA (filter-sterilized) rotating at 4 °C at least 1 minute. Beads were then centrifuged at room temperature, 5,000 rpm for 3 minutes. The supernatant was aspirated and an equal volume of fresh lysis solution was added, with or without salt, and the bead slurry was kept on ice.

Two days after the transfection experiments, cells were gently washed with 1XPBS and then, while on ice, 200 µl Lysis Solution was applied to the cells (see recipe above, with or without 100 mM NaCl and with Complete EDTA-free Protease Inhibitor Cocktail Tablets, Roche, per manufacturer's instructions). On ice, cells were scraped, transferred to 1.5 ml eppendorf tubes, aspirated with a 25 G needle 15 times, rotated at 4 °C for 30 minutes, and then centrifuged at 13,000 rpm for 15 minutes at 4 °C. Keeping samples on ice, the supernatant was transferred to a new eppendorf tube. For total protein lysate, 100 µl of each sample was placed in a separate eppendorf tube, combined with 50 µl of 5X loading buffer, incubated at 70 °C for 5 minutes, and then stored at -80°C. For the GST

pull-down experiments, the samples were incubated with 50 μ l beads (as prepared above), rotating for 2.5 hours at 4 °C. The pull-down samples were centrifuged at 5,000 rpm for 2 minutes at room temperature and the supernatant was carefully aspirated. The pull-down samples were then washed 3 times in 1 ml Lysis Solution (recipe above, with or without salt, with protease inhibitor), rotating for 2 minutes at 4 °C for each wash and spinning down as before. Finally, 100 μ l 2X loading buffer was added to the bead pellet, resuspended by flicking, and denatured at 70 °C for 5 minutes. Samples were placed on ice for 2 minutes, centrifuged at 13,000 rpm for 3 minutes at room temperature. The supernatant was transferred to a new tube and stored at -80 °C. 20 μ l was loaded into each lane for Western blot analyses. Primary antibody was 1:1000, Secondary 1:1500.

2.6 *In vitro* Radio-labeled CHD7 Pull-Down

CHD7 was radio-labeled with S methionine using TNT Promega kit, according to manufacturer's protocol. Reagents were mixed, incubated at 30 °C for 2 hour, and stored at -80 °C overnight. B2L1 cells (characterized by having a mutated protease) were transformed with GST-SMAD1: 1 μ l DNA was added to cells, samples were placed on ice for 30 minutes, followed by a heat shock incubation in a 42 °C water bath for 90 sec, then ice for 2 minutes. 1 ml LB media was added and the sample was incubated at 37°C for 1 hour. 50 μ l was plated and incubated at 37 °C overnight. Inoculated media was treated with 300 μ l IPTG to induce the expression of the insert (GST-SMAD1) and cultured for 4 hours before it was collected. The pellet was resuspended in TT Buffer, pH 8.0, to a total volume of 15 ml.

3. Results

3.1 Over 300 Candidates Obtained from the Yeast Two-Hybrid Screen

To identify protein-protein interactions with the BMP specific R-SMAD, SMAD1, an embryonic mouse heart cDNA library was screened in a yeast two-hybrid experiment.³⁴ The bait, SMAD1, was fused to the GAL4 DNA binding domain (*Smad1*-pGBD). The prey, cDNA obtained from E9.5-E11.5 mouse hearts, was fused to the GAL4 DNA activation domain (prey-pGAD). Over 300 individual clones were obtained from the yeast two-hybrid screen. PCR analyses using primers 5' and 3' of the pGAD vector multiple cloning site (MCS) confirmed the presence of 329 candidate genes ranging from about 700 base pairs (bp) to over 1,500 bp in length (Figure 1A). Sequence analyses validated 73 candidate genes, from 298 clones (Figure 1B, Table 1). Several of these are known SMAD-interacting proteins, such as SMAD4, SMURF1, SMURF2, STUB1, and ZFYVE9.³⁵⁻³⁹ Candidates were prioritized for further analyses based on experimental evidence of their roles in heart development, associations with human disease, and their functions as transcription regulators. For high priority candidates, a second yeast two-hybrid screen was performed to confirm the interaction with SMAD1 and to test for an interaction with Transforming Growth Factor- β (TGF β)-specific SMAD2 (Figure 2 and Figure 3).¹ CCAR1, CHAF1A, CHD7, EPS15, and TAX1BP1 interacted with SMAD1 and SMAD2, suggesting that they can participate in both BMP and TGF β signaling pathways. HBP1 interacted only with SMAD1 and not with SMAD2, indicating that it functions specifically in the BMP signaling pathway. COMMD1, however, interacted with the pGBD vector and was therefore a false positive.

3.2 CHD7 Interacts with SMAD1

CHD7 is implicated in several aspects of heart development in animal models, is associated with human congenital heart defects, and functions as a transcriptional regulator, so we decided to further explore its interaction with SMAD1. Two identical clones of *Chd7* were obtained from the yeast two-hybrid screen (Figure 4A and 4B). Sequence analyses revealed that the clones aligned with mouse *Chd7* mRNA from nucleotides (nt) 7230-8266, which includes exons 32-35. The clone contained 8 nt of intronic sequence at the 5' end and 51 nt of intronic sequence at the 3' end that introduced a stop codon, resulting in a 1,096 nt transcript. The *Chd7* clone contained the two C-terminal BRK domains that are characteristic of the CHD6-9 subfamily (Figure 4C).^{19, 20} Due to the unique sequences flanking the clone, it may represent a heart-specific *Chd7* transcript.

The interaction of the CHD7 clone with SMAD1 was confirmed with a GST pull-down experiment performed in mammalian cells. The *Chd7* clone was inserted into a GST vector, creating a GST-CHD7 fusion protein. COSM6 cells were transfected with constitutively active BMP receptor, GST or GST-CHD7, and HA-SMAD1. While there was non-specific interaction between HA-SMAD1 and GST, HA-SMAD1 interacted more strongly with GST-CHD7 and this interaction was more specific under 100 mM salt conditions (Figure 5A). Lastly, an *in vitro* pull-down experiment further confirmed that the CHD7 clone can interact with SMAD1 (Figure 5B).

4. Discussion

To identify novel effectors of the BMP signaling pathway during heart development, we screened an embryonic mouse heart cDNA library.³⁴ The cDNA library was isolated from over 600 hearts between the stages E9.5-E11.5, a dynamic developmental period. During this time, the once seemingly quiescent linear heart tube undergoes tremendous morphological changes. At E9.5, the looping heart tube consists of an outer myocardial layer and an inner endocardial layer of cells, separated by an extracellular matrix called the cardiac jelly. The cardiac jelly enables crosstalk between the myocardium and endocardium, resulting in regional cardiomyocyte proliferation and demarcation of the future atrial and ventricular chambers. At E10.0-E10.5, chamber formation continues with septation, valve development, and myocardial wall morphogenesis. Outflow tract development is concurrently taking place, with contributions from the cardiac NCC population. By E11.5, the pro-epicardial cells have migrated around and enveloped the heart, forming the epicardium. The epicardium regulates myocardial wall development, contributes to endocardial cushion morphogenesis, and later in development it coordinates the formation of the coronary vasculature with the development of the myocardium.⁴⁰⁻⁴² Therefore, the cDNA library potentially contains candidates from different cardiac cell populations with functions in multiple aspects of early heart development.

We have identified an interaction between CHD7 and SMAD1, an intracellular transducer of BMP signaling pathways. The interaction with SMAD1 was confirmed in mammalian cells with GST pull-down experiments and *in vitro* pull-down assays. CHD7 interacted with SMAD2 in the yeast two-hybrid and may therefore have roles

downstream of the TGF β signaling pathway as well, although this needs to be confirmed with future experiments. The CHD7-SMAD1 interaction likely has implications for transcription regulation as both proteins bind DNA in cooperation with other cofactors to regulate gene expression.^{1, 12-18}

Two identical clones of *Chd7* were obtained from the yeast two-hybrid screen. The CHD7 clones aligned with the C-terminal end of the mouse *Chd7* transcript. However, the clones had intronic sequences at the 5' and 3' ends. Therefore, they may be representative of a new CHD7 isoform with unique expression and function in the developing mouse heart. The CHD7 clones contained the BRK domains characteristic of chromodomain helicase DNA binding proteins 6-9.^{19, 20} BRK domains are conserved in CHD7 homologs from *Drosophila* to humans, suggesting that they are important for CHD7 biological functions.^{43, 44} BRK domains are also found in the BRG1 family of chromatin remodeling enzymes and are thought to have protein-protein binding activities as well as chromodomain helicase activities.^{43, 45, 46} Full length CHD7 binds DNA at thousands of sites, including many enhancer sites, and shares binding sites with several cofactors including SMAD1, SOX2, and BRG1.^{47, 48} It was recently reported that CHD7 interacts with CHD8, which is part of a large protein complex that includes H3K4 methyltransferase and CHD9.^{12, 49-51} Taken together, these data suggest that CHD7 interacts via its BRK domain with SMAD1 to regulate gene transcription by (1) changing accessibility to target genes via chromatin unwinding, (2) bringing enhancer and promoter elements together, and/or (3) participating in developmentally regulated multi-protein complexes.⁴⁷

Animal models have provided insight into CHD7's conserved cardiogenic roles. The cardiac phenotypes of *Chd7*-null mouse embryos were not characterized in detail, however, deletion of *Chd7* in mice did not appear to affect cardiac induction or looping.³⁰ Mice heterozygous for a loss-of-function *Chd7* mutation had defects in septation, aortic arch morphogenesis, and outflow tract development.^{29, 30, 32} In *Xenopus*, loss of *Chd7* disrupted NCC gene expression and migration, ultimately causing misalignment of the outflow tract.³³ Haploinsufficiency for *CHD7* in humans causes similar congenital heart anomalies.^{27, 28} The defects in aortic arch patterning and outflow tract development associated with mutations in *CHD7* strongly suggest that it is required for these processes. However, it is unclear if *CHD7* has direct roles in the cardiac NCC population that contributes to the aortic arches and outflow tract, or if is instead important in the pharyngeal ectoderm which signals to the migratory cardiac NCC.^{52, 53} In the mouse, *CHD7* is expressed in the developing myocardium, outflow tract, NCC, and pharyngeal ectoderm.³⁰⁻³² Future studies using conditional inactivation of *Chd7* in specific cardiac cell types will help delineate its roles during cardiogenesis.

The roles of *CHD7* and its BRK domains during heart development remain to be determined. Mutations associated with CHARGE syndrome occur indiscriminately throughout *CHD7*.²⁶ Pathologic allelic variants in *CHD7* include nonsense, frameshift, and missense mutations, as well as deletions.^{28, 31, 54-57} Less common are chromosomal abnormalities detected in karyotypes that disrupt *CHD7*. These include balanced chromosomal translocations t(6;8)(6p8p;6q8q) and t(8;13)(q11.2;q22), and an interstitial deletion of 8q11.2-q13.⁵⁸⁻⁶⁰ The mutations are generally predicted to result in mRNA that is targeted for nonsense-mediated decay, removing the entire message.²⁶ No

genotype-phenotype correlation has been identified in CHARGE patients and it is not uncommon for patients with the same mutation to have different phenotypes.^{28, 31, 54, 56, 61} For example, three unrelated individuals with diverse clinical phenotypes had identical mutations in the second BRK domain that introduced a stop codon.³¹ The phenotypic variability in CHARGE patients may be due to mosaicism of *CHD7* mutations and the tissue-specific roles of *CHD7*, the type of mutation, and the diversity of genetic backgrounds which could result in the presence of different modifier genes.

CHD7 is one of three known causative genes in syndromic tracheal-esophageal malformations, the other two genes are *SOX2* and *MYCN*.^{62, 63} Like *CHD7*, *SOX2* and *MYCN* encode proteins that can regulate transcription.^{19, 20, 64, 65} Loss-of-function mutations in *CHD7*, *SOX2*, or *MYCN* cause developmental disorders with overlapping phenotypes including abnormal formation of the trachea and esophagus, as well as mental retardation.^{62, 64, 66} Recently, it was discovered that *CHD7* and *SOX2* are both highly expressed during mouse embryogenesis and can directly interact with each other to regulate common gene targets, including *Mycn*.⁶⁴ Furthermore, *CHD7*, *SOX2*, and *SMAD1* share binding sites in enhancer elements throughout the mouse genome.⁴⁷ Taken together with our results showing a direct interaction between *CHD7* and *SMAD1*, these data suggest that *CHD7*, *SOX2*, and *SMAD1* are part of a transcription regulatory complex with roles in regulating *Mycn* expression during development. This newly discovered *CHD7*-*SOX2*-*MYCN* axis has implications for cardiogenesis. While *Sox2* is not a known regulator of heart formation, other *Sox* genes are important for several aspects of cardiogenesis, including valve and outflow tract formation.⁶⁷⁻⁷³ Likewise, *CHD7* and *MYCN* have roles in septal-valvulogenesis and outflow tract morphogenesis.

^{26-28, 74, 75} *CHD7* mutations are associated with more severe heart defects than mutations in *MYCN*, which is consistent with *CHD7* being an upstream regulator of *MYCN*. *Mycn* has also been identified as a direct transcriptional target of BMP signaling pathways in the developing mouse myocardium.⁷⁶ Both *CHD7* and *MYCN* are implicated in several aspects of heart development and their roles during cardiogenesis warrant further investigation. The next chapter will explore the roles of myocardial *Mycn* during mouse heart development.

References

1. Euler-Taimor G, Heger J. The complex pattern of SMAD signaling in the cardiovascular system. *Cardiovasc Res* 2006;**69**:15-25.
2. Hoodless PA, Haerry T, Abdollah S, Stapleton M, O'Connor MB, Attisano L, et al. MADR1, a MAD-related protein that functions in BMP2 signaling pathways. *Cell* 1996;**85**:489-500.
3. Nishimura R, Kato Y, Chen D, Harris SE, Mundy GR, Yoneda T. Smad5 and DPC4 are key molecules in mediating BMP-2-induced osteoblastic differentiation of the pluripotent mesenchymal precursor cell line C2C12. *J Biol Chem* 1998;**273**:1872-1879.
4. Chen Y, Bhushan A, Vale W. Smad8 mediates the signaling of the ALK-2 [corrected] receptor serine kinase. *Proc Natl Acad Sci U S A* 1997;**94**:12938-12943.
5. Chen D, Zhao M, Harris SE, Mi Z. Signal transduction and biological functions of bone morphogenetic proteins. *Front Biosci* 2004;**9**:349-358.
6. Balemans W, Van Hul W. Extracellular regulation of BMP signaling in vertebrates: a cocktail of modulators. *Dev Biol* 2002;**250**:231-250.
7. Barbara NP, Wrana JL, Letarte M. Endoglin is an accessory protein that interacts with the signaling receptor complex of multiple members of the transforming growth factor-beta superfamily. *J Biol Chem* 1999;**274**:584-594.
8. Miyazono K, Maeda S, Imamura T. BMP receptor signaling: transcriptional targets, regulation of signals, and signaling cross-talk. *Cytokine Growth Factor Rev* 2005;**16**:251-263.
9. Miyazono K, Kamiya Y, Morikawa M. Bone morphogenetic protein receptors and signal transduction. *J Biochem* 2010;**147**:35-51.
10. van Wijk B, Moorman A, van den Hoff M. Role of bone morphogenetic proteins in cardiac differentiation. *Cardiovasc Res* 2007;**74**:244-255.
11. Wang J, Greene SB, Martin JF. BMP signaling in congenital heart disease: New developments and future directions. *Birth Defects Res A Clin Mol Teratol* 2011.
12. Shur I, Benayahu D. Characterization and functional analysis of CReMM, a novel chromodomain helicase DNA-binding protein. *J Mol Biol* 2005;**352**:646-655.
13. Becker PB, Hörz W. ATP-dependent nucleosome remodeling. *Annu Rev Biochem* 2002;**71**:247-273.
14. Eberharter A, Becker PB. ATP-dependent nucleosome remodelling: factors and functions. *J Cell Sci* 2004;**117**:3707-3711.
15. Lusser A, Kadonaga JT. Chromatin remodeling by ATP-dependent molecular machines. *Bioessays* 2003;**25**:1192-1200.
16. Narlikar GJ, Fan HY, Kingston RE. Cooperation between complexes that regulate chromatin structure and transcription. *Cell* 2002;**108**:475-487.
17. Sif S. ATP-dependent nucleosome remodeling complexes: enzymes tailored to deal with chromatin. *J Cell Biochem* 2004;**91**:1087-1098.
18. Smith CL, Peterson CL. ATP-dependent chromatin remodeling. *Curr Top Dev Biol* 2005;**65**:115-148.
19. Hall JA, Georgel PT. CHD proteins: a diverse family with strong ties. *Biochem Cell Biol* 2007;**85**:463-476.
20. Marfella CG, Imbalzano AN. The Chd family of chromatin remodelers. *Mutat Res* 2007;**618**:30-40.

21. Layman WS, McEwen DP, Beyer LA, Lalani SR, Fernbach SD, Oh E, et al. Defects in neural stem cell proliferation and olfaction in *Chd7* deficient mice indicate a mechanism for hyposmia in human CHARGE syndrome. *Hum Mol Genet* 2009;**18**:1909-1923.
22. Zentner GE, Hurd EA, Schnetz MP, Handoko L, Wang C, Wang Z, et al. CHD7 functions in the nucleolus as a positive regulator of ribosomal RNA biogenesis. *Hum Mol Genet* 2010;**19**:3491-3501.
23. Hurd EA, Poucher HK, Cheng K, Raphael Y, Martin DM. The ATP-dependent chromatin remodeling enzyme CHD7 regulates pro-neural gene expression and neurogenesis in the inner ear. *Development* 2010;**137**:3139-3150.
24. Källén K, Robert E, Mastroiacovo P, Castilla EE, Källén B. CHARGE Association in newborns: a registry-based study. *Teratology* 1999;**60**:334-343.
25. Issekutz KA, Graham JM, Prasad C, Smith IM, Blake KD. An epidemiological analysis of CHARGE syndrome: preliminary results from a Canadian study. *Am J Med Genet A* 2005;**133A**:309-317.
26. Zentner GE, Layman WS, Martin DM, Scacheri PC. Molecular and phenotypic aspects of CHD7 mutation in CHARGE syndrome. *Am J Med Genet A* 2010;**152A**:674-686.
27. Searle LC, Graham JM, Prasad C, Blake KD. CHARGE syndrome from birth to adulthood: an individual reported on from 0 to 33 years. *Am J Med Genet A* 2005;**133A**:344-349.
28. Aramaki M, Udaka T, Kosaki R, Makita Y, Okamoto N, Yoshihashi H, et al. Phenotypic spectrum of CHARGE syndrome with CHD7 mutations. *J Pediatr* 2006;**148**:410-414.
29. Bosman EA, Penn AC, Ambrose JC, Kettleborough R, Stemple DL, Steel KP. Multiple mutations in mouse *Chd7* provide models for CHARGE syndrome. *Hum Mol Genet* 2005;**14**:3463-3476.
30. Hurd EA, Capers PL, Blauwkamp MN, Adams ME, Raphael Y, Poucher HK, et al. Loss of *Chd7* function in gene-trapped reporter mice is embryonic lethal and associated with severe defects in multiple developing tissues. *Mamm Genome* 2007;**18**:94-104.
31. Lalani SR, Safiullah AM, Fernbach SD, Harutyunyan KG, Thaller C, Peterson LE, et al. Spectrum of CHD7 mutations in 110 individuals with CHARGE syndrome and genotype-phenotype correlation. *Am J Hum Genet* 2006;**78**:303-314.
32. Randall V, McCue K, Roberts C, Kyriakopoulou V, Beddow S, Barrett AN, et al. Great vessel development requires biallelic expression of *Chd7* and *Tbx1* in pharyngeal ectoderm in mice. *J Clin Invest* 2009;**119**:3301-3310.
33. Bajpai R, Chen DA, Rada-Iglesias A, Zhang J, Xiong Y, Helms J, et al. CHD7 cooperates with PBAF to control multipotent neural crest formation. *Nature* 2010;**463**:958-962.
34. DeBenedittis P, Harmelink C, Chen Y, Wang Q, Jiao K. Characterization of the novel interaction between muskellin and TBX20, a critical cardiogenic transcription factor. *Biochem Biophys Res Commun* 2011.
35. Murakami G, Watabe T, Takaoka K, Miyazono K, Imamura T. Cooperative inhibition of bone morphogenetic protein signaling by Smurf1 and inhibitory Smads. *Mol Biol Cell* 2003;**14**:2809-2817.
36. Lin X, Liang M, Feng XH. Smurf2 is a ubiquitin E3 ligase mediating proteasome-dependent degradation of Smad2 in transforming growth factor-beta signaling. *J Biol Chem* 2000;**275**:36818-36822.
37. Zhang Y, Musci T, Derynck R. The tumor suppressor Smad4/DPC 4 as a central mediator of Smad function. *Curr Biol* 1997;**7**:270-276.
38. Li L, Xin H, Xu X, Huang M, Zhang X, Chen Y, et al. CHIP mediates degradation of Smad proteins and potentially regulates Smad-induced transcription. *Mol Cell Biol* 2004;**24**:856-864.

39. Tsukazaki T, Chiang TA, Davison AF, Attisano L, Wrana JL. SARA, a FYVE domain protein that recruits Smad2 to the TGFbeta receptor. *Cell* 1998;**95**:779-791.
40. Evans SM, Yelon D, Conlon FL, Kirby ML. Myocardial lineage development. *Circ Res* 2010;**107**:1428-1444.
41. Srivastava D. Making or breaking the heart: from lineage determination to morphogenesis. *Cell* 2006;**126**:1037-1048.
42. Olivey HE, Svensson EC. Epicardial-myocardial signaling directing coronary vasculogenesis. *Circ Res* 2010;**106**:818-832.
43. Daubresse G, Deuring R, Moore L, Papoulas O, Zakrajsek I, Waldrip WR, et al. The *Drosophila* kismet gene is related to chromatin-remodeling factors and is required for both segmentation and segment identity. *Development* 1999;**126**:1175-1187.
44. Tamkun JW, Deuring R, Scott MP, Kissinger M, Pattatucci AM, Kaufman TC, et al. brahma: a regulator of *Drosophila* homeotic genes structurally related to the yeast transcriptional activator SNF2/SWI2. *Cell* 1992;**68**:561-572.
45. Doerks T, Copley RR, Schultz J, Ponting CP, Bork P. Systematic identification of novel protein domain families associated with nuclear functions. *Genome Res* 2002;**12**:47-56.
46. Chi T. A BAF-centred view of the immune system. *Nat Rev Immunol* 2004;**4**:965-977.
47. Schnetz MP, Handoko L, Akhtar-Zaidi B, Bartels CF, Pereira CF, Fisher AG, et al. CHD7 targets active gene enhancer elements to modulate ES cell-specific gene expression. *PLoS Genet* 2010;**6**:e1001023.
48. Schnetz MP, Bartels CF, Shastri K, Balasubramanian D, Zentner GE, Balaji R, et al. Genomic distribution of CHD7 on chromatin tracks H3K4 methylation patterns. *Genome Res* 2009;**19**:590-601.
49. Dou Y, Milne TA, Tackett AJ, Smith ER, Fukuda A, Wysocka J, et al. Physical association and coordinate function of the H3 K4 methyltransferase MLL1 and the H4 K16 acetyltransferase MOF. *Cell* 2005;**121**:873-885.
50. Surapureddi S, Viswakarma N, Yu S, Guo D, Rao MS, Reddy JK. PRIC320, a transcription coactivator, isolated from peroxisome proliferator-binding protein complex. *Biochem Biophys Res Commun* 2006;**343**:535-543.
51. Batsukh T, Pieper L, Koszucka AM, von Velsen N, Hoyer-Fender S, Elbracht M, et al. CHD8 interacts with CHD7, a protein which is mutated in CHARGE syndrome. *Hum Mol Genet* 2010;**19**:2858-2866.
52. Basch ML, Bronner-Fraser M. Neural crest inducing signals. *Adv Exp Med Biol* 2006;**589**:24-31.
53. Kameda Y. Hoxa3 and signaling molecules involved in aortic arch patterning and remodeling. *Cell Tissue Res* 2009;**336**:165-178.
54. Jongmans MC, Admiraal RJ, van der Donk KP, Vissers LE, Baas AF, Kapusta L, et al. CHARGE syndrome: the phenotypic spectrum of mutations in the CHD7 gene. *J Med Genet* 2006;**43**:306-314.
55. Wincent J, Holmberg E, Strömland K, Soller M, Mirzaei L, Djureinovic T, et al. CHD7 mutation spectrum in 28 Swedish patients diagnosed with CHARGE syndrome. *Clin Genet* 2008;**74**:31-38.
56. Vissers LE, van Ravenswaaij CM, Admiraal R, Hurst JA, de Vries BB, Janssen IM, et al. Mutations in a new member of the chromodomain gene family cause CHARGE syndrome. *Nat Genet* 2004;**36**:955-957.
57. Bergman JE, de Wijs I, Jongmans MC, Admiraal RJ, Hoefsloot LH, van Ravenswaaij-Arts CM. Exon copy number alterations of the CHD7 gene are not a major cause of CHARGE and CHARGE-like syndrome. *Eur J Med Genet* 2008;**51**:417-425.

58. Hurst JA, Meinecke P, Baraitser M. Balanced t(6;8)(6p8p;6q8q) and the CHARGE association. *J Med Genet* 1991;**28**:54-55.
59. Johnson D, Morrison N, Grant L, Turner T, Fantes J, Connor JM, et al. Confirmation of CHD7 as a cause of CHARGE association identified by mapping a balanced chromosome translocation in affected monozygotic twins. *J Med Genet* 2006;**43**:280-284.
60. Arrington CB, Cowley BC, Nightingale DR, Zhou H, Brothman AR, Viskochil DH. Interstitial deletion 8q11.2-q13 with congenital anomalies of CHARGE association. *Am J Med Genet A* 2005;**133A**:326-330.
61. Sanlaville D, Etchevers HC, Gonzales M, Martinovic J, Clément-Ziza M, Delezoide AL, et al. Phenotypic spectrum of CHARGE syndrome in fetuses with CHD7 truncating mutations correlates with expression during human development. *J Med Genet* 2006;**43**:211-217.
62. Shaw-Smith C. Oesophageal atresia, tracheo-oesophageal fistula, and the VACTERL association: review of genetics and epidemiology. *J Med Genet* 2006;**43**:545-554.
63. Geneviève D, de Pontual L, Amiel J, Sarnacki S, Lyonnet S. An overview of isolated and syndromic oesophageal atresia. *Clin Genet* 2007;**71**:392-399.
64. Engelen E, Akinci U, Bryne JC, Hou J, Gontan C, Moen M, et al. Sox2 cooperates with Chd7 to regulate genes that are mutated in human syndromes. *Nat Genet* 2011;**43**:607-611.
65. Hurlin PJ. N-Myc functions in transcription and development. *Birth Defects Res C Embryo Today* 2005;**75**:340-352.
66. Puc J, Rosenfeld MG. SOX2 and CHD7 cooperatively regulate human disease genes. *Nat Genet* 2011;**43**:505-506.
67. Lee YH, Saint-Jeannet JP. Characterization of molecular markers to assess cardiac cushions formation in *Xenopus*. *Dev Dyn* 2009;**238**:3257-3265.
68. Hoser M, Potzner MR, Koch JM, Bösl MR, Wegner M, Sock E. Sox12 deletion in the mouse reveals nonreciprocal redundancy with the related Sox4 and Sox11 transcription factors. *Mol Cell Biol* 2008;**28**:4675-4687.
69. Sakamoto Y, Hara K, Kanai-Azuma M, Matsui T, Miura Y, Tsunekawa N, et al. Redundant roles of Sox17 and Sox18 in early cardiovascular development of mouse embryos. *Biochem Biophys Res Commun* 2007;**360**:539-544.
70. Zhang C, Basta T, Klymkowsky MW. SOX7 and SOX18 are essential for cardiogenesis in *Xenopus*. *Dev Dyn* 2005;**234**:878-891.
71. Montero JA, Giron B, Arrechedera H, Cheng YC, Scotting P, Chimal-Monroy J, et al. Expression of Sox8, Sox9 and Sox10 in the developing valves and autonomic nerves of the embryonic heart. *Mech Dev* 2002;**118**:199-202.
72. Takash W, Cañizares J, Bonneaud N, Poulat F, Mattéi MG, Jay P, et al. SOX7 transcription factor: sequence, chromosomal localisation, expression, transactivation and interference with Wnt signalling. *Nucleic Acids Res* 2001;**29**:4274-4283.
73. Schilham MW, Oosterwegel MA, Moerer P, Ya J, de Boer PA, van de Wetering M, et al. Defects in cardiac outflow tract formation and pro-B-lymphocyte expansion in mice lacking Sox-4. *Nature* 1996;**380**:711-714.
74. Celli J, van Bokhoven H, Brunner HG. Feingold syndrome: clinical review and genetic mapping. *Am J Med Genet A* 2003;**122A**:294-300.
75. Marcelis CL, Hol FA, Graham GE, Rieu PN, Kellermayer R, Meijer RP, et al. Genotype-phenotype correlations in MYCN-related Feingold syndrome. *Hum Mutat* 2008;**29**:1125-1132.
76. Song L, Yan W, Chen X, Deng CX, Wang Q, Jiao K. Myocardial smad4 is essential for cardiogenesis in mouse embryos. *Circ Res* 2007;**101**:277-285.

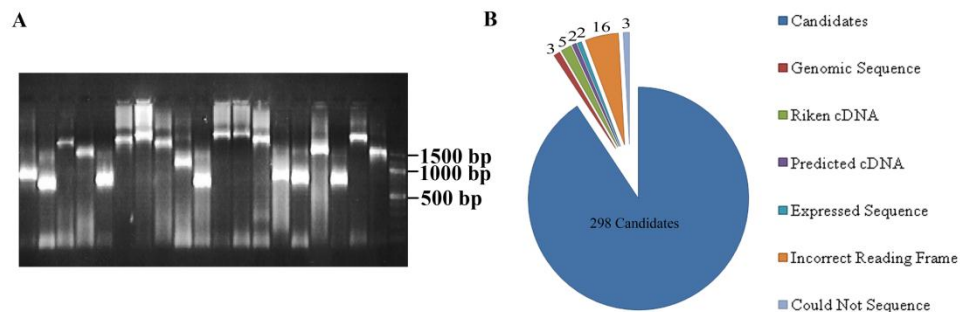


Figure 1. Analyses of candidates. A. Example of PCR analyses on DNA isolated from clones, confirming the presence of candidate genes inserted into pGAD expression vector. PCR analyses were performed using primers 5' and 3' of the pGAD multiple cloning site and results were run on a 1.2% agarose gel. Candidate gene sizes ranged from about 700 base pairs (bp) to over 1,500 bp. B. Sequence analyses of 329 clones validated 298 candidates, representing 73 genes. Other inserts were eliminated because they represented genomic contamination (Genomic Sequence, n=3), were undefined sequences (Riken cDNA, n=5; Predicted cDNA, n=2; Expressed Sequence, n=2), were not in the correct reading frames (n=16), or could not be sequenced (n=3).

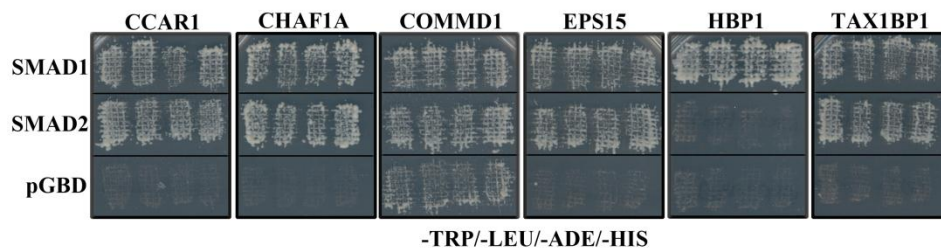


Figure 2. Confirming the SMAD1 interaction in yeast. Growth on media lacking the amino acids tryptophan, leucine, adenine, and histidine (-TRP/-LEU/-ADE/-HIS) indicates a positive interaction with SMAD1, which is specific to the BMP signaling pathway, and with SMAD2 which is specific to the TGF β signaling pathway. CCAR1, CHAF1A, EPS15, and TAX1BP1 interacted with both SMAD1 and SMAD2. HBP1 interacted only with SMAD1. COMMD1 was a false positive, as it interacted with SMAD1, SMAD2, and with the pGBD vector alone.

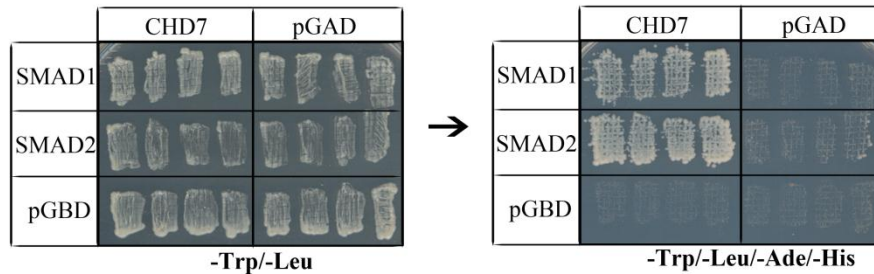


Figure 3. CHD7 interacts with SMAD1 in yeast. A yeast two-hybrid screen confirmed the interaction of CHD7 with SMAD1, and revealed an interaction with SMAD2. Growth on media lacking tryptophan and leucine (-TRP/-LEU) confirms co-transformation (left). Colonies were replica-plated onto media lacking tryptophan, leucine, adenine, and histidine (-TRP/-LEU/-ADE/-HIS) (right). Growth on this media revealed a positive interaction. CHD7 interacted with SMAD1 and SMAD2, suggesting it has a role in both BMP and TGF β signaling pathways, respectively. CHD7 did not interact with the pGBD vector alone, nor did pGBD vector interact with the pGAD vector.

A

7230

```

mChd7 clone -----AGGACAGAGTAATGATAAACCGATTAGACAACATCTGTGAAGCTGTGTGAA
CCCCCTTCAGGACAGAGTAATGATAAACCGATTAGACAACATCTGTGAAGCTGTGTGAA
*****

mChd7 clone AGGCAAATGGCCAGTAAATCGGCGCCAGATGTTTGATTTCCAGGGCCITGTCCTGGGTA
AGGCAAATGGCCAGTAAATCGGCGCCAGATGTTTGATTTCCAGGGCCITGTCCTGGGTA
*****

mChd7 clone CCCACCCTCOGCOGTGGACAGTCCOCTSCAGAAGAGGAGCTTTGCCGAGCTCTCTATGGT
CCCACCCTCOGCOGTGGACAGTCCOCTSCAGAAGAGGAGCTTTGCCGAGCTCTCTATGGT
*****

mChd7 clone CAGCCAGGCCAGCATCAGTGCAGCGAGGACATCACACGCTCTCCTCAGTTGTCCAAGGA
CAGCCAGGCCAGCATCAGTGCAGCGAGGACATCACACGCTCTCCTCAGTTGTCCAAGGA
*****

mChd7 clone TGATGCCTCAACTGTCTGTCCCTCGCCAGCGGCGGGAGGAGAAGGAAAGTTGAAAT
TGATGCCTCAACTGTCTGTCCCTCGCCAGCGGCGGGAGGAGAAGGAAAGTTGAAAT
*****

mChd7 clone CGAGGCTGAAAGAGCTGCCAAGAGGAAACCTTATGGAGATGGTTGCCAGCTTCGAGA
CGAGGCTGAAAGAGCTGCCAAGAGGAAACCTTATGGAGATGGTTGCCAGCTTCGAGA
*****

mChd7 clone GTCTCAGTGGTCTCAGAAAATGGACAGAAAAGTTGTGGACTTATCAAAGGCTCGAG
GTCTCAGTGGTCTCAGAAAATGGACAGAAAAGTTGTGGACTTATCAAAGGCTCGAG
*****

mChd7 clone AGAGGCAACAAGCTCTACCTCAAATTTCTCACTCTTACTTCAAAGTTATCTTGCCTAA
AGAGGCAACAAGCTCTACCTCAAATTTCTCACTCTTACTTCAAAGTTATCTTGCCTAA
*****

mChd7 clone TGTCTCCAGCCAGTGTCTGATGCCCTTAAAGTCTCAGATGGAGCTGCTCCAGCAGGCCCT
TGTCTCCAGCCAGTGTCTGATGCCCTTAAAGTCTCAGATGGAGCTGCTCCAGCAGGCCCT
*****

mChd7 clone TTCACGCACACCACAAGGCATATGCTCAATGGCTCCCTGGTGGATGGAGAGCCCCCAT
TTCACGCACACCACAAGGCATATGCTCAATGGCTCCCTGGTGGATGGAGAGCCCCCAT
*****

mChd7 clone GAAGAGGAGCGAGGCAGGAGGAAAACGTGGAGGGCCTCGACCTACTTTTCATGAGCCA
GAAGAGGAGCGAGGCAGGAGGAAAACGTGGAGGGCCTCGACCTACTTTTCATGAGCCA
*****

mChd7 clone CAAACGGACCCGTTAAGTGCAGAGGATGCTGAGGTGACCAAGCTTTTGAAGAGATAT
CAAACGGACCCGTTAAGTGCAGAGGATGCTGAGGTGACCAAGCTTTTGAAGAGATAT
*****

mChd7 clone AGAGACCCACCATAAGAAACATTCCTTCTCCTGGACAGCTGGACCCCGACACCCGGAT
AGAGACCCACCATAAGAAACATTCCTTCTCCTGGACAGCTGGACCCCGACACCCGGAT
*****

mChd7 clone CCCTGTGATAAACCTTGAAGATGGGACTAGGCTGGTGGGAGAGACGCTCCTAAAAACAA
CCCTGTGATAAACCTTGAAGATGGGACTAGGCTGGTGGGAGAGACGCTCCTAAAAACAA
*****

mChd7 clone GGACTTGGTTGACTGGCTGAACTGCACCCACCTACACTGTCGATATGCCGAGTTATGT
GGACTTGGTTGACTGGCTGAACTGCACCCACCTACACTGTCGATATGCCGAGTTATGT
*****

mChd7 clone ACCAAAGAACACAGACGTGCTGTTTTCTCGTTTTAGAAACCGAAACAGAAACGACATAG
ACCAAAGAACACAGACGTGCTGTTTTCTCGTTTTAGAAACCGAAACAGAAACGACATAG
*****

mChd7 clone ATGTCGAAATCCTAATAAATGGATATTAACTTTGACAGGAGAAAGGGTTCCCTGT
ATGTCGAAATCCTAATAAATGGATATTAACTTTGACAGGAGAAAGGGTTCCCTGT
*****

mChd7 clone TGTAACAAACGAAATGGGAAGAG-----
TGTAACAAACGAAATGGGAAGAGGTAATGCTGGGAAGGGATGGGCAAGGATGGCAA
*****

mChd7 clone -----
ATCACACTTCTTAG

```

8266

B



C



Figure 4. *Chd7* clone. A. Two identical clones of *Chd7* were obtained from the yeast two-hybrid screen. The *Chd7* clones aligned with the mouse *Chd7* transcript (*mChd7*) from nucleotides (nt) 7230-8266. The 5' end of the clone had 8 nt of intronic sequence, and the 3' end had intronic sequence that introduced a stop codon (TAG) after 51 nt. Intronic sequences are highlighted in red. B. In the mouse *Chd7* transcript, the ATG start codon is at 329 nt and the TAA stop codon is at 9,289nt. The *Chd7* clones, represented by the shorter schematic below, were 100% identical to the mouse transcript from 7230-8266 nt, which includes exons 32-35. The intronic sequences are depicted in red. The resulting transcript was 1,096 nt. The unique sequence of the clone may be representative of a new *Chd7* transcript. C. Schematic of the mouse CHD7 protein. Mouse CHD7 is 2,986 amino acids (aa). CHD7 has two Chromodomains (Chromo, 790-857 and 872-937 aa) that condense chromatin. The SNF2 ATPase domain (961-1,246 aa) and Helicase domain (1,284-1,454 aa) are involved in chromatin unwinding. On the C-terminal end of the protein are the SANT and BRK domains. The SANT domain (1,952-2,011 aa) is thought to bind histone tails. The BRK domains (2,553-2,602 and 2,631-2,675 aa) are thought to have helicase and protein-protein binding functions. The clone isolated from the yeast two-hybrid screen aligned with CHD7 from 2,410-2,755 aa, a region containing the BRK domains indicated by the green bar above the protein cartoon.

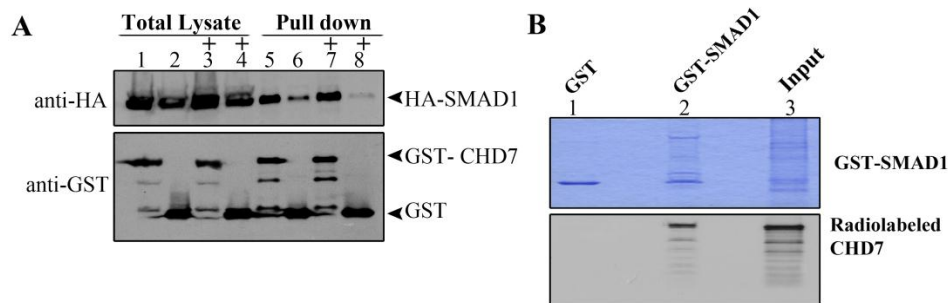


Figure 5. CHD7-SMAD1 interaction in mammalian cells and *in vitro*. A. CHD7-SMAD1 interaction in COSM6 cells. Lanes 1-4 are total protein lysates, Lanes 5-6 are pull-down lysates, + = with 100 mM NaCl. HA-SMAD1 interacts with GST-CHD7 without NaCl (Total Protein Lanes 1 and 2, Pull-down lanes 5 and 6) but the fusion proteins interact more specifically when pulled down with 100 mM NaCl (Total Protein Lanes 3 and 4, Pull-down lanes 7 and 8). B. *In vitro* pull-down assay with GST-SMAD1 and radio-labeled CHD7. An 18 hour exposure showed that radio-labeled CHD7 interacted only with GST-SMAD1 (Lane 2) and not with GST (Lane 1). Lane 3 is 1/10th of probe input.

Table 1. Candidates isolated from the yeast two-hybrid screen.

Gene Symbol (NCBI)	Gene Name (NCBI)	Gene ID (NCBI)	Gene Ontology Process (MGI)	Swisspro ID
<i>Ankrd13a</i>	Ankyrin repeat domain 13a	68420	ND	Q80UP5
<i>Ascc2</i>	Activating signal cointegrator 1 complex subunit 2	75452	DNA-dependent regulation of transcription	Q91WR3
<i>Asxl1</i>	Additional sex combs like 1	228790	Chromatin modification, DNA-dependent regulation of transcription	P59598
<i>Aup1</i>	Ancient ubiquitous protein 1	11993	Metabolic Process	P70295
<i>Aypi1</i>	Arginine vasopressin-induced protein 1	69534	Activation of MAPK activity, Cell cycle	Q9D7H4
<i>Bhlhb9</i>	Basic helix-loop-helix domain containing, class B9	70237	ND	Q6PB60
<i>Cblb</i>	Casitas B-lineage lymphoma b	208650	T cell activation, Signal transduction	Q3TTA7
<i>Ccar1</i> (pJK197)	Cell division cycle and apoptosis regulator 1	67500	RNA splicing, Apoptosis, Cell cycle, DNA-dependent regulation of transcription	Q8CH18
<i>Ccnt1</i>	Cyclin T1	12455	Cell cycle, Cell division, Protein phosphorylation, DNA-dependent regulation of transcription	Q9QWV9
<i>Cep57</i>	Centrosomal protein 57	74360	FGFR signaling pathway, protein homooligomerization, protein translocation into nucleus	Q8CEE0
<i>Chaf1a</i> (pJK198)	Chromatic assembly factor 1, subunit A (p150)	27221	DNA repair and replication, Cell cycle, DNA-dependent regulation of transcription	Q9QWF0
<i>Chd7</i> (pJK208)	Chromodomain helicase DNA binding protein 7	320790	T cell differentiation, Embryonic development, Locomotory behavior, DNA-dependent regulation of transcription, Chromatin modification	A2AJK6
<i>Commd1</i>	COMM domain containing 1	17846	Cellular ion homeostasis, Positive regulator of protein ubiquitination, Negative regulator of NF-kappaB transcription factor activity	Q8K4M5

<i>Dnajb5</i>	DnaJ (Hsp40) homolog, subfamily B, member 5	56323	Negative regulation of transcription from RNA polymerase II promoter, Protein folding	Q89114
<i>Eno1</i>	Enolase 1, alpha non-neuron	13806	Embryonic development, Metabolic process, Negative regulation of cell growth, DNA-dependent negative regulation of transcription	P17182
<i>Epn1</i>	Epsin 1	13854	Endocytosis	Q80VP1
<i>Epn2</i>	Epsin 2	13855	Endocytosis	Q8CHU3
<i>Eps15</i>	Epidermal growth factor receptor pathway substrate 15	13858	Clathrin coat assembly, Protein transport	P42567
<i>Ercc6</i>	Excision repair cross-complementing rodent repair deficiency, complementation group 6	319955	DNA repair, Activation of JNKK and JUN activity, DNA-dependent positive regulation of transcription elongation	A3KMN2
<i>Fbxo42</i>	F-box protein 42	213499	ND	Q6PDJ6
<i>Frm4a</i>	FERM domain containing 4A	209630	ND	Q8BIE6
<i>Grb10</i>	Growth factor receptor bound protein 10	14783	Insulin-like growth factor receptor signaling pathway, Negative regulation of Wnt receptor signaling pathway, Positive regulation of VEGFR signaling pathway	Q60760
<i>Hbp1</i>	High mobility group box transcription factor 1	73389	Wnt receptor signaling pathway, DNA-dependent regulation of transcription	Q8R316
<i>Hnrpa1</i>	Heterogeneous nuclear ribonucleoprotein A1	15382	RNA splicing, mRNA processing and transport, Nuclear export and import	P49312
<i>March7</i>	Membrane-associated ring finger (C3HC4) 7	57438	ND	A2AW82, A2AW83
<i>Mcrs1</i>	Microspherule protein 1	51812	ND	Q99L90
<i>Morc4</i>	Microrchidia 4	75746	ND	A2RSL2
<i>Mrpl19</i>	Mitochondrial ribosomal protein L19	56284	Translation	Q6P8U3

<i>Mtap1s</i>	Microtubule-associated protein 1S	270058	Apoptosis, Microtubule bundle formation, Microtubule cytoskeleton organization	Q8C052
<i>Mybpc3</i>	Myosin binding protein C, cardiac	17868	Cardiac muscle contraction, Cell adhesion, Heart morphogenesis	O70468
<i>Mynn</i>	Myoneurin	80732	DNA-dependent regulation of transcription	Q99MD8
<i>Ncoa3</i>	Nuclear receptor coactivator 3	17979	Developmental growth, Histone acetylation, DNA-dependent regulation of transcription	O09000
<i>Nedd4</i>	Neural precursor cell expressed, developmentally down-regulated gene 4	17999	Negative regulator of VEGFR signaling pathway, Nervous system development, Protein ubiquitination	P46935
<i>Nedd4l</i>	Neural precursor cell expressed, developmentally down-regulated gene 4-like	83814	Negative regulation of sodium ion transport, Protein ubiquitination	Q8CFI0
<i>Patz1</i>	POZ (BTB) and AT hook containing zinc finger 1	56218	T-cell differentiation, Male gonad development, DNA-dependent regulation of transcription	Q80XS2
<i>Phkb</i>	Phosphorylase kinase beta	102093	Carbohydrate metabolic process, Glycogen metabolic process	Q7TSH2
<i>Poldip3</i>	Polymerase (DNA-directed), delta interacting protein 3	73826	Positive regulation of translation	Q8BG81
<i>Polk</i>	Polymerase (DNA directed), kappa	27015	DNA repair, DNA replication, Metabolic process	Q9QUG2
<i>Rbm14</i>	RNA binding motif protein 14	56275	Histone deacetylation, Positive regulation of transcription from RNA polymerase II promoter	Q8C2Q3
<i>Rev1</i>	REV1 homolog (<i>S. cerevisiae</i>)	56210	DNA repair, DNA replication	Q920Q2
<i>Rnf2</i>	Ring finger protein 2	19821	Anterior/posterior axis specification, Histone ubiquitination, Mitotic cell cycle, DNA-dependent regulation of transcription, Protein ubiquitination	Q9CQJ4
<i>Rps27a</i>	Ribosomal protein S27a	78294	MyD88-dependent toll-like receptor signaling pathway, Apoptosis, Cell membrane organization, Ubiquitination, Translational elongation	P62983

<i>Scmh1</i>	Sex comb on midleg homolog 1	29871	Anterior/posterior axis specification, Chromatin remodeling, Regulation of transcription, Spermatogenesis	Q8K214
<i>Sema6d</i>	Sema domain, transmembrane domain (TM), and cytoplasmic domain, (semaphorin) 6D	214968	Cell differentiation, Development, Nervous system development	Q76KF0
<i>Sh3bp4</i>	SH3-domain binding protein 4	98402	Endocytosis	Q921I6
<i>Smad4</i>	MAD homolog 4	17128	TGF β and BMP signaling pathways, Development, Cell death, Cell growth, Proliferation, Regulation of transcription	P97471
<i>Smurf1</i>	SMAD specific E3 ubiquitin protein ligase 1	75788	TGF β and BMP signaling pathways, Cell differentiation, Protein ubiquitination	Q9CUN6
<i>Smurf2</i>	SMAD specific E3 ubiquitin protein ligase 2	66313	BMP signaling pathway, Protein ubiquitination	A2A5Z6
<i>Snip1</i>	Smad nuclear interacting protein 1	76793	I-kappaB kinase/NF kappaB cascade, Production of miRNAs, Regulation of transcription	Q8BIZ6
<i>Stam</i>	Signal transducing adaptor molecule (SH3 domain and ITAM motif) 1	20844	Cellular membrane organization, Intracellular protein transport	P70297
<i>Stam2</i>	Signal transducing adaptor molecule (SH3 domain and ITAM motif) 2	56324	Cellular membrane organization, Intracellular Protein transport	O88811
<i>Stub1</i>	STIP1 homology and U-Box containing protein 1	56424	Protein ubiquitination, Ubiquitin-dependent SMAD protein catabolic process, Protein folding, Protein maturation	Q9WUD1
<i>Supt6h</i>	Suppressor of Ty 6 homolog (S. cerevisiae)	20926	DNA-dependent regulation of transcription elongation	Q62383
<i>Tab2</i>	TGF-beta activated kinase 1/MAP3K7 binding protein 2	68652	MyD88-dependent toll-like receptor signaling pathway, Heart development, Positive regulation of protein kinase activity	Q99K90
<i>Tax1bp1</i>	Tax1 (human T-cell leukemia virus type I) binding protein 1	52440	Apoptosis, Negative regulation of NF-kappaB transcription factor activity	Q3UKC1
<i>Tnip1</i>	TNFAIP3 interacting protein 1	57783	Glycoprotein biosynthetic process	Q9WUU8
<i>Tollip</i>	Toll interacting protein	54473	Inflammatory response, Phosphorylation, Signal transduction	Q9QZ06

<i>Uba52</i>	Ubiquitin A-52 residue ribosomal protein fusion product 1	22186	MyD88-dependent toll-like receptor signaling pathway, Apoptosis, Ubiquitination, Translational elongation	P62984
<i>Ubap1</i>	Ubiquitin-associated protein 1	67123	ND	Q8BH48
<i>Ubb</i>	Ubiquitin B	22187	MyD88-dependent toll-like receptor signaling pathway, Apoptosis, Ubiquitination	P0CG49
<i>Ubqln1</i>	Ubiquilin 1	56085	Apoptosis, Protein ubiquitination, Response to hypoxia	Q8R317
<i>Ubqln2</i>	Ubiquilin 2	54609	ND	Q9QZM0
<i>Ubqln4</i>	Ubiquilin 4	94232	ND	Q99NB8
<i>Uimc1</i>	Ubiquitin interaction motif containing 1	20184	DNA repair, G2/M DNA damage checkpoint, Chromatin modification, DNA-dependent regulation of transcription	Q5U5Q9
<i>Usp13</i>	Ubiquitin specific peptidase 13 (isopeptidase T-3)	72607	ND	D3YYG7
<i>Usp5</i>	Ubiquitin specific peptidase 5 (isopeptidase T)	22225	Positive regulation of proteasomal ubiquitin-dependent protein catabolic process	P56399
<i>Usp28</i>	Ubiquitin specific peptidase 28	235323	DNA damage checkpoint, DNA repair, Cell proliferation, Protein deubiquitination	Q5I043
<i>Zfp251</i>	Zinc finger protein 251	71591	ND	Q6PCX8
<i>Zfp326</i>	Zinc finger protein 326	54367	DNA-dependent regulation of transcription	O88291
<i>Zfp784</i>	Zinc finger protein 784	654801	DNA-dependent regulation of transcription	Q8BI69
<i>Zfyve9</i>	Zinc finger, FYVE domain containing 9	230597	Regulation of TGF β signaling pathway (Smad interacting)	Q80XL0
<i>Zfp598</i>	Zinc finger protein 598	213753	ND	Q80YR4
<i>Zmynd11</i>	Zinc finger, MYND domain containing 11	66505	DNA-dependent regulation of transcription	Q8R5C8

BMP, Bone Morphogenetic Protein; FGFR, Fibroblast growth factor receptor; TGF β , Transforming growth factor beta; VEGFR: Vascular endothelial growth factor receptor; pJK, plasmid designation for lab use.

MYOCARDIAL MYCN IS ESSENTIAL FOR MOUSE VENTRICULAR WALL
MORPHOGENESIS

by

CRISTINA M. HARMELINK, PAIGE DEBENEDITTIS, AND KAI JIAO

In preparation for *BMC Developmental Biology*

Format adapted for dissertation

1. Introduction

The heart is the first organ to develop and function during embryogenesis. In order to sustain the growing embryo, heart muscle must rapidly expand through cardiomyocyte proliferation and differentiation.^{1,2} The relatively unproliferative nonchamber myocardium along the inner curvature of the heart includes the atrioventricular canal (AVC), the outflow tract, and the inflow tract.^{3,4} Atrial and ventricular chamber myocardium is characterized by highly proliferative cardiomyocytes.^{1,3,4} After rightward looping, proliferating cardiomyocytes increase chamber mass and volume by contributing to the thickening myocardial wall and to the trabecular myocardium on the luminal side of the ventricles (Supplemental Figure 1).^{1,2,5,6} Trabecular myocardium consists of subendocardial muscular projections created by organized layers of differentiated cardiomyocytes.² It has multiple roles during early heart development including coordinating conduction and enhancing contractile force to support continuing embryonic development.^{2,5} Later in development, the trabecular myocardium is incorporated into the compact myocardium, papillary muscles, and the interventricular septum (IVS).² Abnormalities in ventricular myocardial wall morphogenesis cause embryonic lethality in mice and adult cardiomyopathies in humans.⁷⁻¹⁵

MYCN is a member of the conserved MYC family of basic transcription factors involved in development and disease.¹⁶⁻³⁰ There are four closely related *MYC* genes in mammals: *CMYC*, *MYCN*, *MYCL*, and *MYCS*.¹⁷ *CMYC* and *MYCN*, perhaps the best characterized of the MYC proteins, are broadly expressed in complementary temporal-spatial patterns.³¹ *MYCN* has an N-terminal transcription activating domain and a C-terminal DNA-binding domain (Supplemental Figure 2). It interacts with MAX proteins to activate

transcription and with MIZ-1 to repress transcription.^{16, 17, 32-34} Multiple developmental signaling pathways converge on MYC proteins and, depending on the cellular context, they can promote proliferation and growth, inhibit differentiation, and regulate apoptosis.^{16, 17, 35} Haploinsufficiency for *MYCN* is associated with Feingold syndrome (FS, OMIM 164280), a rare developmental disorder characterized in part by congenital heart defects (CHDs).^{19, 30, 36-39} Heart anomalies are variable and include ventricle septal defect (VSD), abnormal valvulogenesis, outflow tract septation defects and aberrant development of the aortic arch.^{37, 40} Pathogenic mutations disrupt the *MYCN* DNA binding domain and include frameshift mutations, missense mutations, and deletions that result in nonsense-mediated decay of the transcript or a truncated protein.^{30, 40}

Mouse models have provided insight into *Mycn*'s conserved roles in development and disease. Global deletion or severe reduction of *MYCN* in mice causes phenotypes that are similar to but more severe than those associated with FS. *Mycn*-depletion results in embryonic lethality between E10.5 and E12.5 due to defective organogenesis.²⁰⁻²⁴ Tissue-specific deletion or overexpression of *Mycn* revealed that it has roles in the growth, morphogenesis, and patterning of the limbs, lungs, inner ears, and brain.^{18, 25, 26, 41, 42} *Mycn* is a positive regulator of proliferation, but it regulates cell survival and differentiation in a tissue-specific manner.^{18, 25, 26, 41-43} Conditional removal of *Mycn* from the developing limbs causes reduced apoptosis, while increased apoptosis was seen in the *Mycn*-depleted lungs and liver.^{25, 26, 43} Cell differentiation was sensitive to *MYCN* levels in the developing limbs, lungs, and brain, but not in the inner ears.^{18, 25, 26, 41}

Mycn-depletion disrupts normal heart development and, consistent with its role in human heart development, the cardiac phenotypes observed in *Mycn*-depleted mouse models are

complex and variable. Mice null for *Mycn* or with reduced MYCN protein to 15% of normal had heart defects such as delayed development with no septa-valvulogenesis, lack of IVS formation, and underdeveloped ventricular myocardial walls.²⁰⁻²³ These studies provided evidence that *Mycn* potentially has roles in several key cardiogenic processes, yet the mutant hearts were not characterized in detail. It remains unclear if the reported heart defects were caused by grossly abnormal embryo development. Moreover, global removal of *Mycn* from the developing embryo precludes investigation of its functions within specific cardiac tissues during heart development.

Our lab and others have identified *Mycn* as a transcriptional target of Bone Morphogenetic Protein (BMP) signaling in the developing mouse myocardium.^{44, 45} BMP cytokines are necessary for cardiomyocyte induction, proliferation, and survival during chamber morphogenesis.^{10, 44, 46-59} BMP signaling is also important for AVC valvuloseptal development.^{53, 54, 58-65} In the current study, we tested the hypothesis that myocardial *Mycn* encodes an essential regulator of cardiomyocyte proliferation, survival, size, and differentiation, using a novel mouse model with *Mycn* specifically removed from the myocardium.

2. Methods

2.1 Mice

This study conforms to the Guide for the Care and Use of Laboratory Animals published by the US National Institutes of Health (NIH Publication no. 85–23, revised 1996). All protocols were approved by the Institutional Animal Care and Use Committee at the University of Alabama at Birmingham.

The *cTnt-Cre* and *Mycn*^{loxP} transgenic mouse lines have been described elsewhere.

Mycn^{loxP} mice were provided by R. Eisenman, Fred Hutchinson Cancer Research Center.

^{18, 44} Male *cTnt-Cre;Mycn*^{loxP/wt} mice were mated with *Mycn*^{loxP/loxP} females to conditionally delete *Mycn* from the developing mouse heart. Upon *cTnt-Cre* mediated recombination, the entire coding region of *Mycn* is deleted within the myocardium between embryonic day E9.5 and E10.5. The day of the plug was considered E0.5. Embryos were dissected in 1XPBS and processed for further experiments. Living embryos were defined by beating hearts. Hemorrhage, edema, and dilation of hearts were phenotypes indicative of cardiovascular insufficiency. Controls in all experiments were *cTnt-Cre* negative littermates. Only living embryos were used for experiments.

2.2 Antibodies and reagents

Monoclonal antibodies for MYCN (ab16898, Western blotting (WB), 1 µg/ml), alpha MHC (ab50967, WB 1:1,000), beta MHC (ab11083, WB, 1:75,000; IHC 1:5,000), and MLC1V (ab680, WB, 1:20,000), cardiac Troponin I (ab19615, WB, 1:2,000) were purchased from Abcam. Polyclonal anti-phospho-Histone H3 antibody (06-570, Immunofluorescence (IF), 1:300) was obtained from Upstate Cell Signaling Solutions.

Monoclonal cyclin D1 antibody (556470, WB, 1:2,500; IHC, 1:300) was purchased from BD Biosciences. Polyclonal antibodies for cyclin D2 (sc-593, WB, 1:10,000; IHC, 1:20,000) and myosin light chain 2v (sc-34490, WB, 1:2,500) were from Santa Cruz Biotechnology. Monoclonal antibodies for cardiac actin (A9357, WB, 1:5,000; IHC 1:3,000) and smooth muscle actin (A2547, WB, 1:10,000; IHC 1:3,000), and polyclonal antibody for ID2 (HPA027612, WB 1:500; IHC 1:8,000) were from Sigma. Monoclonal antibodies for cardiac troponin T (WB, 1:2,000; IF 1:200) and beta tubulin (WB, 1:50,000) were provided by the Developmental Studies Hybridoma Bank at the University of Iowa. Anti-p70 S6 kinase polyclonal antibody (9202, WB, 1:2,000; IHC 1:200) was supplied by Cell Signaling. Polyclonal skeletal muscle actin (NBP1-35265, WB, 1:5,000; IHC 1:20,000) antibody was from Novus Biologicals. The myosin light chain 2a antibody (WB, 1:15,000) was from S. Kubalak at the University of South Carolina. Fluorescent wheat germ agglutinin conjugate Oregon Green 488 (IF, 10 µg/ml) was purchased from Invitrogen.

2.3 DNA analyses

Genotyping was performed on tissue from the yolk sac or tail. Tissue samples were incubated with 20mg/ml Proteinase K (PK) in 50mM Tris/ 100 mM EDTA overnight at 55 °C. The *cTnt-Cre* primer pair sequences are: forward primer, 5'-GGCGCGGCAACA CCATTTTT-3', and reverse primer, 5'-TCCGGGCTGCCA CGACCAA-3'. The PCR program used to amplify the *cTnt-Cre* product was: 94 °C for 3 min (1 cycle); 94 °C for 30 sec, 64 °C for 30 sec, 72 °C 30 sec (30 cycles); 72 °C 4 min. The primer pair used to distinguish the floxed versus wild type *Mycn* alleles was: forward primer, 5'-GTCGC

GCTAGTAAGAGCTGAGATC-3', and reverse primer, 5'-CACAGCTCTGGAA
GGTGGGAGAAAGTTGAGCGTCTCC-3.¹⁸ The PCR program was: 94 °C for 3 min (1
cycle); 94 °C for 30 sec, 68 °C for 30 sec, 72 °C for 45 sec (2 cycles); 94 °C for 30 sec, 65
°C for 30 sec, 72 °C for 45 sec (2 cycles); 94 °C for 30 sec, 63 °C for 30 sec, 72 °C for 45
sec (2 cycles); 94 °C for 30 sec, 60 °C for 30 sec, 72 °C for 45 sec (2 cycles); 94 °C for 30
sec, 58 °C for 30 sec, 72 °C for 45 sec (2 cycles); 94 °C for 30 sec, 55 °C for 30 sec, 72 °C
for 45 sec (39 cycles); 72 °C for 4 min. The wild type allele product is 217 base pairs (bp)
and the floxed allele product is 260 bp. The distribution of genotypes of living embryos
was compared with the expected Mendelian ratio and a chi-square test was performed for
statistical analysis, with P<0.05 considered significant. At least 5 litters were examined
for each stage.

Semiquantitative PCR analyses was performed on genomic DNA isolated from pooled
embryonic heart ventricles and whole bodies from *Mycn*^{loxp/loxp} and *cTnt-Cre;Mycn*^{loxp/loxp}
littermates. To extract DNA from PK-digested tissues, an equal volume of
phenol:chloroform (1:1) was added to the sample, vortexed for 10 sec, centrifuged at
13,000 rpm for 5 min, and the aqueous layer was kept. DNA was precipitated with 3
volumes of ice-cold 95% ethanol/ 0.12M NaAc, pH 4.8, at -20 °C overnight. The next
day, the sample was centrifuged at 13,000 rpm for 15 min at 4 °C, washed in 70%
ethanol, air-dried and then resuspended in 50 µl elution buffer (Qiagen). Recombination
of the *Mycn*^{loxp} conditional allele was detected using the forward primer, 5'-GTCGCGCT
AGTAAGAGCTGAGATC-3', and the reverse primers 5'-GGCACACACCTATA
ATCCCAGCTAG-3' and 5'-CACAGCTCTGGAAGGTGGGAGAAAGTTGAGC
GTCTCC-3 to detect the 350 bp product from the recombined allele or the 260 bp

product from the unrecombined allele.¹⁸ The conditions for the *Mycn* PCR are 95 °C for 2 min (1 cycle); 95 °C for 30 sec, 70 °C for 30 sec, 72 °C for 35 sec (28 cycles); 72 °C for 5 min. Primers used to detect *Smad4* were 5'-AAGAGCCACAGGTCAAGCAG-3' and 5'-GGGCAGCGTAGCATATAAGA-3'.⁵⁷ The Smad4 PCR program is: 95 °C for 2 min; 95 °C for 30 sec, 60.5°C for 1 min, 72 °C for 1 min (37 cycles); 72 °C for 5 min.

2.4 Western blot

Embryonic heart ventricles were dissected in PBS and stored at -80 °C. Samples of the same genotype and embryonic stage were pooled and homogenized in laemmli lysis buffer supplemented with protease inhibitor (Roche). Protein samples were quantified with Biorad DCTM Protein Assay according to manufacturer's instructions. Lysates were resolved by SDS-polyacrylamide gel electrophoresis (PAGE) on 10% tris-glycine gels and transferred to PVDF membranes. Membranes were blocked with 5% non-fat dry milk w/v in 0.1% Tween-20/TBS (TBST) and incubated overnight with primary antibodies at 4 °C. After three washes in TBST, membranes were incubated with secondary, HRP-conjugated antibodies for one hour at room temperature. Western blots were analyzed with ImageJ, public domain NIH Image program, developed at the U.S. National Institutes of Health and available on the Internet <http://imagej.nih.gov/ij/>.

2.5 Hematoxylin and Eosin staining

After dissection, embryos were fixed in 4% paraformaldehyde/PBS overnight at 4 °C, washed three times in 1XPBS solution, and dehydrated in ethanol washes: 70% for 1 hour at room temperature, 90% for 1 hour at room temperature, 95% overnight at 4 °C.

The following day, embryos were washed twice in 100% ethanol for a total of two hours at room temperature, cleared with Histo-Clear (National Diagnostics), incubated in a 50:50 Histo-Clear:paraffin wax (McCormick Scientific) solution for one hour at 70 °C, and put through a series of 3 one-hour washes in paraffin wax at 70 °C. Embedded embryos were sectioned 6.5-7 um on a Leica microtome and set onto Superfrost glass slides (Fisher). Slides were cleared in two 5 minute washes of Histo-Clear, and rehydrated in a series of ethanol washes (100% minutes x2, 95%, 90%, 70%, 50%) followed by a 3 minute wash in distilled water.

After rehydration, slides were placed in Mayer's Hematoxylin staining solution for 1 min, rinsed under running tap water for 10 min, incubated in Eosin B staining solution for 2 min, and then dehydrated in 95% and 100% ethanol washes. Slides were cleared in three Histo-Clear washes (1 min, 2 min and 3 min) and mounted with Permount (Fisher).

2.6 Immunohistochemistry (IHC) and immunofluorescence (IF) experiments.

After hydration, slides were put into pre-heated Antigen Retrieval Buffer (10mM citrate buffer, pH 6.0) in a 95 °C water bath for 25 min, and then allowed to cool to room temperature. IHC experiments were performed using Dako EnVision™+ System HRP (DAB) according to manufacturer's protocol. Slides were counterstained with Hematoxylin QS (Vector labs), washed in water, and dehydrated in 95% and 100% ethanol washes followed by three Histo-Clear washes. Slides were mounted with Permount (Fisher). A light microscope (Zeiss AxioCam MRc) with a Zeiss Axio Imager.A1 digital camera and AxioVision AC software were used for imaging. Images were processed with Adobe Photoshop.

For IF experiments, slides were rinsed with 1XTBS after antigen retrieval, permeabilized with TBST for 10 min, rinsed with 1XTBS and blocked in 5% FBS/TBST for 1 hour at room temperature, and then incubated with primary antibody overnight in a humidity chamber at 4°C. The next day, slides were washed with TBST, incubated with fluorescent secondary antibody in the dark for 1 hour at room temperature, washed with TBST in the dark, mounted with DAPI media (Vectashield) and sealed. Slides were protected from light and stored at 4°C until visualization with a Leica HC microscope and Metamorph 6.3R2 software. Images were processed with Adobe Photoshop.

2.7 Detection and quantification of proliferative cardiomyocytes in paraffin-embedded tissues

Cell proliferation experiments were performed on sagittal sections of paraffin-embedded E9.5 embryos using antibodies against phospho-Histone H3 (Upstate) to identify mitotic cells and DAPI to identify nuclei. Proliferation was calculated as total phospho-Histone H3 positive nuclei divided by total nuclei, and the result was expressed as the mean percentage of phospho-Histone H3 positive nuclei/ total number of nuclei. Cells were counted within 4 regions of the heart: the atrial myocardium, atrioventricular canal myocardium, cushion mesenchyme, and ventricular myocardium. Three embryos were analyzed from three different litters, and at least three sections were analyzed for each embryo. A two-tailed, unpaired student's *t* test was used to calculate P value, with $P < 0.05$ considered significant.

2.8 Detection and quantification of apoptotic cardiomyocytes in paraffin-embedded tissues with TUNEL assays

To visualize apoptotic cells, sagittal sections of paraffin-embedded embryos were subjected to terminal transferase-mediated dUTP-biotin nickend labeling (TUNEL) experiments with DeadEndTM Fluorometric TUNEL System (Promega), per manufacturer's protocol. Apoptosis was calculated as the number of positive cells divided by total cell number, and the result was expressed as the mean percentage of apoptotic cells/ total number of cells. Cells were counted within 4 regions of the heart: the atrial myocardium, atrioventricular canal myocardium, cushion mesenchymal cells, and ventricular myocardium. Three embryos were analyzed from three different litters, and at least three sections were analyzed for each embryo. A two-tailed, unpaired student's *t* test was used to calculate P value, with $P < 0.05$ considered significant.

2.9 Cardiomyocyte width measurement

Cardiomyocyte width was measured as previously described.⁵⁸ Briefly, immunostaining experiments were performed on sagittal sections of paraffin-embedded embryos using Wheat Germ Agglutinin Conjugate (WGA, Oregon Green 488, Invitrogen) to outline cells, primary antibodies for cardiac troponin T to distinguish cardiomyocytes, and DAPI mounting media to identify nuclei. Images from comparable regions of the ventricle wall were analyzed for each embryo. To measure cardiomyocyte width, we identified cross sections of cardiomyocytes that cut through the nuclei and measured width as the shortest axis through the middle of the nucleus. For each embryonic stage, 3 embryos were analyzed from 3 different litters, and at least three sections were analyzed for each embryo. A two-tailed, unpaired student's *t* test was used to calculate P value, with $P < 0.05$ considered significant. Results are expressed as mean +/- standard error.

3. Results

3.1 Conditional deletion of *Mycn* in the developing mouse myocardium causes embryonic lethality

To investigate the specific role of myocardial *Mycn* during heart development, *Mycn* was deleted from the myocardium by crossing male *cTnt-Cre;Mycn^{loxp/wt}* mice with *Mycn^{loxp/loxp}* females (Supplemental Figure 3).¹⁸ *cTnt-Cre* efficiently deletes target genes within the cardiomyocyte lineage between embryonic day 9.5 (E9.5) and E10.5.^{44, 54, 66-69} Deletion of *Mycn* was confirmed with PCR analyses on genomic DNA from E10.5 embryos (Figure 1A and 1B, Supplemental Figure 4). The unrecombined *Mycn^{loxp}* allele was reduced in *cTnt-Cre;Mycn^{loxp/loxp}* mutant hearts to approximately 25% of the controls (*Mycn^{loxp/loxp}*). The recombined *Mycn^{loxp}* allele was only detected in mutant hearts. MYCN reduction was confirmed at the protein level with Western blot experiments on proteins extracted from E10.5 and E11.5 ventricles (Figure 1C).

Embryos heterozygous for myocardial *Mycn* (*cTnt-Cre;Mycn^{loxp/wt}*) developed normally and were viable in adulthood. *cTnt-Cre;Mycn^{loxp/loxp}* mutants were recovered at the expected Mendelian frequency until E12.5, at which point they were no longer isolated alive (Figure 1C, Supplemental Table 1). Living embryos were defined by beating hearts. At E12.5, mutants had delayed development and internal hemorrhaging (Figure 1D). This result strongly suggests that deletion of *Mycn* from the myocardium disrupts mouse cardiogenesis, resulting in embryonic lethality due to cardioinsufficiency.

3.2 Myocardial *Mycn* is necessary for ventricular wall morphogenesis

Only living embryos were used for all following experiments. To examine cardiac defects, we performed detailed histological examination on E9.5-E11.5 embryos. Mutants displayed a thin-walled ventricle phenotype at E9.5, which progressively became more pronounced until E11.5, the latest stage of survival, when mutant ventricles were extremely thin and almost completely devoid of trabeculae (Figure 2A through 2F). Atrial myocardium was also noticeably thinner in mutant hearts at E10.5 and E11.5. Development of the cushions and outflow tract appeared to occur normally. Myocardial wall thickening and trabecular layer formation are necessary for proper ventricle contractility and embryo survival. Impaired myocardial wall morphogenesis due to myocardial *Mycn*-depletion likely caused cardiovascular insufficiency, resulting in embryonic lethality.

3.3 Reduced cardiomyocyte proliferation contributes to hypocellular myocardial wall in mutant ventricles

MYCN regulates gene expression programs in a tissue-specific manner to control cellular processes such as proliferation, survival, growth, and differentiation.^{16, 17} To determine if loss of myocardial MYCN altered proliferation, cardiomyocyte number and proliferation were measured at E9.5. A significant reduction in cardiomyocyte number was found in mutant ventricles ($p=0.001$, Figure 3A). Cardiomyocyte proliferation was measured using IF assays with antibodies for phospho-Histone H3, a marker for mitotic cells. Mutants had significantly reduced cardiomyocyte proliferation within the ventricles ($p=0.02$, Figure 3B through 3D).

To test if *Mycn* was necessary for cardiomyocyte survival during cardiogenesis, apoptosis was measured using TUNEL assays. No changes in apoptosis were detected in the mutant hearts from E9.5-E11.5 (Supplemental Figure 5). Therefore, decreased cardiomyocyte proliferation, but not increased apoptosis, contributed to the hypocellular myocardial wall phenotype in mutant ventricles.

3.4 *Mycn* is required for expression of cell cycle regulators CCND1, CCND2, and ID2 in the ventricular myocardium

MYC proteins are important activators of proliferation through their ability to upregulate cell cycle regulatory genes.^{16, 17} To better understand the mechanism whereby MYCN regulates cardiomyocyte proliferation during heart development, we measured the levels of MYCN targets cyclin D1 (CCND1), cyclin D2 (CCND2), and inhibitor of DNA binding 2 (ID2).^{27, 70-73} Proteins were extracted from embryonic ventricles and analyzed with Western blot experiments. All three proteins were significantly decreased in mutant ventricles from E10.5-E11.5 ($p < 0.001$, Figure 4A). These results were confirmed with IHC experiments (Figure 4B through 4G). These data indicate that MYCN promotes cardiomyocyte proliferation at least in part through regulation of *Ccnd1*, *Ccnd2*, and *Id2*.

3.5 Mutant hearts have smaller cardiomyocytes and decreased levels of p70(S6K), a regulator of cell growth

Through its regulation of the cell cycle, ribosome synthesis, and protein translation, MYCN ultimately enhances cell growth.^{16, 17} To investigate if *Mycn* was required for

cardiomyocyte growth, we measured cardiomyocyte width in cross-sections of control and mutant ventricle walls. Cardiomyocytes were stained with anti-cardiac troponin T (TNNT2, red) and cell membranes were labeled with anti-WGA (green, Figure 5A and 5B).⁷⁴ At E9.5 there was no measurable difference between control and mutant cardiomyocytes, but at E10.5 and E11.5 mutant cardiomyocytes were significantly smaller (Figure 5C). To further elucidate how MYCN mediates cardiomyocyte growth, we examined expression of ribosomal protein S6 kinase I (p70 S6K), a regulator of ribosome biogenesis and cell growth.⁷⁵⁻⁷⁹ Western blot experiments on E10.5-E11.5 ventricle proteins revealed that mutants had a noticeable reduction of p70(S6K) (Figure 5D). This was confirmed with IHC assays showing decreased p70(S6K) in E10.5 ventricular myocardium (Figure 5E and 5F). These data suggest that p70S6K is a regulatory target of MYCN in controlling cardiomyocyte size.

3.6 Aberrant cardiac myofilament gene expression in *Mycn*-depleted ventricles

During development, MYCN is necessary for maintaining certain cell types in a proliferative, undifferentiated state.^{18, 25} To determine if MYCN-depletion causes premature cardiomyocyte differentiation, we examined myofilament proteins that have unique expression patterns in embryonic, less differentiated myocardium versus adult, differentiated myocardium. There were no changes in embryonic proteins β -myosin heavy chain (β -MHC), α -smooth muscle actin (α -ACTA2), or α -skeletal actin (α -ACTA1) (Figure 6A). Likewise, mutants did not have increased expression of adult myocardial proteins, α -myosin heavy chain (α -MHC) or α -cardiac actin (α -ACTC1)

(Figure 6A).^{80, 81} While MYCN is necessary for cardiomyocyte proliferation, our results suggest that it is not necessary to maintain cardiomyocytes in an undifferentiated state.

We next analyzed the expression of myofilament proteins necessary for proper cardiomyocyte structure and function. Western blot experiments showed that E10.5-E11.5 mutant ventricles had significantly abnormal expression of myosin light chain 2A (MLC2A, $p < 0.05$), myosin light chain 2v (MLC2V, $p < 0.001$), and cardiac troponin I (TNNI3, $p < 0.001$) (Figure 6B). Loss of normal cardiac structural proteins may contribute to the abnormal myocardial wall formation in mutant hearts.

4. Discussion

MYCN has been established as an important cardiac transcription factor, yet its precise cardiogenic functions are unknown. Haploinsufficiency for *MYCN* causes Feingold syndrome, which is characterized in part by CHDs.^{19, 30, 36-39} Previous reports have shown that global loss of MYCN or severe reduction in MYCN during mouse embryogenesis causes varying and complex CHDs.²⁰⁻²³ In this study, we demonstrated that myocardial *Mycn* has fundamental roles during ventricle wall morphogenesis, including regulation of cardiomyocyte proliferation, size, and cardiac gene expression.

Myocardial-specific deletion of *Mycn* definitively established that the developing myocardium requires MYCN. Mutants invariably manifested hypocellular ventricle chambers with thin myocardial walls and disrupted trabeculation. Embryonic lethality occurred at E12.5, roughly the same time as global knockout mouse models and earlier than the hypomorphic mice.²⁰⁻²³ This result strongly suggests that defective

cardiogenesis due to loss of *Mycn* within the myocardium was the cause of lethality in earlier models.

In the present study, the mutant phenotype was restricted to myocardial wall morphogenesis. Other aspects of cardiac morphogenesis such as AVC cushion development and IVS initiation occurred normally, indicating that myocardial *Mycn* is not necessary for those aspects of cardiogenesis. Interestingly, *Mycn*-null mice displayed abnormal septal-valvulogenesis.²⁰ Based on the results from our current study, we speculate that endocardial, but not myocardial, MYCN is required for proper cushion formation. This idea is substantiated by recent work showing that *Mycn* is a downstream target of BMP2-induced TBX20 regulation in chicken endocardial cushion culture systems.⁸²

Ventricle wall morphogenesis relies heavily on tight regulation of cardiomyocyte proliferation (see Introduction). We found that *Mycn* is essential for maintaining normal cardiomyocyte number and proliferation within the ventricular myocardium as early as E9.5. Concomitant with decreased proliferation, the expression of cell cycle regulators *Ccnd1*, *Ccnd2*, and *Id2* was downregulated. TUNEL experiments revealed that apoptosis did not contribute to the hypocellular wall. This suggests that disrupted cardiomyocyte proliferation was the major cause of hypocellular ventricles in mutant hearts.

BMP10 is a critical regulator of cardiomyocyte proliferation during heart development.¹⁰ Since *Mycn* is a transcriptional target of BMP signaling in the heart we found it particularly interesting that *cTnt-Cre;Mycn^{loxp/loxp}* embryos and *BMP10*-null embryos had similar heart phenotypes.^{10, 44, 45} *BMP10*-null hearts also had thin ventricular walls with

reduced trabeculation, decreased cardiomyocyte proliferation, and no change in apoptosis.¹⁰ These data further support the idea that BMP signaling regulates cardiomyocyte proliferation via *Mycn* during myocardial wall morphogenesis.

Cell proliferation and growth are tightly coupled during development.⁷⁷ Since MYC proteins can promote cell growth we wanted to determine if loss of *Mycn* stunted cardiomyocyte growth in addition to reducing proliferation.^{16, 17} Indeed, loss of myocardial *Mycn* caused a significant size reduction in ventricular cardiomyocytes. This result is consistent with a previous study showing that ectopic expression of *cMyc* led to hypertrophy in adult hearts.⁸³ We further showed that MYCN mediates cardiomyocyte growth in part by maintaining proper expression of p70(S6K) within the ventricles. p70(S6K) is a well-known regulator of cell growth during development and in adult diseases such as cardiac hypertrophy.^{75-79, 84, 85} Given that CMYC is activated by hypertrophic stimuli, our results provide novel insight into a potential MYC-p70(S6K) mechanism during cardiac hypertrophy.^{16, 83, 86-89}

As ventricle development ensues, changes in morphogenesis are accompanied by alterations in cardiac gene expression.⁹⁰ Since myocardial wall development was disrupted in *cTnt-Cre;Mycn^{loxp/loxp}* mutant ventricles, we investigated the possibility that loss of myocardial *Mycn* altered normal cardiac structural gene expression. MYCN has been described as a “molecular switch” that serves to keep cells in a proliferative, undifferentiated state.²⁰ Normally, embryonic cardiomyocytes express *β-Mhc*, *α-Acta1*, and *α-Acta2*. As cardiomyocytes differentiate, embryonic gene expression is

downregulated while adult genes like *α -Mhc* and *Actc1* are upregulated.^{80, 81} Loss of *Mycn* did not result in decreased embryonic proteins or increased expression of adult proteins, revealing that it was not required to prevent premature terminal differentiation of embryonic cardiomyocytes. Indeed, mutant ventricles had decreased α -MHC, a protein that is normally enriched in more differentiated, working myocardium.⁹¹ Additionally, mutant ventricles had consistent reductions in chamber-specific sarcomere proteins MLC1V, MLC2A, and MLC2V, and increased levels of TNNI3.^{91, 92} These results indicate that *Mycn* is required for proper expression of a subset of cardiac genes during ventricular myocardial wall morphogenesis.

In summary, deletion of myocardial *Mycn* resulted in hypoplastic ventricle walls and embryonic lethality at midgestation, likely due to cardioinsufficiency. *Mycn* is necessary for myocardial wall morphogenesis through its regulation of cardiomyocyte proliferation, growth, and cardiac structural gene expression.

Funding

This work was supported by an American Heart Association predoctoral fellowship to Cristina Harmelink [09PRE2261138]; and a UAB faculty development grant to Kai Jiao.

Acknowledgements

We thank R. Eisenman, Fred Hutchinson Cancer Research Center, for providing the *Mycn^{loxP}* mice. MLC2A antibody was kindly provided by S. Kubalak at the University of South Carolina. The TNNT2 and β -tubulin antibodies developed by J. Jung-Ching Lin and M. Klymkowksy, respectively, were obtained from the Developmental Studies Hybridoma Bank developed under the auspices of the NICHD and maintained by The University of Iowa, Department of Biology, Iowa City, IA 52242. We thank members of the Jiao lab for insightful discussions, technical advice, and overall support of this project.

Conflict of Interest: None declared.

References

1. Christoffels VM, Habets PE, Franco D, Campione M, de Jong F, Lamers WH, *et al.* Chamber formation and morphogenesis in the developing mammalian heart. *Dev Biol* 2000;**223**:266-278.
2. Sedmera D, Pexieder T, Vuillemin M, Thompson RP, Anderson RH. Developmental patterning of the myocardium. *Anat Rec* 2000;**258**:319-337.
3. Christoffels VM, Hoogaars WM, Tessari A, Clout DE, Moorman AF, Campione M. T-box transcription factor Tbx2 represses differentiation and formation of the cardiac chambers. *Dev Dyn* 2004;**229**:763-770.
4. Evans SM, Yelon D, Conlon FL, Kirby ML. Myocardial lineage development. *Circ Res* 2010;**107**:1428-1444.
5. Dunwoodie SL. Combinatorial signaling in the heart orchestrates cardiac induction, lineage specification and chamber formation. *Semin Cell Dev Biol* 2007;**18**:54-66.
6. Srivastava D, Olson EN. A genetic blueprint for cardiac development. *Nature* 2000;**407**:221-226.
7. Gassmann M, Casagrande F, Orioli D, Simon H, Lai C, Klein R, *et al.* Aberrant neural and cardiac development in mice lacking the ErbB4 neuregulin receptor. *Nature* 1995;**378**:390-394.
8. Lee KF, Simon H, Chen H, Bates B, Hung MC, Hauser C. Requirement for neuregulin receptor erbB2 in neural and cardiac development. *Nature* 1995;**378**:394-398.
9. Meyer D, Birchmeier C. Multiple essential functions of neuregulin in development. *Nature* 1995;**378**:386-390.
10. Chen H, Shi S, Acosta L, Li W, Lu J, Bao S, *et al.* BMP10 is essential for maintaining cardiac growth during murine cardiogenesis. *Development* 2004;**131**:2219-2231.
11. Lai D, Liu X, Forrai A, Wolstein O, Michalick J, Ahmed I, *et al.* Neuregulin 1 sustains the gene regulatory network in both trabecular and nontrabecular myocardium. *Circ Res* 2010;**107**:715-727.
12. Pignatelli RH, McMahon CJ, Dreyer WJ, Denfield SW, Price J, Belmont JW, *et al.* Clinical characterization of left ventricular noncompaction in children: a relatively common form of cardiomyopathy. *Circulation* 2003;**108**:2672-2678.
13. Weiford BC, Subbarao VD, Mulhern KM. Noncompaction of the ventricular myocardium. *Circulation* 2004;**109**:2965-2971.
14. Xing Y, Ichida F, Matsuoka T, Isobe T, Ikemoto Y, Higaki T, *et al.* Genetic analysis in patients with left ventricular noncompaction and evidence for genetic heterogeneity. *Mol Genet Metab* 2006;**88**:71-77.
15. Klaassen S, Probst S, Oechslin E, Gerull B, Krings G, Schuler P, *et al.* Mutations in sarcomere protein genes in left ventricular noncompaction. *Circulation* 2008;**117**:2893-2901.
16. Hurlin PJ. N-Myc functions in transcription and development. *Birth Defects Res C Embryo Today* 2005;**75**:340-352.
17. Adhikary S, Eilers M. Transcriptional regulation and transformation by Myc proteins. *Nat Rev Mol Cell Biol* 2005;**6**:635-645.
18. Knoepfler PS, Cheng PF, Eisenman RN. N-myc is essential during neurogenesis for the rapid expansion of progenitor cell populations and the inhibition of neuronal differentiation. *Genes Dev* 2002;**16**:2699-2712.

19. Brunner HG, Winter RM. Autosomal dominant inheritance of abnormalities of the hands and feet with short palpebral fissures, variable microcephaly with learning disability, and oesophageal/duodenal atresia. *J Med Genet* 1991;**28**:389-394.
20. Charron J, Malynn BA, Fisher P, Stewart V, Jeannotte L, Goff SP, *et al.* Embryonic lethality in mice homozygous for a targeted disruption of the N-myc gene. *Genes Dev* 1992;**6**:2248-2257.
21. Moens CB, Stanton BR, Parada LF, Rossant J. Defects in heart and lung development in compound heterozygotes for two different targeted mutations at the N-myc locus. *Development* 1993;**119**:485-499.
22. Sawai S, Shimono A, Wakamatsu Y, Palmes C, Hanaoka K, Kondoh H. Defects of embryonic organogenesis resulting from targeted disruption of the N-myc gene in the mouse. *Development* 1993;**117**:1445-1455.
23. Stanton BR, Perkins AS, Tessarollo L, Sassoon DA, Parada LF. Loss of N-myc function results in embryonic lethality and failure of the epithelial component of the embryo to develop. *Genes Dev* 1992;**6**:2235-2247.
24. Moens CB, Auerbach AB, Conlon RA, Joyner AL, Rossant J. A targeted mutation reveals a role for N-myc in branching morphogenesis in the embryonic mouse lung. *Genes Dev* 1992;**6**:691-704.
25. Okubo T, Knoepfler PS, Eisenman RN, Hogan BL. Nmyc plays an essential role during lung development as a dosage-sensitive regulator of progenitor cell proliferation and differentiation. *Development* 2005;**132**:1363-1374.
26. Ota S, Zhou ZQ, Keene DR, Knoepfler P, Hurlin PJ. Activities of N-Myc in the developing limb link control of skeletal size with digit separation. *Development* 2007;**134**:1583-1592.
27. Kenney AM, Cole MD, Rowitch DH. Nmyc upregulation by sonic hedgehog signaling promotes proliferation in developing cerebellar granule neuron precursors. *Development* 2003;**130**:15-28.
28. Kenney AM, Widlund HR, Rowitch DH. Hedgehog and PI-3 kinase signaling converge on Nmyc1 to promote cell cycle progression in cerebellar neuronal precursors. *Development* 2004;**131**:217-228.
29. Strieder V, Lutz W. Regulation of N-myc expression in development and disease. *Cancer Lett* 2002;**180**:107-119.
30. van Bokhoven H, Celli J, van Reeuwijk J, Rinne T, Glaudemans B, van Beusekom E, *et al.* MYCN haploinsufficiency is associated with reduced brain size and intestinal atresias in Feingold syndrome. *Nat Genet* 2005;**37**:465-467.
31. Hurlin PJ, Quéva C, Eisenman RN. Mnt, a novel Max-interacting protein is coexpressed with Myc in proliferating cells and mediates repression at Myc binding sites. *Genes Dev* 1997;**11**:44-58.
32. Peukert K, Staller P, Schneider A, Carmichael G, Hänel F, Eilers M. An alternative pathway for gene regulation by Myc. *EMBO J* 1997;**16**:5672-5686.
33. Blackwell TK, Kretzner L, Blackwood EM, Eisenman RN, Weintraub H. Sequence-specific DNA binding by the c-Myc protein. *Science* 1990;**250**:1149-1151.
34. Amati B, Dalton S, Brooks MW, Littlewood TD, Evan GI, Land H. Transcriptional activation by the human c-Myc oncoprotein in yeast requires interaction with Max. *Nature* 1992;**359**:423-426.
35. Charron J, Gagnon JF, Cadrin-Girard JF. Identification of N-myc regulatory regions involved in embryonic expression. *Pediatr Res* 2002;**51**:48-56.

36. Geneviève D, de Pontual L, Amiel J, Sarnacki S, Lyonnet S. An overview of isolated and syndromic oesophageal atresia. *Clin Genet* 2007;**71**:392-399.
37. Celli J, van Bokhoven H, Brunner HG. Feingold syndrome: clinical review and genetic mapping. *Am J Med Genet A* 2003;**122A**:294-300.
38. Büttiker V, Wojtulewicz J, Wilson M. Imperforate anus in Feingold syndrome. *Am J Med Genet* 2000;**92**:166-169.
39. Piersall LD, Dowton SB, McAlister WH, Waggoner DJ. Vertebral anomalies in a new family with ODED syndrome. *Clin Genet* 2000;**57**:444-448.
40. Marcelis CL, Hol FA, Graham GE, Rieu PN, Kellermayer R, Meijer RP, et al. Genotype-phenotype correlations in MYCN-related Feingold syndrome. *Hum Mutat* 2008;**29**:1125-1132.
41. Domínguez-Frutos E, López-Hernández I, Vendrell V, Neves J, Gallozzi M, Gutsche K, et al. N-myc Controls Proliferation, Morphogenesis, and Patterning of the Inner Ear. *J Neurosci* 2011;**31**:7178-7189.
42. Kopecky B, Santi P, Johnson S, Schmitz H, Fritzscht B. Conditional deletion of N-Myc disrupts neurosensory and non-sensory development of the ear. *Dev Dyn* 2011;**240**:1373-1390.
43. Giroux S, Charron J. Defective development of the embryonic liver in N-myc-deficient mice. *Dev Biol* 1998;**195**:16-28.
44. Song L, Yan W, Chen X, Deng CX, Wang Q, Jiao K. Myocardial smad4 is essential for cardiogenesis in mouse embryos. *Circ Res* 2007;**101**:277-285.
45. Cai CL, Zhou W, Yang L, Bu L, Qyang Y, Zhang X, et al. T-box genes coordinate regional rates of proliferation and regional specification during cardiogenesis. *Development* 2005;**132**:2475-2487.
46. Azhar M, Schultz JJ, Grupp I, Dorn GW, Meneton P, Molin DG, et al. Transforming growth factor beta in cardiovascular development and function. *Cytokine Growth Factor Rev* 2003;**14**:391-407.
47. Barnett JV, Desgrosellier JS. Early events in valvulogenesis: a signaling perspective. *Birth Defects Res C Embryo Today* 2003;**69**:58-72.
48. Délot EC, Bahamonde ME, Zhao M, Lyons KM. BMP signaling is required for septation of the outflow tract of the mammalian heart. *Development* 2003;**130**:209-220.
49. Délot EC. Control of endocardial cushion and cardiac valve maturation by BMP signaling pathways. *Mol Genet Metab* 2003;**80**:27-35.
50. Waite KA, Eng C. From developmental disorder to heritable cancer: it's all in the BMP/TGF-beta family. *Nat Rev Genet* 2003;**4**:763-773.
51. Judge DP, Dietz HC. Marfan's syndrome. *Lancet* 2005;**366**:1965-1976.
52. Loeyls BL, Schwarze U, Holm T, Callewaert BL, Thomas GH, Pannu H, et al. Aneurysm syndromes caused by mutations in the TGF-beta receptor. *N Engl J Med* 2006;**355**:788-798.
53. Song L, Fässler R, Mishina Y, Jiao K, Baldwin HS. Essential functions of Alk3 during AV cushion morphogenesis in mouse embryonic hearts. *Dev Biol* 2007;**301**:276-286.
54. Jiao K, Kulesa H, Tompkins K, Zhou Y, Batts L, Baldwin HS, et al. An essential role of Bmp4 in the atrioventricular septation of the mouse heart. *Genes Dev* 2003;**17**:2362-2367.
55. McFadden DG, Olson EN. Heart development: learning from mistakes. *Curr Opin Genet Dev* 2002;**12**:328-335.
56. Srivastava D. Building a heart: implications for congenital heart disease. *J Nucl Cardiol* 2003;**10**:63-70.

57. Zaffran S, Frasch M. Early signals in cardiac development. *Circ Res* 2002;**91**:457-469.
58. Gaussin V, Morley GE, Cox L, Zwijsen A, Vance KM, Emile L, *et al.* Alk3/Bmpr1a receptor is required for development of the atrioventricular canal into valves and annulus fibrosus. *Circ Res* 2005;**97**:219-226.
59. Gaussin V, Van de Putte T, Mishina Y, Hanks MC, Zwijsen A, Huylebroeck D, *et al.* Endocardial cushion and myocardial defects after cardiac myocyte-specific conditional deletion of the bone morphogenetic protein receptor ALK3. *Proc Natl Acad Sci U S A* 2002;**99**:2878-2883.
60. Sugi Y, Yamamura H, Okagawa H, Markwald RR. Bone morphogenetic protein-2 can mediate myocardial regulation of atrioventricular cushion mesenchymal cell formation in mice. *Dev Biol* 2004;**269**:505-518.
61. Ma L, Lu MF, Schwartz RJ, Martin JF. Bmp2 is essential for cardiac cushion epithelial-mesenchymal transition and myocardial patterning. *Development* 2005;**132**:5601-5611.
62. Rivera-Feliciano J, Tabin CJ. Bmp2 instructs cardiac progenitors to form the heart-valve-inducing field. *Dev Biol* 2006;**295**:580-588.
63. Wang J, Sridurongrit S, Dudas M, Thomas P, Nagy A, Schneider MD, *et al.* Atrioventricular cushion transformation is mediated by ALK2 in the developing mouse heart. *Dev Biol* 2005;**286**:299-310.
64. Park C, Lavine K, Mishina Y, Deng CX, Ornitz DM, Choi K. Bone morphogenetic protein receptor 1A signaling is dispensable for hematopoietic development but essential for vessel and atrioventricular endocardial cushion formation. *Development* 2006;**133**:3473-3484.
65. Desgrosellier JS, Mundell NA, McDonnell MA, Moses HL, Barnett JV. Activin receptor-like kinase 2 and Smad6 regulate epithelial-mesenchymal transformation during cardiac valve formation. *Dev Biol* 2005;**280**:201-210.
66. Wang Q, Sigmund CD, Lin JJ. Identification of cis elements in the cardiac troponin T gene conferring specific expression in cardiac muscle of transgenic mice. *Circ Res* 2000;**86**:478-484.
67. Wang Q, Reiter RS, Huang QQ, Jin JP, Lin JJ. Comparative studies on the expression patterns of three troponin T genes during mouse development. *Anat Rec* 2001;**263**:72-84.
68. Chen JW, Zhou B, Yu QC, Shin SJ, Jiao K, Schneider MD, *et al.* Cardiomyocyte-specific deletion of the coxsackievirus and adenovirus receptor results in hyperplasia of the embryonic left ventricle and abnormalities of sinuatrial valves. *Circ Res* 2006;**98**:923-930.
69. Ilagan R, Abu-Issa R, Brown D, Yang YP, Jiao K, Schwartz RJ, *et al.* Fgf8 is required for anterior heart field development. *Development* 2006;**133**:2435-2445.
70. Bouchard C, Thieke K, Maier A, Saffrich R, Hanley-Hyde J, Ansorge W, *et al.* Direct induction of cyclin D2 by Myc contributes to cell cycle progression and sequestration of p27. *EMBO J* 1999;**18**:5321-5333.
71. Bouchard C, Dittrich O, Kiermaier A, Dohmann K, Menkel A, Eilers M, *et al.* Regulation of cyclin D2 gene expression by the Myc/Max/Mad network: Myc-dependent TRRAP recruitment and histone acetylation at the cyclin D2 promoter. *Genes Dev* 2001;**15**:2042-2047.
72. Lasorella A, Boldrini R, Dominici C, Donfrancesco A, Yokota Y, Inserra A, *et al.* Id2 is critical for cellular proliferation and is the oncogenic effector of N-myc in human neuroblastoma. *Cancer Res* 2002;**62**:301-306.

73. Lasorella A, Nosedà M, Beyna M, Yokota Y, Iavarone A. Id2 is a retinoblastoma protein target and mediates signalling by Myc oncoproteins. *Nature* 2000;**407**:592-598.
74. Condorelli G, Drusco A, Stassi G, Bellacosa A, Roncarati R, Iaccarino G, *et al.* Akt induces enhanced myocardial contractility and cell size in vivo in transgenic mice. *Proc Natl Acad Sci U S A* 2002;**99**:12333-12338.
75. Shima H, Pende M, Chen Y, Fumagalli S, Thomas G, Kozma SC. Disruption of the p70(s6k)/p85(s6k) gene reveals a small mouse phenotype and a new functional S6 kinase. *EMBO J* 1998;**17**:6649-6659.
76. Fingar DC, Salama S, Tsou C, Harlow E, Blenis J. Mammalian cell size is controlled by mTOR and its downstream targets S6K1 and 4EBP1/eIF4E. *Genes Dev* 2002;**16**:1472-1487.
77. Ahuja P, Sdek P, MacLellan WR. Cardiac myocyte cell cycle control in development, disease, and regeneration. *Physiol Rev* 2007;**87**:521-544.
78. Crackower MA, Oudit GY, Kozieradzki I, Sarao R, Sun H, Sasaki T, *et al.* Regulation of myocardial contractility and cell size by distinct PI3K-PTEN signaling pathways. *Cell* 2002;**110**:737-749.
79. Shioi T, Kang PM, Douglas PS, Hampe J, Yballe CM, Lawitts J, *et al.* The conserved phosphoinositide 3-kinase pathway determines heart size in mice. *EMBO J* 2000;**19**:2537-2548.
80. Morkin E. Control of cardiac myosin heavy chain gene expression. *Microsc Res Tech* 2000;**50**:522-531.
81. Clément S, Stouffs M, Bettiol E, Kampf S, Krause KH, Chaponnier C, *et al.* Expression and function of alpha-smooth muscle actin during embryonic-stem-cell-derived cardiomyocyte differentiation. *J Cell Sci* 2007;**120**:229-238.
82. Shelton EL, Yutzey KE. Tbx20 regulation of endocardial cushion cell proliferation and extracellular matrix gene expression. *Dev Biol* 2007;**302**:376-388.
83. Xiao G, Mao S, Baumgarten G, Serrano J, Jordan MC, Roos KP, *et al.* Inducible activation of c-Myc in adult myocardium in vivo provokes cardiac myocyte hypertrophy and reactivation of DNA synthesis. *Circ Res* 2001;**89**:1122-1129.
84. Pereira AH, Clemente CF, Cardoso AC, Theizen TH, Rocco SA, Judice CC, *et al.* MEF2C silencing attenuates load-induced left ventricular hypertrophy by modulating mTOR/S6K pathway in mice. *PLoS One* 2009;**4**:e8472.
85. Takano H, Komuro I, Zou Y, Kudoh S, Yamazaki T, Yazaki Y. Activation of p70 S6 protein kinase is necessary for angiotensin II-induced hypertrophy in neonatal rat cardiac myocytes. *FEBS Lett* 1996;**379**:255-259.
86. Malynn BA, de Alboran IM, O'Hagan RC, Bronson R, Davidson L, DePinho RA, *et al.* N-myc can functionally replace c-myc in murine development, cellular growth, and differentiation. *Genes Dev* 2000;**14**:1390-1399.
87. Kim S, Li Q, Dang CV, Lee LA. Induction of ribosomal genes and hepatocyte hypertrophy by adenovirus-mediated expression of c-Myc in vivo. *Proc Natl Acad Sci U S A* 2000;**97**:11198-11202.
88. Izumo S, Nadal-Ginard B, Mahdavi V. Protooncogene induction and reprogramming of cardiac gene expression produced by pressure overload. *Proc Natl Acad Sci U S A* 1988;**85**:339-343.
89. Green NK, Franklyn JA, Ohanian V, Heagerty AM, Gammage MD. Transfection of cardiac muscle: effects of overexpression of c-myc and c-fos proto-oncogene proteins in primary cultures of neonatal rat cardiac myocytes. *Clin Sci (Lond)* 1997;**92**:181-188.

90. Moorman AF, Christoffels VM. Cardiac chamber formation: development, genes, and evolution. *Physiol Rev* 2003;**83**:1223-1267.
91. Franco D, Lamers WH, Moorman AF. Patterns of expression in the developing myocardium: towards a morphologically integrated transcriptional model. *Cardiovasc Res* 1998;**38**:25-53.
92. O'Brien TX, Lee KJ, Chien KR. Positional specification of ventricular myosin light chain 2 expression in the primitive murine heart tube. *Proc Natl Acad Sci U S A* 1993;**90**:5157-5161.
93. Thomas WD, Raif A, Hansford L, Marshall G. N-myc transcription molecule and oncoprotein. *Int J Biochem Cell Biol* 2004;**36**:771-775.

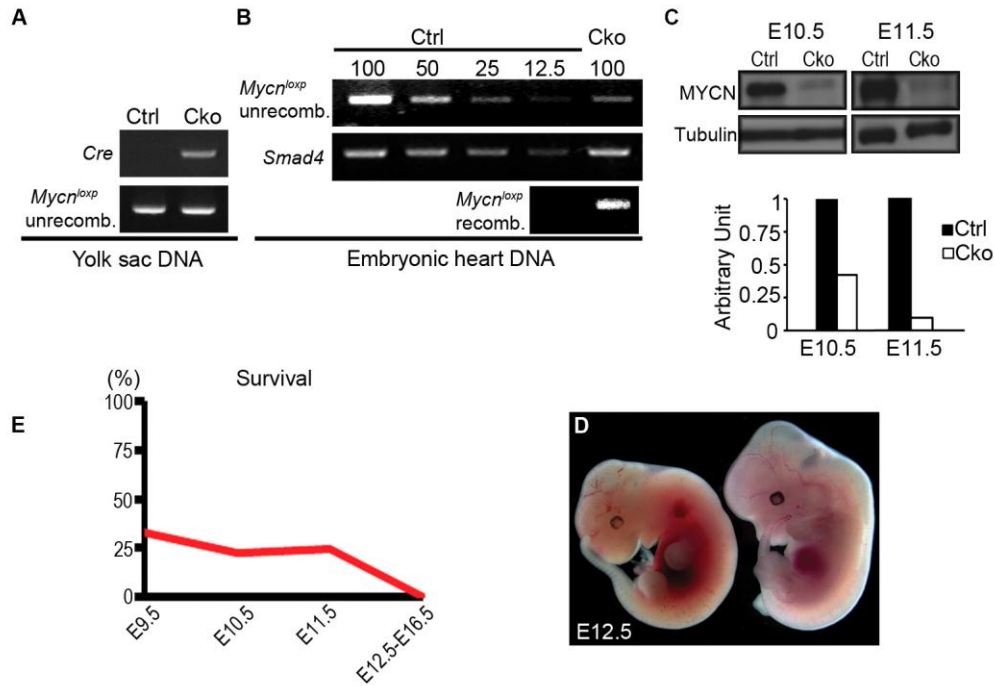


Figure 1. Conditional deletion of *Mycn* from the myocardium caused embryonic lethality. A, PCR analyses on genomic DNA from embryo yolk sacs with primers for *Cre* and unrecombined *Mycn^{loxp}*. B, Genomic DNA from control (*Mycn^{loxp/loxp}*) and mutant (*cTnt-Cre;Mycn^{loxp/loxp}*) hearts was analyzed with semiquantitative PCR using primers for unrecombined *Mycn^{loxp}* (top). Lanes 1-4 are control samples with 100, 50, 25 and 12.5 ng of input DNA. Lane 5 is mutant sample with 100ng of input DNA. The unrecombined *Mycn^{loxp}* allele was reduced in mutant hearts to roughly 25% of the control. *Smad4* primers were used as a loading control (middle). Bottom, heart DNA was analyzed with PCR using primers for the recombined *Mycn^{loxp}* allele, which was only in mutant hearts. C, Western blot analyses on ventricle proteins confirmed loss of MYCN. Samples were pooled from at least five embryos for each experiment. β -tubulin was the loading control. D, No living mutants were recovered after E11.5. At least nine litters were collected at each stage. E, A dead mutant embryo at E12.5 (left) was underdeveloped and displayed hemorrhaging, compared to a littermate control (right). Ctrl, control; Cko, conditional knockout.

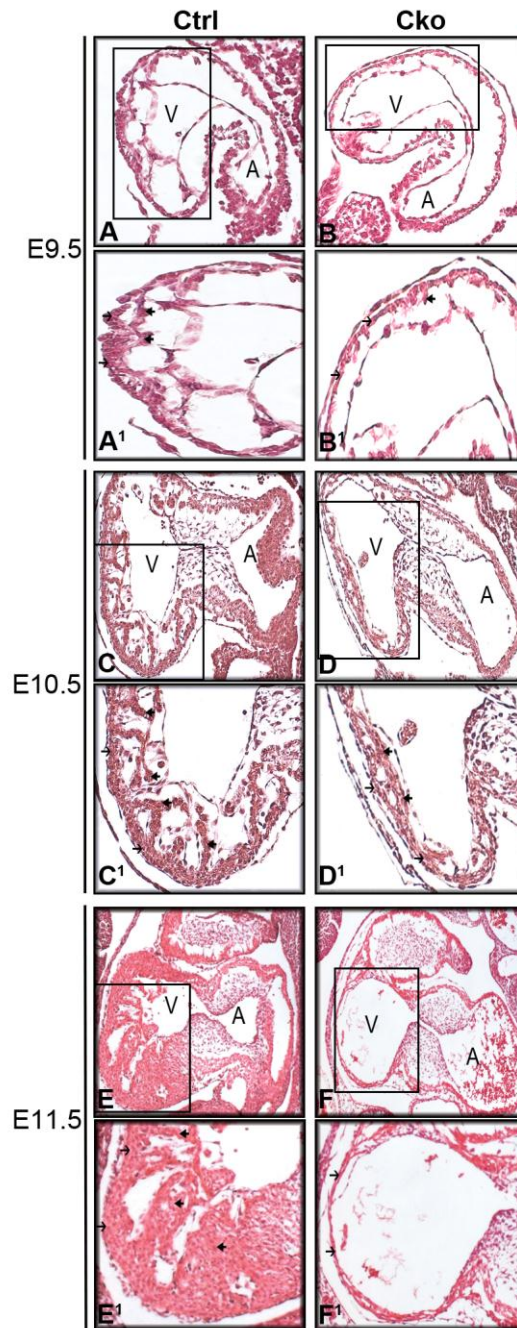


Figure 2. Histological analyses of *cTnt-Cre;Mycn^{loxp/loxp}* hearts revealed thin myocardial walls. A-F, Hematoxylin/eosin-stained sagittal sections of embryos from E9.5 (A-B¹), E10.5 (C-D¹), and E11.5 (E-F¹). A¹-F¹ correspond to boxed regions of A-F, respectively. Open arrows point to ventricular myocardial wall. Closed arrows point to trabeculae. Ctrl, control; Cko, conditional knockout; A, atria; V, ventricle.

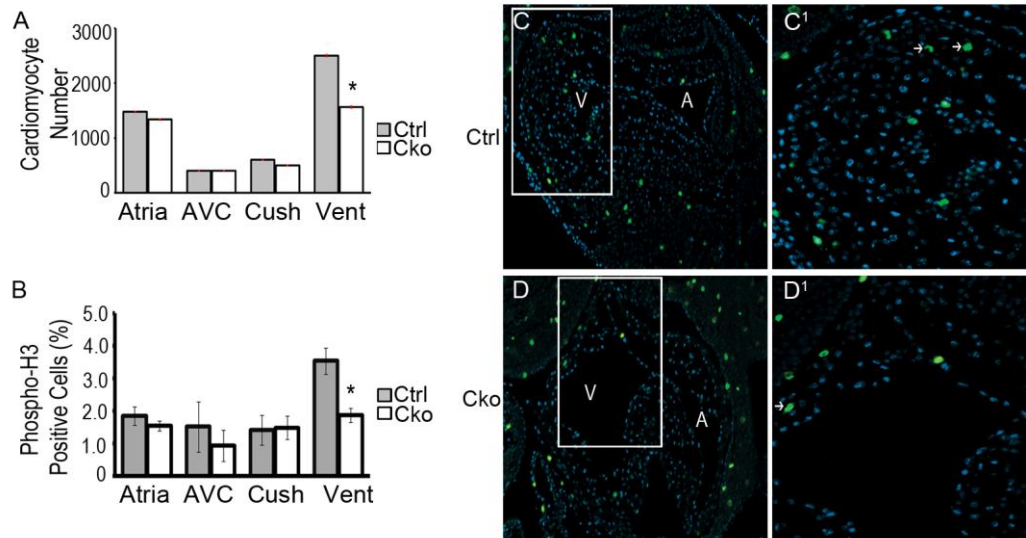


Figure. 3. Analyses of cardiomyocyte number and proliferation at E9.5. A, Sagittal sections were stained with DAPI and total nuclei were counted within cushion mesenchyme and myocardium of the atria, AVC, and ventricles. Three embryos were analyzed from three litters, and at least three sections were analyzed per embryo. Mutant ventricles had a significant decrease in cardiomyocyte number (Student's *t* test, $p=0.001$). B, Proliferation experiments were performed with phospho-Histone H3 (pH3) antibodies to identify mitotic cells and DAPI to identify nuclei. Cells were counted within cushion mesenchyme and myocardium of the atria, AVC, and ventricles. Proliferation was calculated as total pH3-positive nuclei/total nuclei. Data were shown as mean \pm Standard Error. Three embryos were analyzed from three litters, and at least three sections were analyzed for each embryo. Cardiomyocyte proliferation was significantly decreased in mutant ventricles (Student's *t* test, $p<0.02$). C-D, Representative images from immunostaining on control (C-C¹) and mutant (D-D¹) embryos. C¹ and D¹ correspond to boxed regions of C and D. Arrows point to examples of pH3-positive cardiomyocytes (green). Nuclei were stained with DAPI (blue). Ctrl, control; Cko, conditional knockout; A, atria; AVC, atrioventricular canal; Cush, endocardial cushion; V or Vent, ventricle; *, statistically significant.

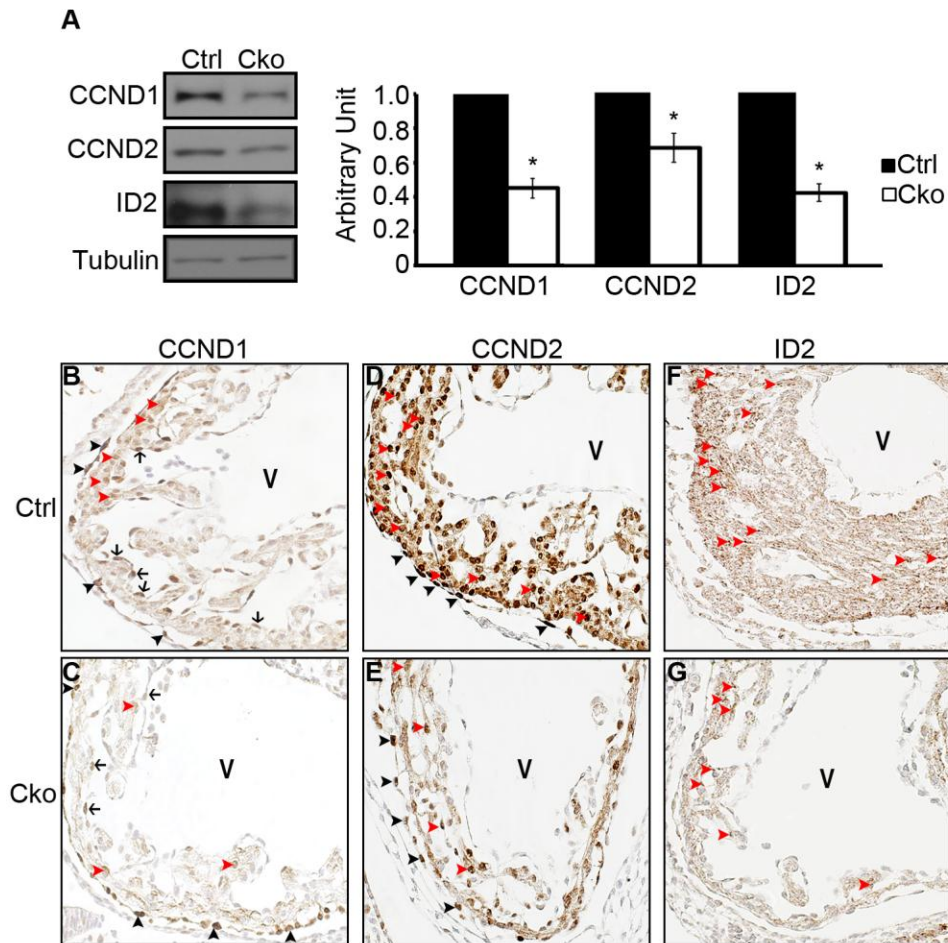


Figure 4. Mutant ventricular myocardium had reduced expression of CCND1, CCND2, and ID2. A, Western blot experiments on E10.5-E11.5 ventricle proteins showed significantly decreased expression of cell cycle regulators (Student's *t* test, $p < 0.001$). β -tubulin was the loading control. Proteins were pooled from at least five ventricles per experiment. Experiments were repeated at least three times. B-G, Immunohistochemistry for CCND1, CCND2, and ID2 on controls (B, D, F) and mutants (C, E, G) confirmed decreased expression within the mutant ventricular myocardium. Red arrowheads point to examples of CCND1-, CCND2-, or ID2-positive cardiomyocytes, black arrows point to examples of CCND1-positive endocardial cells, and black arrowheads point to examples of positive epicardial cells. CCND1 expression was also reduced in mutant endocardium; this is likely secondary to the myocardial defect, as *cTnt-Cre* specifically inactivates target genes in myocardial cells. Epicardial expression of CCND1 and CCND2 was not altered. Ctrl, control; Cko, conditional knockout; V, ventricle; *, statistically significant.

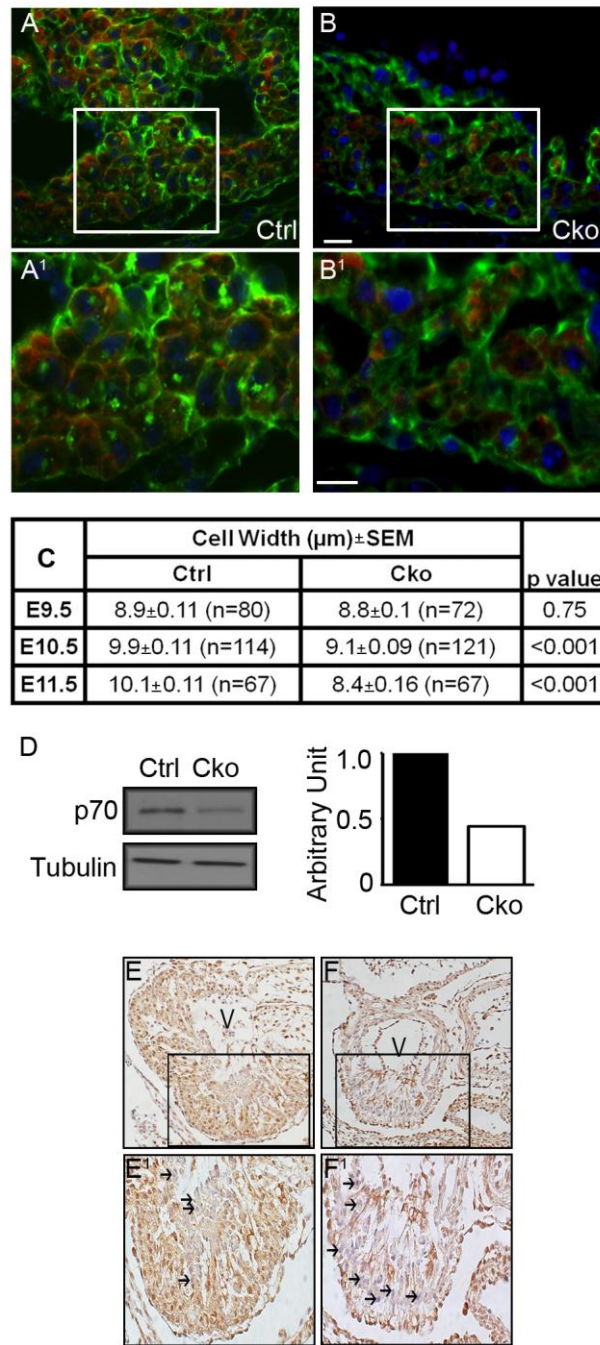


Figure 5. Measurement of cardiomyocyte size. A-B, Representative sections of E10.5 control (A-A¹) and mutant (B-B¹) ventricle myocardium. A¹ and B¹ correspond to boxed regions of A and B. Cardiomyocytes were labeled with anti-TNNT2 (red), cell membranes were labeled with WGA (green), and nuclei were labeled with DAPI (blue). Bar=10 μm . C, Cardiomyocyte width, the shortest axis through the middle of the nucleus, was measured in comparable regions of E9.5-E11.5 ventricle myocardium. Mutant

cardiomyocytes were significantly smaller at E10.5 and E11.5 (Student's *t* test, $p < 0.001$.) For each stage, three embryos were analyzed from three different litters, and at least three sections were analyzed per embryo. Results are expressed as mean \pm standard error. D. Western blot assays on E10.5-E11.5 ventricle proteins revealed a decrease in p70(S6K). Protein samples were pooled from at least five ventricles. β -tubulin was the loading control. E-F, Loss of p70(S6K) was confirmed with immunohistochemistry on E10.5 control (E-E¹) and mutant (F-F¹) ventricles. E¹ and F¹ correspond to boxed areas of E and F. Arrows point to examples of p70(S6K)-negative cardiomyocytes. Ctrl, control; Cko, conditional knockout; V, ventricle.

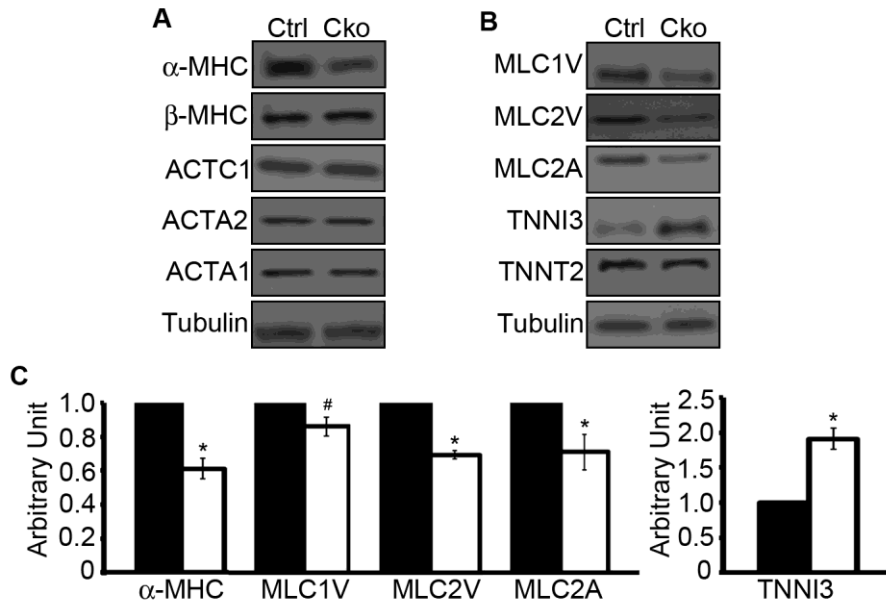
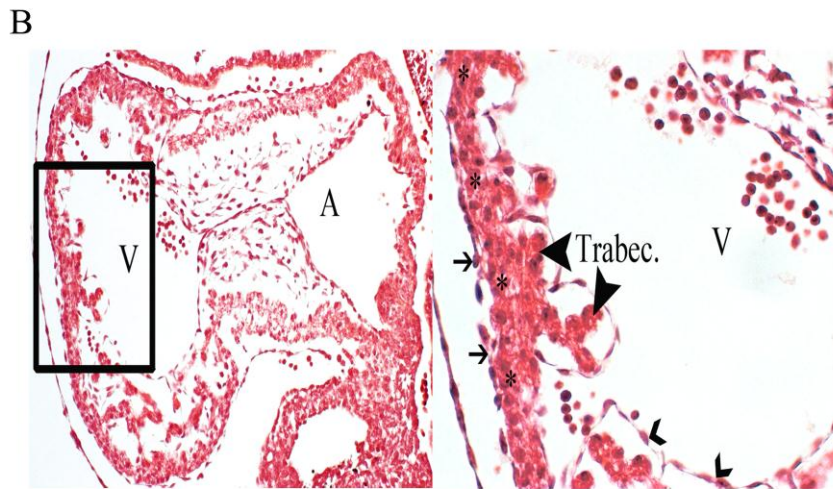
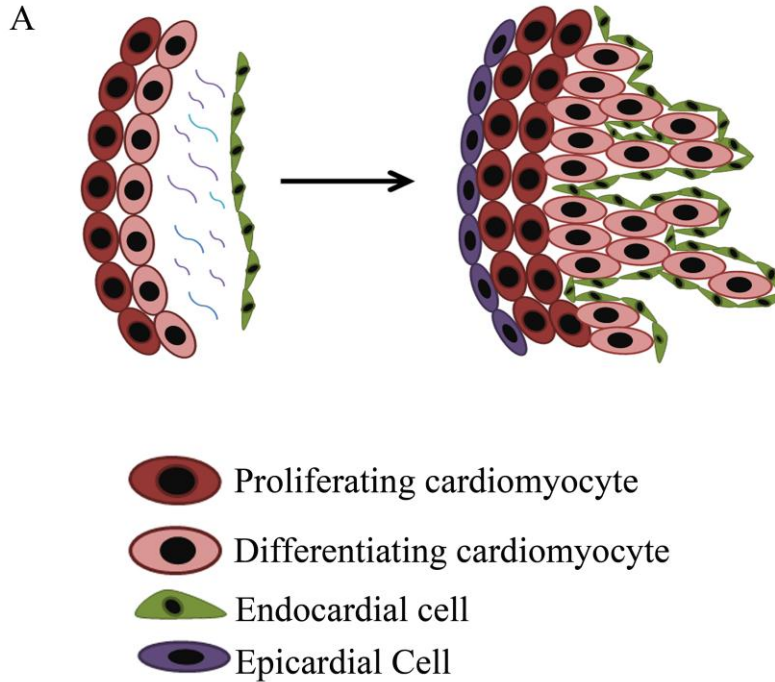
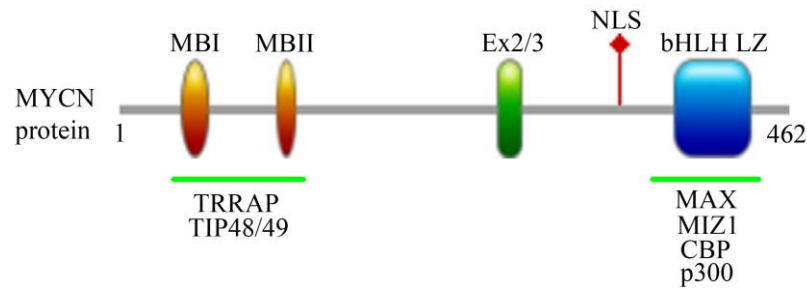


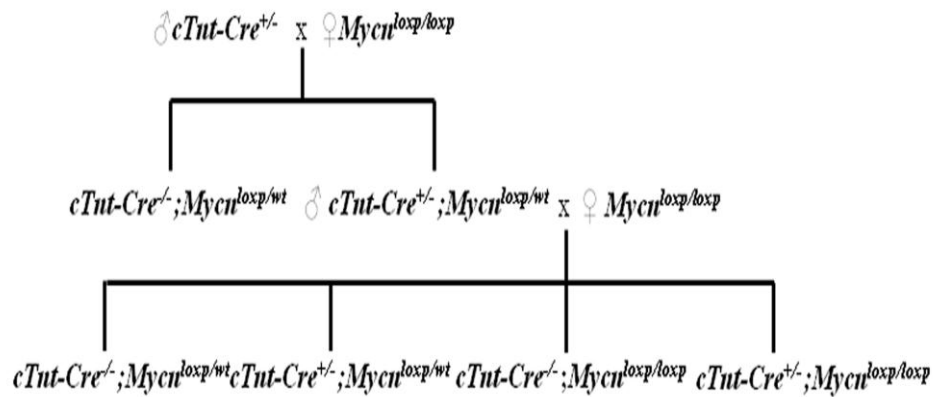
Figure 6. Examination of myofilament proteins. A, Western blot analyses on E10.5-E11.5 ventricle proteins showed that mutant cardiomyocytes did not prematurely differentiate. Loading control was β -tubulin. Ventricle proteins were pooled from at least five embryos. B, Western blot experiments on E10.5-E11.5 ventricle proteins showed that mutants had aberrant expression of MLC1V, MLC2A, MLC2V, and TNNI3. β -tubulin was the loading control. Proteins were pooled from at least five ventricles per experiment. C, Quantification of Western blot results revealed significant changes in α -MHC ($p < 0.005$), MLC2A ($p < 0.05$), MLC2V ($p < 0.001$) and TNNI3 ($p < 0.001$). Reduction of MLC1V also occurred, but it did not reach statistical significance ($p = 0.07$). Ctrl, control; Cko, conditional knockout; *, statistically significant.



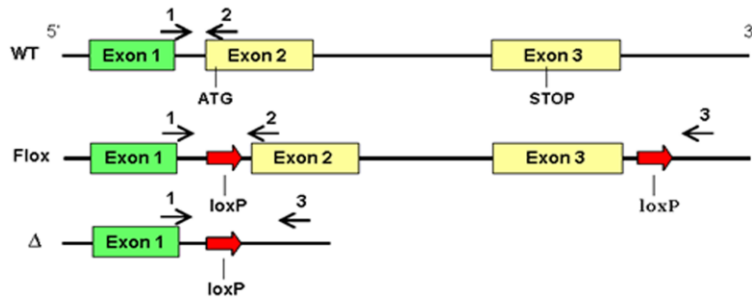
Supplemental Figure 1. Myocardial wall formation. A. Left: cardiomyocytes on the outer edge of the ventricular chamber (red) are highly proliferative. They contribute to the expanding myocardial wall. Cardiomyocytes on the luminal aspect of the ventricle (pink) lose their proliferative capacity and differentiate. The myocardium is separated from the endocardium (green) by the extracellular matrix (ECM) called the cardiac jelly. Right: differentiated cardiomyocytes form muscular projections call trabeculae, which provide contractile force for the developing heart. The epicardium (purple) envelops the heart. B. Example of an E10.5 wild type mouse heart. On the left is a hematoxylin/eosin stained sagittal section. The boxed region corresponds to the magnified region shown on the right. A, atria; V, ventricle; filled arrowheads point to trabecular myocardium; arrowheads point to endocardium; open arrows point to epicardium.



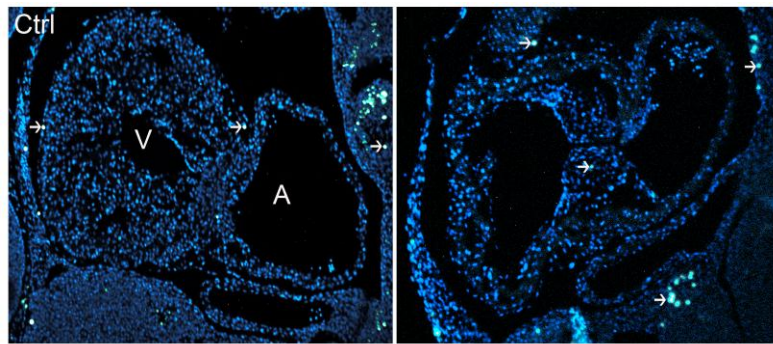
Supplemental Figure 2. The mouse MYCN protein. MYCN is 462 amino acids (aa). The N-terminal contains conserved MYC BOXES (MBI, 44-63aa, and MBII, 110-123aa) that are involved in MYCN turnover and transcription regulation activities. MYCN recruits cofactors involved in chromatin modification through MBII such as TRRAP, a component of complexes that have histone acetyltransferase activity. MBII is also necessary for interactions with TIP48 and TIP49, which are components of ATP-dependent chromatin remodeling complexes. The exon 2 and exon 3 boundary (Ex2/3) is at 262-278 aa. A nuclear localization signal (NLS) is located at 345 aa. The C-terminal region of the MYCN protein contains the basic helix-loop-helix leucine zipper (bHLH-LZ) domain from 384-436 aa. This domain mediates MYCN and MAX interactions in the HLH-LZ region. Formation of the MYCN-MAX heterodimer is required for MYCN transcription activation, and the MYCN-MIZ1 interaction is associated with transcription repression. MYCN binds DNA with the basic amino acids immediately N-terminal to the HLH-LZ domains. It preferentially binds the E-box sequence CACGTG *in vitro*, but can bind other sequences. Additionally, the C-terminal region binds with cofactors as well. Histone acetyltransferases cAMP-response-element-binding protein (CBP) and p300 interact with MYCN's C-terminus.^{16, 17, 93} Protein interacting regions are shown with a green bar. MB, MYC boxes; Ex2/3, boundary of exons 2 and 3; NLS, nuclear localization signal; bHLH-LZ, basic helix-loop-helix leucine zipper; TRRAP, Transformation/transcription domain-associated protein; TIP48 and 49, TATA box-binding protein interacting proteins. The MYCN protein schematic was created using Prosite MyDomains (<http://us.expasy.org/tools/mydomains/>).



Supplemental Figure 3. Breeding strategy. To generate $cTnt-Cre^{+/-}; Mycn^{loxp/loxp}$ mice, male $cTnt-Cre^{+/-}$ and female $Mycn^{loxp/loxp}$ mice were crossed. Male $cTnt-Cre^{+/-}; Mycn^{loxp/wt}$ mice generated from the first cross were mated with female $Mycn^{loxp/loxp}$ mice. Mutant embryos have the *Cre* recombinase gene and are heterozygous or homozygous for $Mycn^{loxp/loxp}$ allele. $cTnt-Cre^{-/-}; Mycn^{loxp/loxp}$ and $cTnt-Cre^{-/-}; Mycn^{loxp/wt}$ embryos are controls. *cTnt*, cardiac troponin T; *loxp*, floxed allele; wt, wild type allele.



Supplemental Figure 4. *Mycn* allele and primer design. *Mycn* has three exons. The translational initiation codon of *Mycn* is in the second exon. The floxed *Mycn* allele has *loxP* sites inserted 5' of exon 2 and 3' of exon 3, targeting the entire coding region for deletion by *Cre* recombinase. Primers are indicated by arrows above gene schematic. Primers 1 and 2 were used to detect the wildtype (WT) and Floxed (Flox) alleles. Primers 1 and 3 were used to detect recombined allele (Δ). The WT product is 217 base pairs (bp), the Flox product is 260 bp, and the recombined (Δ) product is 350 bp.¹⁸



Supplemental Figure 5. Representative image of TUNEL staining on sagittal sections of control and mutant embryos at E11.5. No change in cardiomyocyte survival was detected in E11.5 mutant hearts (similar results for E9.5-E10.5, data not shown). Apoptosis was calculated as the number of positive cells (green) divided by total cell number (DAPI, blue), and the result was expressed as the mean percentage of apoptotic cells/ total number of cells. Cells were counted within 4 heart areas: atrial myocardium, atrioventricular canal myocardium, cushion mesenchyme, and ventricular myocardium. Three embryos were analyzed from three different litters, and at least three sections were analyzed for each embryo. Ctrl, control; Cko, conditional knockout; V, ventricle; A, atria. Arrows show examples of pH3-positive nuclei.

Supplementary Table I. Recovery of Living Mutant Embryos

Embryonic Stage	Living Embryos Observed (Embryos Expected)				Total	p Value
	<i>Mycn</i> ^{loxp/wt}	<i>Mycn</i> ^{loxp/loxp}	<i>cTnt-Cre;Mycn</i> ^{loxp/wt}	<i>cTnt-Cre;Mycn</i> ^{loxp/loxp}		
E9.5	30 (27)	33 (27)	20 (27)	26 (27)	109	0.3
E10.5	28 (27)	26 (27)	28 (27)	24 (27)	106	0.8
E11.5	57 (55)	55 (55)	56 (55)	50 (55)	218	0.2
E12.5-E16.5	9 (8)	14 (8)	10 (8)	0 (8)	33	<0.005

Genotypes of embryos recovered from E9.5-E12.5. The number of recovered living embryos for each genotype is shown at each corresponding stage, along with the expected Mendelian frequency in parenthesis. Chi square test was used to determine p value.

SUMMARY AND FUTURE DIRECTIONS

Heart development is tightly regulated by cardiogenic signaling pathways. The BMP signaling pathway regulates multiple aspects of heart development through regulation of downstream gene targets. BMP signals are transduced from the cell membrane to the nucleus by SMAD1, SMAD5, and SMAD8. The outcomes of the BMP signaling pathway can be modulated by intracellular protein interactions with SMAD proteins. We have investigated two aspects of BMP signaling by identifying SMAD1-interacting proteins during mouse cardiogenesis and exploring the functions of a known BMP transcriptional target, *Mycn*, in the developing myocardium.

Chromodomain Helicase DNA Binding Protein 7 (CHD7) Interacts with SMAD1

Our first goal was to identify novel SMAD1-interacting proteins during mouse cardiogenesis. We screened a cDNA library obtained from embryonic day (E) 9.5-E11.5 mouse hearts with SMAD1 as bait in a yeast two-hybrid experiment.²³² Over three hundred possible candidates were initially isolated and then narrowed down to 73 valid candidate genes. Of these, two were identical *Chd7* sequences that appear to encode a novel isoform. The *Chd7* isoform contained a portion of the C-terminal CHD7 mRNA, flanked by intronic sequences. The CHD7 clone had two BRK domains thought to have protein-protein binding functions and chromodomain helicase activities.^{233, 234} The

interaction between the CHD7 isoform and SMAD1 was confirmed with GST pull-down and *in vitro* pull-down experiments. SMAD1 likely interacts with CHD7's BRK domains, but future experiments are needed to confirm the SMAD1-interacting region. The CHD7 isoform was also able to interact with SMAD2, which is specific to the TGF β signaling pathway. However, the interaction with SMAD2 needs to be confirmed in other cell types and *in vitro* with pull-down experiments. Both TGF β and BMP signaling pathways are essential for multiple aspects of heart development. The roles of CHD7 in BMP- or TGF β - mediated cardiogenic processes are unclear.

Future Directions: Roles of CHD7 during Heart Development

The biological significance of the CHD7 isoform needs to be determined. It would be interesting to perform the following experiments with both the CHD7 isoform and full length CHD7, or the C-terminal end of CHD7 as full-length CHD7 is a large protein (330 kDa). That way, if the CHD7 isoform cannot be validated, we could still investigate full-length CHD7 and its interaction with SMAD1. First, I would like to validate the CHD7 isoform and perhaps identify other heart-specific CHD7 isoforms. To do this, immunoprecipitation (IP) experiments could be performed on embryonic mouse heart protein lysate, followed by mass spectrometry analyses. Next, the temporal and spatial expression patterns of *Chd7* during mouse heart development could be examined in detail using immunohistochemistry and *in situ* hybridization experiments. The expression patterns would provide clues about the roles of CHD7 in different aspects of heart development, such as valve development, myocardial wall formation, and outflow

tract (OFT) morphogenesis. Finally, overexpression and knockdown experiments using primary cardiomyocyte cultures or the immortalized NkL-TAg cardiomyocyte cell line could determine if the *CHD7* isoform influences proliferation, survival, differentiation, and gene expression.²³⁵

The functional relevancy of the *CHD7*-*SMAD1* interaction could be studied by verifying a functional output, identifying DNA binding sites, and discovering DNA binding cofactors. Since *CHD7* and *SMAD1* both regulate transcription in cooperation with other cofactors, their interaction likely has implications for transcription regulation.²³⁶⁻²⁴³ This could be tested with luciferase reporter assays. Second, considering that *CHD7* and *SMAD1* share DNA binding sites and that we have shown a direct *CHD7*-*SMAD1* interaction in our study, it is likely that we could confirm co-localization at common gene targets during mouse cardiogenesis with chromatin immunoprecipitation (ChIP)-seq experiments.^{233, 234} Furthermore, a recent report showed that *CHD7* interacts with its family member *CHD8*, which is part of a large protein-protein complex that modifies chromatin structure and gene regulation.^{236, 244-246} *SMAD1* may participate in the *CHD7*-*CHD8* complex as a linker protein and/or as a DNA binding cofactor. To explore this possibility and to identify other cofactors, IP experiments could be performed followed by mass spectrometry to identify proteins that bind to *CHD7*.

The molecular functions and tissue-specific requirements of *CHD7* are not completely understood, but it appears to have roles in multiple aspects of heart morphogenesis. Haploinsufficiency for *CHD7* is associated with CHARGE syndrome (OMIM 608892). The heart defects caused by *CHD7* haploinsufficiency are variable and include OFT septation and alignment defects, atrioventricular canal (AVC) defects

(poorly formed or absent septation between chambers), atrial septal defects (ASD), and ventricular septal defects (VSD).^{247, 248} The hearts of mouse models heterozygous for loss of function mutations in *Chd7* were not characterized in detail, but were reported to have VSD and defects in OFT development.^{249, 250} Disruption of *Chd7* in *Xenopus* caused aberrant cardiac neural crest cell (CNCC) gene expression and migration, resulting in abnormal OFT positioning.²⁵¹ Taken together, these data strongly suggest that *Chd7* has functions in OFT morphogenesis and in myocardium formation. Conditional gene inactivation in transgenic mouse models could be used to define *Chd7*'s roles in different cardiac cell populations. To investigate CHD7 functions in OFT morphogenesis, it could be conditionally removed from CNCC, which contribute to the developing OFT, using *Wnt1-Cre*, or from the pharyngeal endoderm, which signals to the CNCC, with *Tbx1-Cre* or *Foxg1-Cre*.^{209, 247, 248, 252, 253} Likewise, to understand the role of CHD7 in the myocardium, it could be conditionally deleted from the developing myocardium using *Nkx2.5-Cre* or *cTnt-Cre*.^{144, 247, 248, 254}

Roles of MYCN in the Developing Mouse Myocardium

The second goal was to explore the role of myocardial *Mycn* using a transgenic mouse model with *Mycn* deleted specifically from the myocardium. Myocardial *Mycn*-depletion resulted in embryonic lethality, likely due to the thin-walled phenotype in mutant mice. The results of this study reveal that *Mycn* is a critical mediator of myocardial wall formation as a regulator of cardiomyocyte proliferation, size, and cardiac gene expression. The phenotype of the *cTnt-Cre;Mycn^{loxp/loxp}* hearts can likely be

attributed to the cumulative effect of multiple, small changes in gene expression resulting in aberrations in critical cellular processes. Contrary to previous studies reporting that MYCN has roles in preventing premature terminal differentiation, our data strongly suggest that MYCN does not regulate cardiomyocyte maturation.

Myocardial wall morphogenesis: E7.5-E9.5. MYCN's role as a regulator of numerous cellular processes such as proliferation, differentiation, and metabolism, make it well-suited to govern the development of the myocardial wall.²⁵⁵ While we have provided evidence that this is indeed the case, MYCN's niche during myocardial wall morphogenesis has not yet been exhaustively explored. For instance, the *cTnt-Cre; Mycn^{loxp/loxp}* hearts were not analyzed at the initial stages of ventricle chamber specification, between E8.0-E8.5.^{18, 133, 256} *cTnt-Cre* induces recombination at E7.5 in the cardiomyocyte lineage, efficiently deleting target genes between E9.5-E10.5.^{192, 257} We have shown that *cTnt-Cre; Mycn^{loxp/loxp}* ventricular MYCN is reduced to approximately 25% of normal at E10.5. However, the *cTnt-Cre; Mycn^{loxp/loxp}* mice displayed noticeably thin myocardial walls as early as E9.5. Therefore, by E9.5, MYCN protein levels were already below the threshold needed for normal myocardial wall development. Two important avenues of investigation could be followed to help fully characterize *cTnt-Cre; Mycn^{loxp/loxp}* hearts. First, it would be interesting to delineate the initial stages of the mutant phenotype. Myocardial MYCN may be depleted sufficiently between E8.0-E9.0 to disrupt the initial stages of chamber specification within the linear heart tube. Morphology of E8.0-E9.0 *cTnt-Cre; Mycn^{loxp/loxp}* hearts could be analyzed with hematoxylin/eosin staining on paraffin-embedded embryos. Secondly, in hand with the morphological studies, future experiments can more thoroughly measure the sensitivity of

the myocardium to MYCN-depletion. *Mycn* mRNA could be measured with quantitative real-time PCR (qRT-PCR) on RNA isolated from *cTnt-Cre;Mycn^{loxp/loxp}* and control hearts, and with whole mount *in situ* hybridization experiments on E7.5-E9.5 embryos. These experiments would provide a more thorough time course of events leading to embryonic lethality in the *cTnt-Cre;Mycn^{loxp/loxp}* mice.

Myocardial wall morphogenesis: E9.5-E11.5. Chamber morphogenesis relies on regionally controlled cardiomyocyte proliferation and differentiation. Myocardium can be classified as nonchamber myocardium and working, chamber myocardium. Nonchamber myocardium of the inner curvature, OFT, AVC, and conduction system is relatively nonproliferative. Chamber myocardium, on the other hand, is highly proliferative beginning around E9.5 in mouse embryos. Cardiomyocytes on the outer curvature of the ventricle chambers proliferate rapidly and contribute to the expanding wall. On the luminal side of the ventricles, cardiomyocytes lose their proliferative capacity and become more differentiated. They develop into sub-endocardial muscular projections called trabeculae that generate contractile force and coordinate the intraventricular conduction.^{18, 133, 256}

The signaling cascades that regulate myocardial wall formation are complex and are not completely defined. They involve crosstalk between the myocardium, endocardium, and epicardium. Three of the major signaling pathways include the Neuregulin 1 (NRG1), BMP10, and retinoid acid (RA) signaling pathways.^{139, 258-267} It has been established that BMP signaling regulates *Mycn* expression, but it is possible that MYCN's role in myocardial wall morphogenesis is not restricted to the BMP signaling pathway.^{144, 268} MYCN may regulate the expression of proteins involved in NRG1 or RA

signaling pathways. Additionally, MYCN may regulate BMP10 through a feedback mechanism. Future experiments could examine the expression of signaling components such as NRG1 and its receptors ERBB2/4, RA receptors, or BMP10 in *cTnt-Cre*; *Mycn*^{loxp/loxp} hearts using *in situ* hybridization and immunohistochemistry assays. Furthermore, *Mycn* may be a transcriptional target of signaling pathways other than myocardial BMP. To determine this, MYCN expression could be measured in transgenic mice with disrupted NRG1 or RA signaling using *in situ* hybridization, immunostaining, and Western blot experiments.^{258-261, 263, 264, 266, 267} Alternatively, *in vitro* experiments could be performed to determine if MYCN expression changes in response to alterations in NRG1 or RA signaling. In these experiments, cultured primary cardiomyocytes or cultured embryonic hearts could be treated with either agonists (NRG1 or RA stimulation) or antagonists (ERBB2/4 or RA receptor inhibitors) and MYCN expression could be analyzed using Western blot and qRT PCR assays.

Cardiomyocyte maturation and ventricle chamber formation. MYCN maintains some cell types in a proliferative, undifferentiated embryonic state.^{269, 270} If MYCN has such a function during heart development, then loss of myocardial MYCN would have resulted in premature cardiomyocyte differentiation and loss of proliferation. This would have accounted for the thin-walled mutant phenotype in *cTnt-Cre*; *Mycn*^{loxp/loxp} hearts because, if the cardiomyocytes had prematurely matured and could no longer proliferate, the myocardial wall would have lost its source of cells and would not be able to expand. We had already determined that myocardial MYCN-depletion resulted in significantly decreased cardiomyocyte proliferation. To investigate MYCN's role in cardiomyocyte maturation, we examined the expression of myofilament proteins that

have unique expression patterns in the embryonic and adult myocardium. We expected to see a reduction in embryonic markers and an increase in adult markers. However, there were no changes in embryonic proteins, β -myosin heavy chain (β -MHC), α -smooth muscle actin (α -ACTA2), or α -skeletal actin (α -ACTA1).^{271, 272} Adult myofilament proteins, α -myosin heavy chain (α -MHC) and α -cardiac actin (α -ACTC1), were not increased.^{271, 272} Indeed, α -MHC expression was decreased in *cTnt-Cre;Mycn^{loxp/loxp}* ventricles. This could be due to loss of the trabecular myocardium in which α -MHC is enriched during development.¹³⁹ Thus, our data strongly suggest that MYCN is not required for maintaining cardiomyocytes in their embryonic state.

Loss of myocardial MYCN disrupts the expression of a subset of genes within the ventricles whose expression is important for cardiomyocyte structure and function. Myosin light chain 2A (MLC2A) and myosin light chain 2v (MLC2V,) were significantly decreased, while cardiac troponin I (TNNI3) was significantly increased.^{273, 274} So it appears that MYCN is required for a subset of the cardiac gene expression, but MYCN's roles in ventricular myocardial wall development require further investigation. First, it remains unknown if these genes are direct or indirectly regulated by MYCN. Future experiments using luciferase reporter assays, EMSA, and CHIP-Seq could clarify this issue. Second, the changes in expression patterns were not examined in detail. To better understand the altered gene expression in mutant hearts, *in situ* hybridization or immunohistochemistry experiments could be performed on frontal sections. This would help determine if MYCN has regional regulatory roles on cardiac gene expression during heart development. Third, future experiments could investigate other informative markers involved in myocardial regionalization and specialization. These include, but are not

limited to, markers such as *Nkx2.5*, *Tbx20*, *Tbx2*, *Hand1/2*, *Irx4*, *Cited1*, *Nppa* (*Anf*), *Cx40/43*, and *Smpx* (*Chisel*).^{18, 158, 159, 162, 256, 261, 268, 275} As mentioned above, *in situ* hybridization on frontal sections would determine if and how these markers are altered in *cTnt-Cre;Mycn^{loxp/loxp}* hearts. Fourth, to prioritize MYCN targets during heart wall formation and to obtain an overview of the major cardiogenic pathways affected by myocardial MYCN, microarray experiments could be performed on RNA from *cTnt-Cre;Mycn^{loxp/loxp}* and control ventricular tissue. These analyses would provide more comprehensive understanding of the MYCN-mediated cardiac gene network during myocardial wall formation.

Future Directions: MYCN and Epigenetic Regulation

Acetylation and methylation. Chromatin is responsive to cues that alter its structure and affect gene expression.²⁷⁶ MYCN provides such cues. It binds thousands of DNA sequences transiently, but it is thought to have longer-lasting and more widespread effects via chromatin structure modification of expansive genomic regions.^{255, 277} MYCN can promote gene transcription by keeping chromatin in an active configuration, called euchromatin. As discussed in Chapter 3, MYCN interacts with histone acetyltransferases (HATs), which add acetyl groups to histones and are associated with active chromatin configuration.^{255, 276, 278} MYCN likely interacts with histone lysine methyltransferases as well, since MYCN initiates and maintains both histone acetylation at lysine 9 (AcK9) and trimethylation of lysine 4 (tri-MeK4).²⁷⁷ Also, MYCN-depletion in neural stem cells caused nuclear condensation, thought to be due to tightly packed

chromatin, or heterochromatin.²⁶⁹ Conversely, CMYC can repress transcription by recruiting DNA-methyltransferase 3 α (DNMT3 α) which results in DNA hypermethylation.²⁷⁸ Based on the conservation of CMYC and MYCN, and the association of MYCN binding sites with hypermethylated DNA, it is quite possible that MYCN can also interact with methyltransferases.^{279, 280} As with MYCN's other roles, it may regulate chromatin modification in stage-specific patterns that depend on the cell context. In the future, changes in acetylation and methylation patterns could be examined in *cTnt-Cre;Mycn^{loxp/loxp}* ventricles compared to controls. Experiments that would enable this investigation include ChIP-chip experiments, using antibodies for MYCN, AcK9 and triMeK4.^{277, 280} DNA methylation patterns could be examined with methylation-dependent immunoprecipitation (meDIP) followed by hybridization to an array or high-throughput sequencing.²⁸⁰

microRNA. microRNA (miRNA) are short, non-coding RNA that regulate many cellular processes through post-transcriptional silencing of mRNA. miRNA are about 21-25 nucleotides in length and they interact with the 3' untranslated region (UTR) of mRNA in a sequence-specific manner to promote their degradation.⁴²⁻⁴⁴ During heart development, miRNA have roles in the regulating cardiomyocyte proliferation, differentiation, and conduction.^{42, 44, 281} Studies have revealed that MYCN upregulates miRNA and, in turn, *Mycn* is a miRNA target.²⁸²⁻²⁸⁶ Future experiments could determine if myocardial MYCN regulates gene expression indirectly through miRNA-mediated degradation during heart development. RNA isolated from *cTnt-Cre; Mycn^{loxp/loxp}* and control ventricles could be analyzed with miRNA microarrays and real time PCR (RT-PCR) to see if loss of *Mycn* in the myocardium results in altered miRNA

expression. Also, it would be interesting to determine if *Mycn* expression is changed in mouse models with altered miRNA. For example, overexpression of *microRNA-1-1* in the developing mouse heart causes hypoplastic ventricles and reduced cardiomyocyte proliferation, similar to the *cTnt-Cre;Mycn^{loxp/loxp}* mutant phenotype.²⁸⁷ The similar phenotypes suggest that *Mycn* mRNA is a critical target of *microRNA-1-1*.

Future Directions: MYCN in Other Cardiogenic Processes

In our study, the phenotype of *cTnt-Cre;Mycn^{loxp/loxp}* hearts was restricted to the myocardium. However, there is evidence that suggests that MYCN has roles in other aspects of heart development. For instance, MYCN may have roles in the development of the cushions, the primordial valve structures. In mice, global deletion of *Mycn* halted the initial steps of cushion formation.²⁸⁸ Additionally, studies using chicken tissue culture systems have shown that a BMP-TBX20-MYCN axis mediates proliferation and gene expression required for proper cushion development.²⁸⁹ Also, defective valvulogenesis has been reported in people with Feingold syndrome (FS), for example missing or malformed tricuspid valves.^{290, 291} Thus, it appears that endocardial MYCN is important for the induction of cushion formation and/or for later steps in cushion morphogenesis.

MYCN may also have roles in OFT development. MYCN is expressed in mouse and chicken CNCC, a population of cells that contributes to the developing OFT.²⁹²⁻²⁹⁶ FS patients have defects in OFT septation and aortic arch development.^{290, 291} Together, these data strongly suggest that MYCN has roles in the cardiac CNCC.

Lastly, our results suggest that myocardial MYCN does not have roles specific to the first or second heart fields (FHF or SHF, respectively). As discussed in the first chapter, the FHF contributes primarily to the left ventricle and the SHF contributes to the right ventricle.^{6, 7, 9, 10} As we did not observe any obvious differences between left or right ventricle morphology in *cTnt-Cre;Mycn^{loxp/loxp}* hearts, it appears that MYCN is uniformly required for ventricle myocardial wall morphogenesis. To confirm that MYCN does not have heart field-specific roles, future experiments could analyze the expression of FHF markers *Hand1* and *Tbx5*, and SHF markers *Fgf10* and *Isl1* in *cTnt-Cre;Mycn^{loxp/loxp}* hearts using *in situ* hybridization and immunohistochemistry on frontal sections.^{7, 13, 14, 16, 17}

Future studies using transgenic mouse models could be used to conditionally delete *Mycn* from specific cell populations. *Mycn* could be removed from the endocardium using *Tie2-Cre* to investigate its roles in cushion development and from the CNCC using *Wnt1-Cre* to explore its functions in OFT morphogenesis.^{201, 209} To delineate its potential roles in the FHF and SHF, *Mycn* can be removed from the FHF progenitors with *Nkx2.5-Cre*, although *Nkx2.5* has roles in the SHF as well, and from SHF progenitors with *Mef2c-Cre* or *Isl1-Cre*.^{12, 254, 297, 298}

Future Directions: MYCN in Adult Heart Disease

MYCN enhances cell growth through regulation of the cell cycle, ribosome synthesis, and protein translation.²⁵⁵ In our study, loss of myocardial *Mycn* caused a significant reduction in ventricular cardiomyocyte size and decreased expression of

p70(S6K), a regulator of cell growth.²⁹⁹⁻³⁰⁴ Future studies using luciferase reporter, ChIP, and EMSA experiments are needed to establish if MYCN directly or indirectly regulates *p70(s6k)*. Nonetheless, cardiomyocyte size and p70(S6K) expression are sensitive to loss of MYCN. While, *Mycn* is not normally expressed in the adult heart, P70(S6K) has roles in cardiac hypertrophy.^{255, 301-305} It is therefore tempting to speculate that aberrant expression of MYCN in the adult myocardium has roles in cardiac hypertrophy. This idea could be explored using transgenic mouse models with overexpression of MYCN in adult myocardium. Future experiments could also explore the possibility that *p70(s6k)* is downstream of CMYC in cardiac hypertrophy. CMYC has roles in cardiac hypertrophy in the adult myocardium, is activated by hypertrophic stimuli, and is highly homologous to MYCN.³⁰⁶⁻³¹⁰ Thus, it is plausible that our results provide insight into a novel CMYC-*p70(s6k)* mechanism during cardiac hypertrophy. This could be tested with luciferase reporter assays and by measuring p70(S6K) expression in an existing model of CMYC overexpression in the myocardium.³⁰⁷

Summary and Significance

CHDs are the most prevalent birth defect in the United States and they are the leading noninfectious cause of infant death.^{3,4,311} Elucidating the molecular mechanisms of heart development will help uncover the underlying causes of CHDs and may have future benefits in diagnosis and treatment of CHDs. *Chd7* and *Mycn* are both highly conserved genes with roles in heart development and disease. As players in cardiogenic BMP signaling pathways, *Chd7* and *Mycn* are implicated in multiple heart developmental

processes. However, their roles in the BMP signaling pathway and independent of BMP signaling are not completely understood. I believe these follow-up studies are necessary to obtain a more complete understanding of the roles of *Chd7* and *Mycn* during heart development. Furthermore, these and other studies will shed light into the pathology of human disease caused by mutations in *CHD7* and *MYCN*.

LIST OF GENERAL REFERENCES

1. Hoffman JI. Incidence of congenital heart disease: II. Prenatal incidence. *Pediatr Cardiol* 1995;**16**:155-165.
2. Pierpont ME, Basson CT, Benson DW, Gelb BD, Giglia TM, Goldmuntz E, *et al.* Genetic basis for congenital heart defects: current knowledge: a scientific statement from the American Heart Association Congenital Cardiac Defects Committee, Council on Cardiovascular Disease in the Young: endorsed by the American Academy of Pediatrics. *Circulation* 2007;**115**:3015-3038.
3. Lenfant C. Report of the Task Force on Research in Pediatric Cardiovascular Disease. *Circulation* 2002;**106**:1037-1042.
4. Benson DW. The genetics of congenital heart disease: a point in the revolution. *Cardiol Clin* 2002;**20**:385-394, vi.
5. Hoffman JI, Kaplan S. The incidence of congenital heart disease. *J Am Coll Cardiol* 2002;**39**:1890-1900.
6. Abu-Issa R, Kirby ML. Patterning of the heart field in the chick. *Dev Biol* 2008;**319**:223-233.
7. Cai CL, Liang X, Shi Y, Chu PH, Pfaff SL, Chen J, *et al.* Isl1 identifies a cardiac progenitor population that proliferates prior to differentiation and contributes a majority of cells to the heart. *Dev Cell* 2003;**5**:877-889.
8. Meilhac SM, Esner M, Kelly RG, Nicolas JF, Buckingham ME. The clonal origin of myocardial cells in different regions of the embryonic mouse heart. *Dev Cell* 2004;**6**:685-698.
9. Waldo KL, Hutson MR, Ward CC, Zdanowicz M, Stadt HA, Kumiski D, *et al.* Secondary heart field contributes myocardium and smooth muscle to the arterial pole of the developing heart. *Dev Biol* 2005;**281**:78-90.
10. Zaffran S, Kelly RG, Meilhac SM, Buckingham ME, Brown NA. Right ventricular myocardium derives from the anterior heart field. *Circ Res* 2004;**95**:261-268.
11. Dyer LA, Kirby ML. The role of secondary heart field in cardiac development. *Dev Biol* 2009;**336**:137-144.
12. Black BL. Transcriptional pathways in second heart field development. *Semin Cell Dev Biol* 2007;**18**:67-76.
13. Bruneau BG, Nemer G, Schmitt JP, Charron F, Robitaille L, Caron S, *et al.* A murine model of Holt-Oram syndrome defines roles of the T-box transcription factor Tbx5 in cardiogenesis and disease. *Cell* 2001;**106**:709-721.
14. Kelly RG, Brown NA, Buckingham ME. The arterial pole of the mouse heart forms from Fgf10-expressing cells in pharyngeal mesoderm. *Dev Cell* 2001;**1**:435-440.

15. Schwartz RJ, Olson EN. Building the heart piece by piece: modularity of cis-elements regulating Nkx2-5 transcription. *Development* 1999;**126**:4187-4192.
16. Takeuchi JK, Ohgi M, Koshiha-Takeuchi K, Shiratori H, Sakaki I, Ogura K, *et al.* Tbx5 specifies the left/right ventricles and ventricular septum position during cardiogenesis. *Development* 2003;**130**:5953-5964.
17. Yuan S, Schoenwolf GC. Islet-1 marks the early heart rudiments and is asymmetrically expressed during early rotation of the foregut in the chick embryo. *Anat Rec* 2000;**260**:204-207.
18. Evans SM, Yelon D, Conlon FL, Kirby ML. Myocardial lineage development. *Circ Res* 2010;**107**:1428-1444.
19. Srivastava D. Making or breaking the heart: from lineage determination to morphogenesis. *Cell* 2006;**126**:1037-1048.
20. Chen D, Zhao M, Harris SE, Mi Z. Signal transduction and biological functions of bone morphogenetic proteins. *Front Biosci* 2004;**9**:349-358.
21. van Wijk B, Moorman A, van den Hoff M. Role of bone morphogenetic proteins in cardiac differentiation. *Cardiovasc Res* 2007;**74**:244-255.
22. Macías-Silva M, Hoodless PA, Tang SJ, Buchwald M, Wrana JL. Specific activation of Smad1 signaling pathways by the BMP7 type I receptor, ALK2. *J Biol Chem* 1998;**273**:25628-25636.
23. Koenig BB, Cook JS, Wolsing DH, Ting J, Tiesman JP, Correa PE, *et al.* Characterization and cloning of a receptor for BMP-2 and BMP-4 from NIH 3T3 cells. *Mol Cell Biol* 1994;**14**:5961-5974.
24. ten Dijke P, Yamashita H, Sampath TK, Reddi AH, Estevez M, Riddle DL, *et al.* Identification of type I receptors for osteogenic protein-1 and bone morphogenetic protein-4. *J Biol Chem* 1994;**269**:16985-16988.
25. Yamashita H, ten Dijke P, Huylebroeck D, Sampath TK, Andries M, Smith JC, *et al.* Osteogenic protein-1 binds to activin type II receptors and induces certain activin-like effects. *J Cell Biol* 1995;**130**:217-226.
26. Nohno T, Ishikawa T, Saito T, Hosokawa K, Noji S, Wolsing DH, *et al.* Identification of a human type II receptor for bone morphogenetic protein-4 that forms differential heteromeric complexes with bone morphogenetic protein type I receptors. *J Biol Chem* 1995;**270**:22522-22526.
27. Rosenzweig BL, Imamura T, Okadome T, Cox GN, Yamashita H, ten Dijke P, *et al.* Cloning and characterization of a human type II receptor for bone morphogenetic proteins. *Proc Natl Acad Sci U S A* 1995;**92**:7632-7636.
28. Kawabata M, Chytil A, Moses HL. Cloning of a novel type II serine/threonine kinase receptor through interaction with the type I transforming growth factor-beta receptor. *J Biol Chem* 1995;**270**:5625-5630.
29. Cárcamo J, Zentella A, Massagué J. Disruption of transforming growth factor beta signaling by a mutation that prevents transphosphorylation within the receptor complex. *Mol Cell Biol* 1995;**15**:1573-1581.
30. Wieser R, Wrana JL, Massagué J. GS domain mutations that constitutively activate T beta R-I, the downstream signaling component in the TGF-beta receptor complex. *EMBO J* 1995;**14**:2199-2208.

31. Hoodless PA, Haerry T, Abdollah S, Stapleton M, O'Connor MB, Attisano L, *et al.* MADR1, a MAD-related protein that functions in BMP2 signaling pathways. *Cell* 1996;**85**:489-500.
32. Nishimura R, Kato Y, Chen D, Harris SE, Mundy GR, Yoneda T. Smad5 and DPC4 are key molecules in mediating BMP-2-induced osteoblastic differentiation of the pluripotent mesenchymal precursor cell line C2C12. *J Biol Chem* 1998;**273**:1872-1879.
33. Chen Y, Bhushan A, Vale W. Smad8 mediates the signaling of the ALK-2 [corrected] receptor serine kinase. *Proc Natl Acad Sci U S A* 1997;**94**:12938-12943.
34. Qin BY, Lam SS, Correia JJ, Lin K. Smad3 allosterically links TGF-beta receptor kinase activation to transcriptional control. *Genes Dev* 2002;**16**:1950-1963.
35. Miyazono K, Kamiya Y, Morikawa M. Bone morphogenetic protein receptors and signal transduction. *J Biochem* 2010;**147**:35-51.
36. Yamaguchi K, Shirakabe K, Shibuya H, Irie K, Oishi I, Ueno N, *et al.* Identification of a member of the MAPKKK family as a potential mediator of TGF-beta signal transduction. *Science* 1995;**270**:2008-2011.
37. Shibuya H, Iwata H, Masuyama N, Gotoh Y, Yamaguchi K, Irie K, *et al.* Role of TAK1 and TAB1 in BMP signaling in early *Xenopus* development. *EMBO J* 1998;**17**:1019-1028.
38. Nohe A, Keating E, Knaus P, Petersen NO. Signal transduction of bone morphogenetic protein receptors. *Cell Signal* 2004;**16**:291-299.
39. Roux PP, Blenis J. ERK and p38 MAPK-activated protein kinases: a family of protein kinases with diverse biological functions. *Microbiol Mol Biol Rev* 2004;**68**:320-344.
40. Kinbara K, Goldfinger LE, Hansen M, Chou FL, Ginsberg MH. Ras GTPases: integrins' friends or foes? *Nat Rev Mol Cell Biol* 2003;**4**:767-776.
41. Vanhaesebroeck B, Leever SJ, Ahmadi K, Timms J, Katso R, Driscoll PC, *et al.* Synthesis and function of 3-phosphorylated inositol lipids. *Annu Rev Biochem* 2001;**70**:535-602.
42. Cordes KR, Srivastava D. MicroRNA regulation of cardiovascular development. *Circ Res* 2009;**104**:724-732.
43. Bartel DP. MicroRNAs: genomics, biogenesis, mechanism, and function. *Cell* 2004;**116**:281-297.
44. Liu N, Olson EN. MicroRNA regulatory networks in cardiovascular development. *Dev Cell* 2010;**18**:510-525.
45. Ji R, Cheng Y, Yue J, Yang J, Liu X, Chen H, *et al.* MicroRNA expression signature and antisense-mediated depletion reveal an essential role of MicroRNA in vascular neointimal lesion formation. *Circ Res* 2007;**100**:1579-1588.
46. Davis BN, Hilyard AC, Lagna G, Hata A. SMAD proteins control DROSHA-mediated microRNA maturation. *Nature* 2008;**454**:56-61.
47. Warner DR, Bhattacharjee V, Yin X, Singh S, Mukhopadhyay P, Pisano MM, *et al.* Functional interaction between Smad, CREB binding protein, and p68 RNA helicase. *Biochem Biophys Res Commun* 2004;**324**:70-76.

48. Fukuda T, Yamagata K, Fujiyama S, Matsumoto T, Koshida I, Yoshimura K, *et al.* DEAD-box RNA helicase subunits of the Drosha complex are required for processing of rRNA and a subset of microRNAs. *Nat Cell Biol* 2007;**9**:604-611.
49. Davis BN, Hilyard AC, Nguyen PH, Lagna G, Hata A. Smad proteins bind a conserved RNA sequence to promote microRNA maturation by Drosha. *Mol Cell* 2010;**39**:373-384.
50. Yuasa S, Itabashi Y, Koshimizu U, Tanaka T, Sugimura K, Kinoshita M, *et al.* Transient inhibition of BMP signaling by Noggin induces cardiomyocyte differentiation of mouse embryonic stem cells. *Nat Biotechnol* 2005;**23**:607-611.
51. McMahon JA, Takada S, Zimmerman LB, Fan CM, Harland RM, McMahon AP. Noggin-mediated antagonism of BMP signaling is required for growth and patterning of the neural tube and somite. *Genes Dev* 1998;**12**:1438-1452.
52. Bachiller D, Klingensmith J, Kemp C, Belo JA, Anderson RM, May SR, *et al.* The organizer factors Chordin and Noggin are required for mouse forebrain development. *Nature* 2000;**403**:658-661.
53. Matzuk MM, Lu N, Vogel H, Sellheyer K, Roop DR, Bradley A. Multiple defects and perinatal death in mice deficient in follistatin. *Nature* 1995;**374**:360-363.
54. Sneddon JB, Zhen HH, Montgomery K, van de Rijn M, Tward AD, West R, *et al.* Bone morphogenetic protein antagonist gremlin 1 is widely expressed by cancer-associated stromal cells and can promote tumor cell proliferation. *Proc Natl Acad Sci U S A* 2006;**103**:14842-14847.
55. Frank NY, Kho AT, Schatton T, Murphy GF, Molloy MJ, Zhan Q, *et al.* Regulation of myogenic progenitor proliferation in human fetal skeletal muscle by BMP4 and its antagonist Gremlin. *J Cell Biol* 2006;**175**:99-110.
56. Balemans W, Van Hul W. Extracellular regulation of BMP signaling in vertebrates: a cocktail of modulators. *Dev Biol* 2002;**250**:231-250.
57. Onichtchouk D, Chen YG, Dosch R, Gawantka V, Delius H, Massagué J, *et al.* Silencing of TGF-beta signalling by the pseudoreceptor BAMBI. *Nature* 1999;**401**:480-485.
58. Jin W, Yun C, Kim HS, Kim SJ. TrkC binds to the bone morphogenetic protein type II receptor to suppress bone morphogenetic protein signaling. *Cancer Res* 2007;**67**:9869-9877.
59. Sammar M, Stricker S, Schwabe GC, Sieber C, Hartung A, Hanke M, *et al.* Modulation of GDF5/BRI-b signalling through interaction with the tyrosine kinase receptor Ror2. *Genes Cells* 2004;**9**:1227-1238.
60. Samad TA, Rebbapragada A, Bell E, Zhang Y, Sidis Y, Jeong SJ, *et al.* DRAGON, a bone morphogenetic protein co-receptor. *J Biol Chem* 2005;**280**:14122-14129.
61. Barbara NP, Wrana JL, Letarte M. Endoglin is an accessory protein that interacts with the signaling receptor complex of multiple members of the transforming growth factor-beta superfamily. *J Biol Chem* 1999;**274**:584-594.
62. Desgrosellier JS, Mundell NA, McDonnell MA, Moses HL, Barnett JV. Activin receptor-like kinase 2 and Smad6 regulate epithelial-mesenchymal transformation during cardiac valve formation. *Dev Biol* 2005;**280**:201-210.

63. Murakami G, Watabe T, Takaoka K, Miyazono K, Imamura T. Cooperative inhibition of bone morphogenetic protein signaling by Smurf1 and inhibitory Smads. *Mol Biol Cell* 2003;**14**:2809-2817.
64. Kavsak P, Rasmussen RK, Causing CG, Bonni S, Zhu H, Thomsen GH, *et al.* Smad7 binds to Smurf2 to form an E3 ubiquitin ligase that targets the TGF beta receptor for degradation. *Mol Cell* 2000;**6**:1365-1375.
65. Ebisawa T, Fukuchi M, Murakami G, Chiba T, Tanaka K, Imamura T, *et al.* Smurf1 interacts with transforming growth factor-beta type I receptor through Smad7 and induces receptor degradation. *J Biol Chem* 2001;**276**:12477-12480.
66. Imamura T, Takase M, Nishihara A, Oeda E, Hanai J, Kawabata M, *et al.* Smad6 inhibits signalling by the TGF-beta superfamily. *Nature* 1997;**389**:622-626.
67. Hata A, Lagna G, Massagué J, Hemmati-Brivanlou A. Smad6 inhibits BMP/Smad1 signaling by specifically competing with the Smad4 tumor suppressor. *Genes Dev* 1998;**12**:186-197.
68. Hanyu A, Ishidou Y, Ebisawa T, Shimanuki T, Imamura T, Miyazono K. The N domain of Smad7 is essential for specific inhibition of transforming growth factor-beta signaling. *J Cell Biol* 2001;**155**:1017-1027.
69. Pera EM, Ikeda A, Eivers E, De Robertis EM. Integration of IGF, FGF, and anti-BMP signals via Smad1 phosphorylation in neural induction. *Genes Dev* 2003;**17**:3023-3028.
70. Sapkota G, Alarcón C, Spagnoli FM, Brivanlou AH, Massagué J. Balancing BMP signaling through integrated inputs into the Smad1 linker. *Mol Cell* 2007;**25**:441-454.
71. Fuentealba LC, Eivers E, Ikeda A, Hurtado C, Kuroda H, Pera EM, *et al.* Integrating patterning signals: Wnt/GSK3 regulates the duration of the BMP/Smad1 signal. *Cell* 2007;**131**:980-993.
72. Suzawa M, Tamura Y, Fukumoto S, Miyazono K, Fujita T, Kato S, *et al.* Stimulation of Smad1 transcriptional activity by Ras-extracellular signal-regulated kinase pathway: a possible mechanism for collagen-dependent osteoblastic differentiation. *J Bone Miner Res* 2002;**17**:240-248.
73. Xu X, Yin Z, Hudson JB, Ferguson EL, Frasch M. Smad proteins act in combination with synergistic and antagonistic regulators to target Dpp responses to the Drosophila mesoderm. *Genes Dev* 1998;**12**:2354-2370.
74. Frasch M. Induction of visceral and cardiac mesoderm by ectodermal Dpp in the early Drosophila embryo. *Nature* 1995;**374**:464-467.
75. Yin Z, Frasch M. Regulation and function of tinman during dorsal mesoderm induction and heart specification in Drosophila. *Dev Genet* 1998;**22**:187-200.
76. Schultheiss TM, Burch JB, Lassar AB. A role for bone morphogenetic proteins in the induction of cardiac myogenesis. *Genes Dev* 1997;**11**:451-462.
77. Somi S, Buffing AA, Moorman AF, Van Den Hoff MJ. Dynamic patterns of expression of BMP isoforms 2, 4, 5, 6, and 7 during chicken heart development. *Anat Rec A Discov Mol Cell Evol Biol* 2004;**279**:636-651.
78. Waldo KL, Kumiski DH, Wallis KT, Stadt HA, Hutson MR, Platt DH, *et al.* Conotruncal myocardium arises from a secondary heart field. *Development* 2001;**128**:3179-3188.

79. Tirosh-Finkel L, Elhanany H, Rinon A, Tzahor E. Mesoderm progenitor cells of common origin contribute to the head musculature and the cardiac outflow tract. *Development* 2006;**133**:1943-1953.
80. Zhang H, Bradley A. Mice deficient for BMP2 are nonviable and have defects in amnion/chorion and cardiac development. *Development* 1996;**122**:2977-2986.
81. Dudley AT, Robertson EJ. Overlapping expression domains of bone morphogenetic protein family members potentially account for limited tissue defects in BMP7 deficient embryos. *Dev Dyn* 1997;**208**:349-362.
82. Solloway MJ, Robertson EJ. Early embryonic lethality in Bmp5;Bmp7 double mutant mice suggests functional redundancy within the 60A subgroup. *Development* 1999;**126**:1753-1768.
83. Alsan BH, Schultheiss TM. Regulation of avian cardiogenesis by Fgf8 signaling. *Development* 2002;**129**:1935-1943.
84. Barron M, Gao M, Lough J. Requirement for BMP and FGF signaling during cardiogenic induction in non-precardiac mesoderm is specific, transient, and cooperative. *Dev Dyn* 2000;**218**:383-393.
85. Tirosh-Finkel L, Zeisel A, Brodt-Ivenshitz M, Shamaï A, Yao Z, Seger R, *et al.* BMP-mediated inhibition of FGF signaling promotes cardiomyocyte differentiation of anterior heart field progenitors. *Development* 2010;**137**:2989-3000.
86. Winnier G, Blessing M, Labosky PA, Hogan BL. Bone morphogenetic protein-4 is required for mesoderm formation and patterning in the mouse. *Genes Dev* 1995;**9**:2105-2116.
87. Andrée B, Duprez D, Vorbusch B, Arnold HH, Brand T. BMP-2 induces ectopic expression of cardiac lineage markers and interferes with somite formation in chicken embryos. *Mech Dev* 1998;**70**:119-131.
88. Schlange T, Andrée B, Arnold HH, Brand T. BMP2 is required for early heart development during a distinct time period. *Mech Dev* 2000;**91**:259-270.
89. Jamali M, Karamboulas C, Rogerson PJ, Skerjanc IS. BMP signaling regulates Nkx2-5 activity during cardiomyogenesis. *FEBS Lett* 2001;**509**:126-130.
90. Liberatore CM, Searcy-Schrick RD, Vincent EB, Yutzey KE. Nkx-2.5 gene induction in mice is mediated by a Smad consensus regulatory region. *Dev Biol* 2002;**244**:243-256.
91. Shi Y, Katsev S, Cai C, Evans S. BMP signaling is required for heart formation in vertebrates. *Dev Biol* 2000;**224**:226-237.
92. Lien CL, McAnally J, Richardson JA, Olson EN. Cardiac-specific activity of an Nkx2-5 enhancer requires an evolutionarily conserved Smad binding site. *Dev Biol* 2002;**244**:257-266.
93. Reiter JF, Verkade H, Stainier DY. Bmp2b and Oep promote early myocardial differentiation through their regulation of gata5. *Dev Biol* 2001;**234**:330-338.
94. Schultheiss TM, Xydias S, Lassar AB. Induction of avian cardiac myogenesis by anterior endoderm. *Development* 1995;**121**:4203-4214.
95. Brown CO, Chi X, Garcia-Gras E, Shirai M, Feng XH, Schwartz RJ. The cardiac determination factor, Nkx2-5, is activated by mutual cofactors GATA-4 and Smad1/4 via a novel upstream enhancer. *J Biol Chem* 2004;**279**:10659-10669.

96. Arsenian S, Weinhold B, Oelgeschläger M, Rütter U, Nordheim A. Serum response factor is essential for mesoderm formation during mouse embryogenesis. *EMBO J* 1998;**17**:6289-6299.
97. Wang D, Chang PS, Wang Z, Sutherland L, Richardson JA, Small E, *et al.* Activation of cardiac gene expression by myocardin, a transcriptional cofactor for serum response factor. *Cell* 2001;**105**:851-862.
98. Callis TE, Cao D, Wang DZ. Bone morphogenetic protein signaling modulates myocardin transactivation of cardiac genes. *Circ Res* 2005;**97**:992-1000.
99. Ishida W, Hamamoto T, Kusanagi K, Yagi K, Kawabata M, Takehara K, *et al.* Smad6 is a Smad1/5-induced smad inhibitor. Characterization of bone morphogenetic protein-responsive element in the mouse Smad6 promoter. *J Biol Chem* 2000;**275**:6075-6079.
100. Ladd AN, Yatskievych TA, Antin PB. Regulation of avian cardiac myogenesis by activin/TGFbeta and bone morphogenetic proteins. *Dev Biol* 1998;**204**:407-419.
101. Mishina Y, Suzuki A, Ueno N, Behringer RR. Bmpr encodes a type I bone morphogenetic protein receptor that is essential for gastrulation during mouse embryogenesis. *Genes Dev* 1995;**9**:3027-3037.
102. Dewulf N, Verschueren K, Lonnoy O, Morén A, Grimsby S, Vande Spiegle K, *et al.* Distinct spatial and temporal expression patterns of two type I receptors for bone morphogenetic proteins during mouse embryogenesis. *Endocrinology* 1995;**136**:2652-2663.
103. Gu Z, Reynolds EM, Song J, Lei H, Feijen A, Yu L, *et al.* The type I serine/threonine kinase receptor ActRIA (ALK2) is required for gastrulation of the mouse embryo. *Development* 1999;**126**:2551-2561.
104. Mishina Y, Crombie R, Bradley A, Behringer RR. Multiple roles for activin-like kinase-2 signaling during mouse embryogenesis. *Dev Biol* 1999;**213**:314-326.
105. Yi SE, Daluiski A, Pederson R, Rosen V, Lyons KM. The type I BMP receptor BMPRII is required for chondrogenesis in the mouse limb. *Development* 2000;**127**:621-630.
106. Ehrman LA, Yutzey KE. Lack of regulation in the heart forming region of avian embryos. *Dev Biol* 1999;**207**:163-175.
107. Stern CD, Yu RT, Kakizuka A, Kintner CR, Mathews LS, Vale WW, *et al.* Activin and its receptors during gastrulation and the later phases of mesoderm development in the chick embryo. *Dev Biol* 1995;**172**:192-205.
108. Feijen A, Goumans MJ, van den Eijnden-van Raaij AJ. Expression of activin subunits, activin receptors and follistatin in postimplantation mouse embryos suggests specific developmental functions for different activins. *Development* 1994;**120**:3621-3637.
109. Beppu H, Kawabata M, Hamamoto T, Chytil A, Minowa O, Noda T, *et al.* BMP type II receptor is required for gastrulation and early development of mouse embryos. *Dev Biol* 2000;**221**:249-258.
110. Matzuk MM, Kumar TR, Vassalli A, Bickenbach JR, Roop DR, Jaenisch R, *et al.* Functional analysis of activins during mammalian development. *Nature* 1995;**374**:354-356.

111. Oh SP, Li E. The signaling pathway mediated by the type IIB activin receptor controls axial patterning and lateral asymmetry in the mouse. *Genes Dev* 1997;**11**:1812-1826.
112. Song J, Oh SP, Schrewe H, Nomura M, Lei H, Okano M, *et al.* The type II activin receptors are essential for egg cylinder growth, gastrulation, and rostral head development in mice. *Dev Biol* 1999;**213**:157-169.
113. Faure S, de Santa Barbara P, Roberts DJ, Whitman M. Endogenous patterns of BMP signaling during early chick development. *Dev Biol* 2002;**244**:44-65.
114. Tremblay KD, Dunn NR, Robertson EJ. Mouse embryos lacking Smad1 signals display defects in extra-embryonic tissues and germ cell formation. *Development* 2001;**128**:3609-3621.
115. Chang H, Zwijsen A, Vogel H, Huylebroeck D, Matzuk MM. Smad5 is essential for left-right asymmetry in mice. *Dev Biol* 2000;**219**:71-78.
116. Yang X, Castilla LH, Xu X, Li C, Gotay J, Weinstein M, *et al.* Angiogenesis defects and mesenchymal apoptosis in mice lacking SMAD5. *Development* 1999;**126**:1571-1580.
117. Sirard C, de la Pompa JL, Elia A, Itie A, Mirtsos C, Cheung A, *et al.* The tumor suppressor gene Smad4/Dpc4 is required for gastrulation and later for anterior development of the mouse embryo. *Genes Dev* 1998;**12**:107-119.
118. Chu GC, Dunn NR, Anderson DC, Oxburgh L, Robertson EJ. Differential requirements for Smad4 in TGFbeta-dependent patterning of the early mouse embryo. *Development* 2004;**131**:3501-3512.
119. Buckingham M, Meilhac S, Zaffran S. Building the mammalian heart from two sources of myocardial cells. *Nat Rev Genet* 2005;**6**:826-835.
120. Tzahor E, Lassar AB. Wnt signals from the neural tube block ectopic cardiogenesis. *Genes Dev* 2001;**15**:255-260.
121. Schneider VA, Mercola M. Wnt antagonism initiates cardiogenesis in *Xenopus laevis*. *Genes Dev* 2001;**15**:304-315.
122. Marvin MJ, Di Rocco G, Gardiner A, Bush SM, Lassar AB. Inhibition of Wnt activity induces heart formation from posterior mesoderm. *Genes Dev* 2001;**15**:316-327.
123. Lickert H, Kutsch S, Kanzler B, Tamai Y, Taketo MM, Kemler R. Formation of multiple hearts in mice following deletion of beta-catenin in the embryonic endoderm. *Dev Cell* 2002;**3**:171-181.
124. Pandur P, Läsche M, Eisenberg LM, Kühl M. Wnt-11 activation of a non-canonical Wnt signalling pathway is required for cardiogenesis. *Nature* 2002;**418**:636-641.
125. Abdul-Ghani M, Dufort D, Stiles R, De Repentigny Y, Kothary R, Megeney LA. Wnt11 promotes cardiomyocyte development by caspase-mediated suppression of canonical Wnt signals. *Mol Cell Biol* 2011;**31**:163-178.
126. Eisenberg CA, Gourdie RG, Eisenberg LM. Wnt-11 is expressed in early avian mesoderm and required for the differentiation of the quail mesoderm cell line QCE-6. *Development* 1997;**124**:525-536.
127. Chapman SC, Brown R, Lees L, Schoenwolf GC, Lumsden A. Expression analysis of chick Wnt and frizzled genes and selected inhibitors in early chick patterning. *Dev Dyn* 2004;**229**:668-676.

128. Garriock RJ, D'Agostino SL, Pilcher KC, Krieg PA. Wnt11-R, a protein closely related to mammalian Wnt11, is required for heart morphogenesis in *Xenopus*. *Dev Biol* 2005;**279**:179-192.
129. Matsui T, Raya A, Kawakami Y, Callol-Massot C, Capdevila J, Rodríguez-Esteban C, *et al.* Noncanonical Wnt signaling regulates midline convergence of organ primordia during zebrafish development. *Genes Dev* 2005;**19**:164-175.
130. Terami H, Hidaka K, Katsumata T, Iio A, Morisaki T. Wnt11 facilitates embryonic stem cell differentiation to Nkx2.5-positive cardiomyocytes. *Biochem Biophys Res Commun* 2004;**325**:968-975.
131. Nakajima Y, Yamagishi T, Ando K, Nakamura H. Significance of bone morphogenetic protein-4 function in the initial myofibrillogenesis of chick cardiogenesis. *Dev Biol* 2002;**245**:291-303.
132. Bachiller D, Klingensmith J, Shneyder N, Tran U, Anderson R, Rossant J, *et al.* The role of chordin/Bmp signals in mammalian pharyngeal development and DiGeorge syndrome. *Development* 2003;**130**:3567-3578.
133. Sedmera D, Pexieder T, Vuillemin M, Thompson RP, Anderson RH. Developmental patterning of the myocardium. *Anat Rec* 2000;**258**:319-337.
134. Dunwoodie SL. Combinatorial signaling in the heart orchestrates cardiac induction, lineage specification and chamber formation. *Semin Cell Dev Biol* 2007;**18**:54-66.
135. Pignatelli RH, McMahan CJ, Dreyer WJ, Denfield SW, Price J, Belmont JW, *et al.* Clinical characterization of left ventricular noncompaction in children: a relatively common form of cardiomyopathy. *Circulation* 2003;**108**:2672-2678.
136. Xing Y, Ichida F, Matsuoka T, Isobe T, Ikemoto Y, Higaki T, *et al.* Genetic analysis in patients with left ventricular noncompaction and evidence for genetic heterogeneity. *Mol Genet Metab* 2006;**88**:71-77.
137. Neuhaus H, Rosen V, Thies RS. Heart specific expression of mouse BMP-10 a novel member of the TGF-beta superfamily. *Mech Dev* 1999;**80**:181-184.
138. Somi S, Buffing AA, Moorman AF, Van Den Hoff MJ. Expression of bone morphogenetic protein-10 mRNA during chicken heart development. *Anat Rec A Discov Mol Cell Evol Biol* 2004;**279**:579-582.
139. Chen H, Shi S, Acosta L, Li W, Lu J, Bao S, *et al.* BMP10 is essential for maintaining cardiac growth during murine cardiogenesis. *Development* 2004;**131**:2219-2231.
140. Grego-Bessa J, Luna-Zurita L, del Monte G, Bolós V, Melgar P, Arandilla A, *et al.* Notch signaling is essential for ventricular chamber development. *Dev Cell* 2007;**12**:415-429.
141. Kim RY, Robertson EJ, Solloway MJ. Bmp6 and Bmp7 are required for cushion formation and septation in the developing mouse heart. *Dev Biol* 2001;**235**:449-466.
142. Gaussin V, Van de Putte T, Mishina Y, Hanks MC, Zwijsen A, Huylebroeck D, *et al.* Endocardial cushion and myocardial defects after cardiac myocyte-specific conditional deletion of the bone morphogenetic protein receptor ALK3. *Proc Natl Acad Sci U S A* 2002;**99**:2878-2883.
143. Azhar M, Wang PY, Frugier T, Koishi K, Deng C, Noakes PG, *et al.* Myocardial deletion of Smad4 using a novel α skeletal muscle actin Cre recombinase

- transgenic mouse causes misalignment of the cardiac outflow tract. *Int J Biol Sci* 2010;**6**:546-555.
144. Song L, Yan W, Chen X, Deng CX, Wang Q, Jiao K. Myocardial smad4 is essential for cardiogenesis in mouse embryos. *Circ Res* 2007;**101**:277-285.
 145. Qi X, Yang G, Yang L, Lan Y, Weng T, Wang J, *et al.* Essential role of Smad4 in maintaining cardiomyocyte proliferation during murine embryonic heart development. *Dev Biol* 2007;**311**:136-146.
 146. Wang J, Xu N, Feng X, Hou N, Zhang J, Cheng X, *et al.* Targeted disruption of Smad4 in cardiomyocytes results in cardiac hypertrophy and heart failure. *Circ Res* 2005;**97**:821-828.
 147. Christoffels VM, Smits GJ, Kispert A, Moorman AF. Development of the pacemaker tissues of the heart. *Circ Res* 2010;**106**:240-254.
 148. Moorman AF, Christoffels VM. Cardiac chamber formation: development, genes, and evolution. *Physiol Rev* 2003;**83**:1223-1267.
 149. Virágh S, Challice CE. The development of the conduction system in the mouse embryo heart. I. The first embryonic A-V conduction pathway. *Dev Biol* 1977;**56**:382-396.
 150. Virágh S, Challice CE. The development of the conduction system in the mouse embryo heart. II. Histogenesis of the atrioventricular node and bundle. *Dev Biol* 1977;**56**:397-411.
 151. Virágh S, Challice CE. The development of the conduction system in the mouse embryo heart. *Dev Biol* 1982;**89**:25-40.
 152. de Jong F, Opthof T, Wilde AA, Janse MJ, Charles R, Lamers WH, *et al.* Persisting zones of slow impulse conduction in developing chicken hearts. *Circ Res* 1992;**71**:240-250.
 153. Valderrábano M, Chen F, Dave AS, Lamp ST, Klitzner TS, Weiss JN. Atrioventricular ring reentry in embryonic mouse hearts. *Circulation* 2006;**114**:543-549.
 154. Rentschler S, Zander J, Meyers K, France D, Levine R, Porter G, *et al.* Neuregulin-1 promotes formation of the murine cardiac conduction system. *Proc Natl Acad Sci U S A* 2002;**99**:10464-10469.
 155. Yamada M, Revelli JP, Eichele G, Barron M, Schwartz RJ. Expression of chick Tbx-2, Tbx-3, and Tbx-5 genes during early heart development: evidence for BMP2 induction of Tbx2. *Dev Biol* 2000;**228**:95-105.
 156. Ma L, Lu MF, Schwartz RJ, Martin JF. Bmp2 is essential for cardiac cushion epithelial-mesenchymal transition and myocardial patterning. *Development* 2005;**132**:5601-5611.
 157. Aanhaanen WT, Brons JF, Domínguez JN, Rana MS, Norden J, Airik R, *et al.* The Tbx2+ primary myocardium of the atrioventricular canal forms the atrioventricular node and the base of the left ventricle. *Circ Res* 2009;**104**:1267-1274.
 158. Habets PE, Moorman AF, Clout DE, van Roon MA, Lingbeek M, van Lohuizen M, *et al.* Cooperative action of Tbx2 and Nkx2.5 inhibits ANF expression in the atrioventricular canal: implications for cardiac chamber formation. *Genes Dev* 2002;**16**:1234-1246.

159. Christoffels VM, Hoogaars WM, Tessari A, Clout DE, Moorman AF, Campione M. T-box transcription factor *Tbx2* represses differentiation and formation of the cardiac chambers. *Dev Dyn* 2004;**229**:763-770.
160. Harrelson Z, Kelly RG, Goldin SN, Gibson-Brown JJ, Bollag RJ, Silver LM, *et al.* *Tbx2* is essential for patterning the atrioventricular canal and for morphogenesis of the outflow tract during heart development. *Development* 2004;**131**:5041-5052.
161. Shirai M, Imanaka-Yoshida K, Schneider MD, Schwartz RJ, Morisaki T. T-box 2, a mediator of Bmp-Smad signaling, induced hyaluronan synthase 2 and *Tgfbeta2* expression and endocardial cushion formation. *Proc Natl Acad Sci U S A* 2009;**106**:18604-18609.
162. Singh R, Horsthuis T, Farin HF, Grieskamp T, Norden J, Petry M, *et al.* *Tbx20* interacts with smads to confine *tbx2* expression to the atrioventricular canal. *Circ Res* 2009;**105**:442-452.
163. Rutenberg JB, Fischer A, Jia H, Gessler M, Zhong TP, Mercola M. Developmental patterning of the cardiac atrioventricular canal by Notch and Hairy-related transcription factors. *Development* 2006;**133**:4381-4390.
164. Kokubo H, Miyagawa-Tomita S, Nakazawa M, Saga Y, Johnson RL. Mouse *hesr1* and *hesr2* genes are redundantly required to mediate Notch signaling in the developing cardiovascular system. *Dev Biol* 2005;**278**:301-309.
165. Gaussin V, Morley GE, Cox L, Zwijsen A, Vance KM, Emile L, *et al.* *Alk3/Bmpr1a* receptor is required for development of the atrioventricular canal into valves and annulus fibrosus. *Circ Res* 2005;**97**:219-226.
166. Stroud DM, Gaussin V, Burch JB, Yu C, Mishina Y, Schneider MD, *et al.* Abnormal conduction and morphology in the atrioventricular node of mice with atrioventricular canal targeted deletion of *Alk3/Bmpr1a* receptor. *Circulation* 2007;**116**:2535-2543.
167. Aanhaanen WT, Boukens BJ, Sizarov A, Wakker V, de Gier-de Vries C, van Ginneken AC, *et al.* Defective *Tbx2*-dependent patterning of the atrioventricular canal myocardium causes accessory pathway formation in mice. *J Clin Invest* 2011;**121**:534-544.
168. Lalani SR, Thakuria JV, Cox GF, Wang X, Bi W, Bray MS, *et al.* 20p12.3 microdeletion predisposes to Wolff-Parkinson-White syndrome with variable neurocognitive deficits. *J Med Genet* 2009;**46**:168-175.
169. de Lange FJ, Moorman AF, Anderson RH, Männer J, Soufan AT, de Gier-de Vries C, *et al.* Lineage and morphogenetic analysis of the cardiac valves. *Circ Res* 2004;**95**:645-654.
170. Kisanuki YY, Hammer RE, Miyazaki J, Williams SC, Richardson JA, Yanagisawa M. *Tie2-Cre* transgenic mice: a new model for endothelial cell-lineage analysis in vivo. *Dev Biol* 2001;**230**:230-242.
171. Gittenberger-de Groot AC, Vrancken Peeters MP, Bergwerff M, Mentink MM, Poelmann RE. Epicardial outgrowth inhibition leads to compensatory mesothelial outflow tract collar and abnormal cardiac septation and coronary formation. *Circ Res* 2000;**87**:969-971.
172. Kirby ML, Gale TF, Stewart DE. Neural crest cells contribute to normal aorticopulmonary septation. *Science* 1983;**220**:1059-1061.

173. Kirby ML, Waldo KL. Neural crest and cardiovascular patterning. *Circ Res* 1995;**77**:211-215.
174. Waldo K, Miyagawa-Tomita S, Kumiski D, Kirby ML. Cardiac neural crest cells provide new insight into septation of the cardiac outflow tract: aortic sac to ventricular septal closure. *Dev Biol* 1998;**196**:129-144.
175. Jiang X, Rowitch DH, Soriano P, McMahon AP, Sucov HM. Fate of the mammalian cardiac neural crest. *Development* 2000;**127**:1607-1616.
176. Edmonds LD, James LM. Temporal trends in the birth prevalence of selected congenital malformations in the Birth Defects Monitoring Program/Commission on Professional and Hospital Activities, 1979-1989. *Teratology* 1993;**48**:647-649.
177. Smith KA, Joziassse IC, Chocron S, van Dinther M, Guryev V, Verhoeven MC, *et al.* Dominant-negative ALK2 allele associates with congenital heart defects. *Circulation* 2009;**119**:3062-3069.
178. Joziassse IC, Smith KA, Chocron S, van Dinther M, Guryev V, van de Smagt JJ, *et al.* ALK2 mutation in a patient with Down's syndrome and a congenital heart defect. *Eur J Hum Genet* 2011;**19**:389-393.
179. Lyons KM, Pelton RW, Hogan BL. Organogenesis and pattern formation in the mouse: RNA distribution patterns suggest a role for bone morphogenetic protein-2A (BMP-2A). *Development* 1990;**109**:833-844.
180. Abdelwahid E, Rice D, Pelliniemi LJ, Jokinen E. Overlapping and differential localization of Bmp-2, Bmp-4, Msx-2 and apoptosis in the endocardial cushion and adjacent tissues of the developing mouse heart. *Cell Tissue Res* 2001;**305**:67-78.
181. Sugi Y, Yamamura H, Okagawa H, Markwald RR. Bone morphogenetic protein-2 can mediate myocardial regulation of atrioventricular cushion mesenchymal cell formation in mice. *Dev Biol* 2004;**269**:505-518.
182. Rivera-Feliciano J, Tabin CJ. Bmp2 instructs cardiac progenitors to form the heart-valve-inducing field. *Dev Biol* 2006;**295**:580-588.
183. Camenisch TD, Molin DG, Person A, Runyan RB, Gittenberger-de Groot AC, McDonald JA, *et al.* Temporal and distinct TGFbeta ligand requirements during mouse and avian endocardial cushion morphogenesis. *Dev Biol* 2002;**248**:170-181.
184. Camenisch TD, Spicer AP, Brehm-Gibson T, Biesterfeldt J, Augustine ML, Calabro A, *et al.* Disruption of hyaluronan synthase-2 abrogates normal cardiac morphogenesis and hyaluronan-mediated transformation of epithelium to mesenchyme. *J Clin Invest* 2000;**106**:349-360.
185. Yang J, Mani SA, Donaher JL, Ramaswamy S, Itzykson RA, Come C, *et al.* Twist, a master regulator of morphogenesis, plays an essential role in tumor metastasis. *Cell* 2004;**117**:927-939.
186. Luna-Zurita L, Prados B, Grego-Bessa J, Luxán G, del Monte G, Benguría A, *et al.* Integration of a Notch-dependent mesenchymal gene program and Bmp2-driven cell invasiveness regulates murine cardiac valve formation. *J Clin Invest* 2010;**120**:3493-3507.
187. Boyer AS, Ayerinkas II, Vincent EB, McKinney LA, Weeks DL, Runyan RB. TGFbeta2 and TGFbeta3 have separate and sequential activities during epithelial-

- mesenchymal cell transformation in the embryonic heart. *Dev Biol* 1999;**208**:530-545.
188. Yamagishi T, Nakajima Y, Miyazono K, Nakamura H. Bone morphogenetic protein-2 acts synergistically with transforming growth factor-beta3 during endothelial-mesenchymal transformation in the developing chick heart. *J Cell Physiol* 1999;**180**:35-45.
 189. Jones CM, Lyons KM, Hogan BL. Involvement of Bone Morphogenetic Protein-4 (BMP-4) and Vgr-1 in morphogenesis and neurogenesis in the mouse. *Development* 1991;**111**:531-542.
 190. Goldman DC, Donley N, Christian JL. Genetic interaction between Bmp2 and Bmp4 reveals shared functions during multiple aspects of mouse organogenesis. *Mech Dev* 2009;**126**:117-127.
 191. Uchimura T, Komatsu Y, Tanaka M, McCann KL, Mishina Y. Bmp2 and Bmp4 genetically interact to support multiple aspects of mouse development including functional heart development. *Genesis* 2009;**47**:374-384.
 192. Jiao K, Kulesa H, Tompkins K, Zhou Y, Batts L, Baldwin HS, *et al.* An essential role of Bmp4 in the atrioventricular septation of the mouse heart. *Genes Dev* 2003;**17**:2362-2367.
 193. Liu W, Selever J, Wang D, Lu MF, Moses KA, Schwartz RJ, *et al.* Bmp4 signaling is required for outflow-tract septation and branchial-arch artery remodeling. *Proc Natl Acad Sci U S A* 2004;**101**:4489-4494.
 194. Kulesa H, Hogan BL. Generation of a loxP flanked bmp4loxP-lacZ allele marked by conditional lacZ expression. *Genesis* 2002;**32**:66-68.
 195. Kingsley DM, Bland AE, Grubber JM, Marker PC, Russell LB, Copeland NG, *et al.* The mouse short ear skeletal morphogenesis locus is associated with defects in a bone morphogenetic member of the TGF beta superfamily. *Cell* 1992;**71**:399-410.
 196. Jena N, Martín-Seisdedos C, McCue P, Croce CM. BMP7 null mutation in mice: developmental defects in skeleton, kidney, and eye. *Exp Cell Res* 1997;**230**:28-37.
 197. Luo G, Hofmann C, Bronckers AL, Sohocki M, Bradley A, Karsenty G. BMP-7 is an inducer of nephrogenesis, and is also required for eye development and skeletal patterning. *Genes Dev* 1995;**9**:2808-2820.
 198. Solloway MJ, Dudley AT, Bikoff EK, Lyons KM, Hogan BL, Robertson EJ. Mice lacking Bmp6 function. *Dev Genet* 1998;**22**:321-339.
 199. Yamagishi T, Nakajima Y, Nishimatsu S, Nohno T, Ando K, Nakamura H. Expression of bone morphogenetic protein-5 gene during chick heart development: possible roles in valvuloseptal endocardial cushion formation. *Anat Rec* 2001;**264**:313-316.
 200. Lyons KM, Hogan BL, Robertson EJ. Colocalization of BMP 7 and BMP 2 RNAs suggests that these factors cooperatively mediate tissue interactions during murine development. *Mech Dev* 1995;**50**:71-83.
 201. Song L, Fässler R, Mishina Y, Jiao K, Baldwin HS. Essential functions of Alk3 during AV cushion morphogenesis in mouse embryonic hearts. *Dev Biol* 2007;**301**:276-286.
 202. Park C, Lavine K, Mishina Y, Deng CX, Ornitz DM, Choi K. Bone morphogenetic protein receptor 1A signaling is dispensable for hematopoietic

- development but essential for vessel and atrioventricular endocardial cushion formation. *Development* 2006;**133**:3473-3484.
203. Wang J, Sridurongrit S, Dudas M, Thomas P, Nagy A, Schneider MD, *et al.* Atrioventricular cushion transformation is mediated by ALK2 in the developing mouse heart. *Dev Biol* 2005;**286**:299-310.
 204. Stottmann RW, Choi M, Mishina Y, Meyers EN, Klingensmith J. BMP receptor IA is required in mammalian neural crest cells for development of the cardiac outflow tract and ventricular myocardium. *Development* 2004;**131**:2205-2218.
 205. Kaartinen V, Dudas M, Nagy A, Sridurongrit S, Lu MM, Epstein JA. Cardiac outflow tract defects in mice lacking ALK2 in neural crest cells. *Development* 2004;**131**:3481-3490.
 206. Délot EC, Bahamonde ME, Zhao M, Lyons KM. BMP signaling is required for septation of the outflow tract of the mammalian heart. *Development* 2003;**130**:209-220.
 207. Beppu H, Malhotra R, Beppu Y, Lepore JJ, Parmacek MS, Bloch KD. BMP type II receptor regulates positioning of outflow tract and remodeling of atrioventricular cushion during cardiogenesis. *Dev Biol* 2009;**331**:167-175.
 208. Jia Q, McDill BW, Li SZ, Deng C, Chang CP, Chen F. Smad signaling in the neural crest regulates cardiac outflow tract remodeling through cell autonomous and non-cell autonomous effects. *Dev Biol* 2007;**311**:172-184.
 209. Nie X, Deng CX, Wang Q, Jiao K. Disruption of Smad4 in neural crest cells leads to mid-gestation death with pharyngeal arch, craniofacial and cardiac defects. *Dev Biol* 2008;**316**:417-430.
 210. Huang Z, Wang D, Ihida-Stansbury K, Jones PL, Martin JF. Defective pulmonary vascular remodeling in Smad8 mutant mice. *Hum Mol Genet* 2009;**18**:2791-2801.
 211. Wang J, Greene SB, Bonilla-Claudio M, Tao Y, Zhang J, Bai Y, *et al.* Bmp signaling regulates myocardial differentiation from cardiac progenitors through a MicroRNA-mediated mechanism. *Dev Cell* 2010;**19**:903-912.
 212. Lu Y, Thomson JM, Wong HY, Hammond SM, Hogan BL. Transgenic over-expression of the microRNA miR-17-92 cluster promotes proliferation and inhibits differentiation of lung epithelial progenitor cells. *Dev Biol* 2007;**310**:442-453.
 213. Ventura A, Young AG, Winslow MM, Lintault L, Meissner A, Erkeland SJ, *et al.* Targeted deletion reveals essential and overlapping functions of the miR-17 through 92 family of miRNA clusters. *Cell* 2008;**132**:875-886.
 214. Prall OW, Menon MK, Solloway MJ, Watanabe Y, Zaffran S, Bajolle F, *et al.* An Nkx2-5/Bmp2/Smad1 negative feedback loop controls heart progenitor specification and proliferation. *Cell* 2007;**128**:947-959.
 215. Galvin KM, Donovan MJ, Lynch CA, Meyer RI, Paul RJ, Lorenz JN, *et al.* A role for smad6 in development and homeostasis of the cardiovascular system. *Nat Genet* 2000;**24**:171-174.
 216. Allen SP, Bogardi JP, Barlow AJ, Mir SA, Qayyum SR, Verbeek FJ, *et al.* Misexpression of noggin leads to septal defects in the outflow tract of the chick heart. *Dev Biol* 2001;**235**:98-109.

217. Mikawa T, Gourdie RG. Pericardial mesoderm generates a population of coronary smooth muscle cells migrating into the heart along with ingrowth of the epicardial organ. *Dev Biol* 1996;**174**:221-232.
218. Dettman RW, Denetclaw W, Ordahl CP, Bristow J. Common epicardial origin of coronary vascular smooth muscle, perivascular fibroblasts, and intermyocardial fibroblasts in the avian heart. *Dev Biol* 1998;**193**:169-181.
219. Schlueter J, Männer J, Brand T. BMP is an important regulator of proepicardial identity in the chick embryo. *Dev Biol* 2006;**295**:546-558.
220. van Wijk B, van den Berg G, Abu-Issa R, Barnett P, van der Velden S, Schmidt M, *et al.* Epicardium and myocardium separate from a common precursor pool by crosstalk between bone morphogenetic protein- and fibroblast growth factor-signaling pathways. *Circ Res* 2009;**105**:431-441.
221. Liu J, Stainier DY. Tbx5 and Bmp signaling are essential for proepicardium specification in zebrafish. *Circ Res* 2010;**106**:1818-1828.
222. Virágh S, Challice CE. The origin of the epicardium and the embryonic myocardial circulation in the mouse. *Anat Rec* 1981;**201**:157-168.
223. Cai CL, Martin JC, Sun Y, Cui L, Wang L, Ouyang K, *et al.* A myocardial lineage derives from Tbx18 epicardial cells. *Nature* 2008;**454**:104-108.
224. Christoffels VM, Grieskamp T, Norden J, Mommersteeg MT, Rudat C, Kispert A. Tbx18 and the fate of epicardial progenitors. *Nature* 2009;**458**:E8-9; discussion E9-10.
225. Ishii Y, Langberg J, Rosborough K, Mikawa T. Endothelial cell lineages of the heart. *Cell Tissue Res* 2009;**335**:67-73.
226. Ishii Y, Garriock RJ, Navetta AM, Coughlin LE, Mikawa T. BMP signals promote proepicardial protrusion necessary for recruitment of coronary vessel and epicardial progenitors to the heart. *Dev Cell* 2010;**19**:307-316.
227. Kruithof BP, van Wijk B, Somi S, Kruithof-de Julio M, Pérez Pomares JM, Weesie F, *et al.* BMP and FGF regulate the differentiation of multipotential pericardial mesoderm into the myocardial or epicardial lineage. *Dev Biol* 2006;**295**:507-522.
228. Mikawa T, Cohen-Gould L, Fischman DA. Clonal analysis of cardiac morphogenesis in the chicken embryo using a replication-defective retrovirus. III: Polyclonal origin of adjacent ventricular myocytes. *Dev Dyn* 1992;**195**:133-141.
229. Pérez-Pomares JM, Carmona R, González-Iriarte M, Atencia G, Wessels A, Muñoz-Chápuli R. Origin of coronary endothelial cells from epicardial mesothelium in avian embryos. *Int J Dev Biol* 2002;**46**:1005-1013.
230. Winter EM, Gittenberger-de Groot AC. Epicardium-derived cells in cardiogenesis and cardiac regeneration. *Cell Mol Life Sci* 2007;**64**:692-703.
231. Zhou B, Ma Q, Rajagopal S, Wu SM, Domian I, Rivera-Feliciano J, *et al.* Epicardial progenitors contribute to the cardiomyocyte lineage in the developing heart. *Nature* 2008;**454**:109-113.
232. DeBenedittis P, Harmelink C, Chen Y, Wang Q, Jiao K. Characterization of the novel interaction between muskellin and TBX20, a critical cardiogenic transcription factor. *Biochem Biophys Res Commun* 2011.

233. Schnetz MP, Handoko L, Akhtar-Zaidi B, Bartels CF, Pereira CF, Fisher AG, *et al.* CHD7 targets active gene enhancer elements to modulate ES cell-specific gene expression. *PLoS Genet* 2010;**6**:e1001023.
234. Schnetz MP, Bartels CF, Shastri K, Balasubramanian D, Zentner GE, Balaji R, *et al.* Genomic distribution of CHD7 on chromatin tracks H3K4 methylation patterns. *Genome Res* 2009;**19**:590-601.
235. Rybkin II, Markham DW, Yan Z, Bassel-Duby R, Williams RS, Olson EN. Conditional expression of SV40 T-antigen in mouse cardiomyocytes facilitates an inducible switch from proliferation to differentiation. *J Biol Chem* 2003;**278**:15927-15934.
236. Shur I, Benayahu D. Characterization and functional analysis of CReMM, a novel chromodomain helicase DNA-binding protein. *J Mol Biol* 2005;**352**:646-655.
237. Becker PB, Hörz W. ATP-dependent nucleosome remodeling. *Annu Rev Biochem* 2002;**71**:247-273.
238. Eberharter A, Becker PB. ATP-dependent nucleosome remodelling: factors and functions. *J Cell Sci* 2004;**117**:3707-3711.
239. Lusser A, Kadonaga JT. Chromatin remodeling by ATP-dependent molecular machines. *Bioessays* 2003;**25**:1192-1200.
240. Narlikar GJ, Fan HY, Kingston RE. Cooperation between complexes that regulate chromatin structure and transcription. *Cell* 2002;**108**:475-487.
241. Sif S. ATP-dependent nucleosome remodeling complexes: enzymes tailored to deal with chromatin. *J Cell Biochem* 2004;**91**:1087-1098.
242. Smith CL, Peterson CL. ATP-dependent chromatin remodeling. *Curr Top Dev Biol* 2005;**65**:115-148.
243. Euler-Taimor G, Heger J. The complex pattern of SMAD signaling in the cardiovascular system. *Cardiovasc Res* 2006;**69**:15-25.
244. Dou Y, Milne TA, Tackett AJ, Smith ER, Fukuda A, Wysocka J, *et al.* Physical association and coordinate function of the H3 K4 methyltransferase MLL1 and the H4 K16 acetyltransferase MOF. *Cell* 2005;**121**:873-885.
245. Surapureddi S, Viswakarma N, Yu S, Guo D, Rao MS, Reddy JK. PRIC320, a transcription coactivator, isolated from peroxisome proliferator-binding protein complex. *Biochem Biophys Res Commun* 2006;**343**:535-543.
246. Batsukh T, Pieper L, Koszucka AM, von Velsen N, Hoyer-Fender S, Elbracht M, *et al.* CHD8 interacts with CHD7, a protein which is mutated in CHARGE syndrome. *Hum Mol Genet* 2010;**19**:2858-2866.
247. Searle LC, Graham JM, Prasad C, Blake KD. CHARGE syndrome from birth to adulthood: an individual reported on from 0 to 33 years. *Am J Med Genet A* 2005;**133A**:344-349.
248. Aramaki M, Udaka T, Kosaki R, Makita Y, Okamoto N, Yoshihashi H, *et al.* Phenotypic spectrum of CHARGE syndrome with CHD7 mutations. *J Pediatr* 2006;**148**:410-414.
249. Bosman EA, Penn AC, Ambrose JC, Kettleborough R, Stemple DL, Steel KP. Multiple mutations in mouse Chd7 provide models for CHARGE syndrome. *Hum Mol Genet* 2005;**14**:3463-3476.

250. Randall V, McCue K, Roberts C, Kyriakopoulou V, Beddow S, Barrett AN, *et al.* Great vessel development requires biallelic expression of Chd7 and Tbx1 in pharyngeal ectoderm in mice. *J Clin Invest* 2009;**119**:3301-3310.
251. Bajpai R, Chen DA, Rada-Iglesias A, Zhang J, Xiong Y, Helms J, *et al.* CHD7 cooperates with PBAF to control multipotent neural crest formation. *Nature* 2010;**463**:958-962.
252. Arnold JS, Werling U, Braunstein EM, Liao J, Nowotschin S, Edelmann W, *et al.* Inactivation of Tbx1 in the pharyngeal endoderm results in 22q11DS malformations. *Development* 2006;**133**:977-987.
253. Brown CB, Wenning JM, Lu MM, Epstein DJ, Meyers EN, Epstein JA. Cre-mediated excision of Fgf8 in the Tbx1 expression domain reveals a critical role for Fgf8 in cardiovascular development in the mouse. *Dev Biol* 2004;**267**:190-202.
254. Moses KA, DeMayo F, Braun RM, Reecy JL, Schwartz RJ. Embryonic expression of an Nkx2-5/Cre gene using ROSA26 reporter mice. *Genesis* 2001;**31**:176-180.
255. Hurlin PJ. N-Myc functions in transcription and development. *Birth Defects Res C Embryo Today* 2005;**75**:340-352.
256. Christoffels VM, Habets PE, Franco D, Campione M, de Jong F, Lamers WH, *et al.* Chamber formation and morphogenesis in the developing mammalian heart. *Dev Biol* 2000;**223**:266-278.
257. Chen JW, Zhou B, Yu QC, Shin SJ, Jiao K, Schneider MD, *et al.* Cardiomyocyte-specific deletion of the coxsackievirus and adenovirus receptor results in hyperplasia of the embryonic left ventricle and abnormalities of sinuatrial valves. *Circ Res* 2006;**98**:923-930.
258. Meyer D, Birchmeier C. Multiple essential functions of neuregulin in development. *Nature* 1995;**378**:386-390.
259. Lee KF, Simon H, Chen H, Bates B, Hung MC, Hauser C. Requirement for neuregulin receptor erbB2 in neural and cardiac development. *Nature* 1995;**378**:394-398.
260. Gassmann M, Casagranda F, Orioli D, Simon H, Lai C, Klein R, *et al.* Aberrant neural and cardiac development in mice lacking the ErbB4 neuregulin receptor. *Nature* 1995;**378**:390-394.
261. Lai D, Liu X, Forrai A, Wolstein O, Michalick J, Ahmed I, *et al.* Neuregulin 1 sustains the gene regulatory network in both trabecular and nontrabecular myocardium. *Circ Res* 2010;**107**:715-727.
262. Chen J, Kubalak SW, Chien KR. Ventricular muscle-restricted targeting of the RXRalpha gene reveals a non-cell-autonomous requirement in cardiac chamber morphogenesis. *Development* 1998;**125**:1943-1949.
263. Gruber PJ, Kubalak SW, Pexieder T, Sucov HM, Evans RM, Chien KR. RXR alpha deficiency confers genetic susceptibility for aortic sac, conotruncal, atrioventricular cushion, and ventricular muscle defects in mice. *J Clin Invest* 1996;**98**:1332-1343.
264. Kastner P, Messaddeq N, Mark M, Wendling O, Grondona JM, Ward S, *et al.* Vitamin A deficiency and mutations of RXRalpha, RXRbeta and RARalpha lead

- to early differentiation of embryonic ventricular cardiomyocytes. *Development* 1997;**124**:4749-4758.
265. Lavine KJ, Yu K, White AC, Zhang X, Smith C, Partanen J, *et al.* Endocardial and epicardial derived FGF signals regulate myocardial proliferation and differentiation in vivo. *Dev Cell* 2005;**8**:85-95.
266. Lin SC, Dollé P, Ryckebusch L, Nosedá M, Zaffran S, Schneider MD, *et al.* Endogenous retinoic acid regulates cardiac progenitor differentiation. *Proc Natl Acad Sci U S A* 2010;**107**:9234-9239.
267. Sucov HM, Dyson E, Gumeringer CL, Price J, Chien KR, Evans RM. RXR alpha mutant mice establish a genetic basis for vitamin A signaling in heart morphogenesis. *Genes Dev* 1994;**8**:1007-1018.
268. Cai CL, Zhou W, Yang L, Bu L, Qyang Y, Zhang X, *et al.* T-box genes coordinate regional rates of proliferation and regional specification during cardiogenesis. *Development* 2005;**132**:2475-2487.
269. Knoepfler PS, Cheng PF, Eisenman RN. N-myc is essential during neurogenesis for the rapid expansion of progenitor cell populations and the inhibition of neuronal differentiation. *Genes Dev* 2002;**16**:2699-2712.
270. Okubo T, Knoepfler PS, Eisenman RN, Hogan BL. Nmyc plays an essential role during lung development as a dosage-sensitive regulator of progenitor cell proliferation and differentiation. *Development* 2005;**132**:1363-1374.
271. Morkin E. Control of cardiac myosin heavy chain gene expression. *Microsc Res Tech* 2000;**50**:522-531.
272. Clément S, Stouffs M, Bettiol E, Kampf S, Krause KH, Chaponnier C, *et al.* Expression and function of alpha-smooth muscle actin during embryonic-stem-cell-derived cardiomyocyte differentiation. *J Cell Sci* 2007;**120**:229-238.
273. Franco D, Lamers WH, Moorman AF. Patterns of expression in the developing myocardium: towards a morphologically integrated transcriptional model. *Cardiovasc Res* 1998;**38**:25-53.
274. O'Brien TX, Lee KJ, Chien KR. Positional specification of ventricular myosin light chain 2 expression in the primitive murine heart tube. *Proc Natl Acad Sci U S A* 1993;**90**:5157-5161.
275. Singh MK, Christoffels VM, Dias JM, Trowe MO, Petry M, Schuster-Gossler K, *et al.* Tbx20 is essential for cardiac chamber differentiation and repression of Tbx2. *Development* 2005;**132**:2697-2707.
276. Bannister AJ, Kouzarides T. Regulation of chromatin by histone modifications. *Cell Res* 2011;**21**:381-395.
277. Cotterman R, Jin VX, Krig SR, Lemen JM, Wey A, Farnham PJ, *et al.* N-Myc regulates a widespread euchromatic program in the human genome partially independent of its role as a classical transcription factor. *Cancer Res* 2008;**68**:9654-9662.
278. Adhikary S, Eilers M. Transcriptional regulation and transformation by Myc proteins. *Nat Rev Mol Cell Biol* 2005;**6**:635-645.
279. Brenner C, Deplus R, Didelot C, Lorient A, Viré E, De Smet C, *et al.* Myc represses transcription through recruitment of DNA methyltransferase corepressor. *EMBO J* 2005;**24**:336-346.

280. Murphy DM, Buckley PG, Bryan K, Das S, Alcock L, Foley NH, *et al.* Global MYCN transcription factor binding analysis in neuroblastoma reveals association with distinct E-box motifs and regions of DNA hypermethylation. *PLoS One* 2009;**4**:e8154.
281. Zhao Y, Ransom JF, Li A, Vedantham V, von Drehle M, Muth AN, *et al.* Dysregulation of cardiogenesis, cardiac conduction, and cell cycle in mice lacking miRNA-1-2. *Cell* 2007;**129**:303-317.
282. Schulte JH, Horn S, Otto T, Samans B, Heukamp LC, Eilers UC, *et al.* MYCN regulates oncogenic MicroRNAs in neuroblastoma. *Int J Cancer* 2008;**122**:699-704.
283. Northcott PA, Fernandez-L A, Hagan JP, Ellison DW, Grajkowska W, Gillespie Y, *et al.* The miR-17/92 polycistron is up-regulated in sonic hedgehog-driven medulloblastomas and induced by N-myc in sonic hedgehog-treated cerebellar neural precursors. *Cancer Res* 2009;**69**:3249-3255.
284. Ma L, Young J, Prabhala H, Pan E, Mestdagh P, Muth D, *et al.* miR-9, a MYC/MYCN-activated microRNA, regulates E-cadherin and cancer metastasis. *Nat Cell Biol* 2010;**12**:247-256.
285. Cole KA, Attiyeh EF, Mosse YP, Laquaglia MJ, Diskin SJ, Brodeur GM, *et al.* A functional screen identifies miR-34a as a candidate neuroblastoma tumor suppressor gene. *Mol Cancer Res* 2008;**6**:735-742.
286. Wei JS, Song YK, Durinck S, Chen QR, Cheuk AT, Tsang P, *et al.* The MYCN oncogene is a direct target of miR-34a. *Oncogene* 2008;**27**:5204-5213.
287. Zhao Y, Samal E, Srivastava D. Serum response factor regulates a muscle-specific microRNA that targets Hand2 during cardiogenesis. *Nature* 2005;**436**:214-220.
288. Charron J, Malynn BA, Fisher P, Stewart V, Jeannotte L, Goff SP, *et al.* Embryonic lethality in mice homozygous for a targeted disruption of the N-myc gene. *Genes Dev* 1992;**6**:2248-2257.
289. Shelton EL, Yutzey KE. Tbx20 regulation of endocardial cushion cell proliferation and extracellular matrix gene expression. *Dev Biol* 2007;**302**:376-388.
290. Celli J, van Bokhoven H, Brunner HG. Feingold syndrome: clinical review and genetic mapping. *Am J Med Genet A* 2003;**122A**:294-300.
291. Marcelis CL, Hol FA, Graham GE, Rieu PN, Kellermayer R, Meijer RP, *et al.* Genotype-phenotype correlations in MYCN-related Feingold syndrome. *Hum Mutat* 2008;**29**:1125-1132.
292. Downs KM, Martin GR, Bishop JM. Contrasting patterns of myc and N-myc expression during gastrulation of the mouse embryo. *Genes Dev* 1989;**3**:860-869.
293. Hirning U, Schmid P, Schulz WA, Rettenberger G, Hameister H. A comparative analysis of N-myc and c-myc expression and cellular proliferation in mouse organogenesis. *Mech Dev* 1991;**33**:119-125.
294. Kato K, Kanamori A, Wakamatsu Y, *al. e.* Tissue Distribution of N-myc Expression in the Early Organogenesis Period of the Mouse Embryo. *Development, Growth and Differentiation* 1991;**33**:29-36.
295. Sawai S, Kato K, Wakamatsu Y, Kondoh H. Organization and expression of the chicken N-myc gene. *Mol Cell Biol* 1990;**10**:2017-2026.

296. Stanton BR, Perkins AS, Tessarollo L, Sassoon DA, Parada LF. Loss of N-myc function results in embryonic lethality and failure of the epithelial component of the embryo to develop. *Genes Dev* 1992;**6**:2235-2247.
297. Heidt AB, Black BL. Transgenic mice that express Cre recombinase under control of a skeletal muscle-specific promoter from *mef2c*. *Genesis* 2005;**42**:28-32.
298. Yang L, Cai CL, Lin L, Qyang Y, Chung C, Monteiro RM, *et al.* Isl1Cre reveals a common Bmp pathway in heart and limb development. *Development* 2006;**133**:1575-1585.
299. Shima H, Pende M, Chen Y, Fumagalli S, Thomas G, Kozma SC. Disruption of the p70(s6k)/p85(s6k) gene reveals a small mouse phenotype and a new functional S6 kinase. *EMBO J* 1998;**17**:6649-6659.
300. Fingar DC, Salama S, Tsou C, Harlow E, Blenis J. Mammalian cell size is controlled by mTOR and its downstream targets S6K1 and 4EBP1/eIF4E. *Genes Dev* 2002;**16**:1472-1487.
301. Ahuja P, Sdek P, MacLellan WR. Cardiac myocyte cell cycle control in development, disease, and regeneration. *Physiol Rev* 2007;**87**:521-544.
302. Crackower MA, Oudit GY, Koziarzki I, Sarao R, Sun H, Sasaki T, *et al.* Regulation of myocardial contractility and cell size by distinct PI3K-PTEN signaling pathways. *Cell* 2002;**110**:737-749.
303. Shioi T, Kang PM, Douglas PS, Hampe J, Yballe CM, Lawitts J, *et al.* The conserved phosphoinositide 3-kinase pathway determines heart size in mice. *EMBO J* 2000;**19**:2537-2548.
304. Takano H, Komuro I, Zou Y, Kudoh S, Yamazaki T, Yazaki Y. Activation of p70 S6 protein kinase is necessary for angiotensin II-induced hypertrophy in neonatal rat cardiac myocytes. *FEBS Lett* 1996;**379**:255-259.
305. Pereira AH, Clemente CF, Cardoso AC, Theizen TH, Rocco SA, Judice CC, *et al.* MEF2C silencing attenuates load-induced left ventricular hypertrophy by modulating mTOR/S6K pathway in mice. *PLoS One* 2009;**4**:e8472.
306. Malynn BA, de Alboran IM, O'Hagan RC, Bronson R, Davidson L, DePinho RA, *et al.* N-myc can functionally replace c-myc in murine development, cellular growth, and differentiation. *Genes Dev* 2000;**14**:1390-1399.
307. Xiao G, Mao S, Baumgarten G, Serrano J, Jordan MC, Roos KP, *et al.* Inducible activation of c-Myc in adult myocardium in vivo provokes cardiac myocyte hypertrophy and reactivation of DNA synthesis. *Circ Res* 2001;**89**:1122-1129.
308. Kim S, Li Q, Dang CV, Lee LA. Induction of ribosomal genes and hepatocyte hypertrophy by adenovirus-mediated expression of c-Myc in vivo. *Proc Natl Acad Sci U S A* 2000;**97**:11198-11202.
309. Izumo S, Nadal-Ginard B, Mahdavi V. Protooncogene induction and reprogramming of cardiac gene expression produced by pressure overload. *Proc Natl Acad Sci U S A* 1988;**85**:339-343.
310. Green NK, Franklyn JA, Ohanian V, Heagerty AM, Gammage MD. Transfection of cardiac muscle: effects of overexpression of c-myc and c-fos proto-oncogene proteins in primary cultures of neonatal rat cardiac myocytes. *Clin Sci (Lond)* 1997;**92**:181-188.
311. Hoffman JL. Congenital heart disease: incidence and inheritance. *Pediatr Clin North Am* 1990;**37**:25-43.

APPENDIX

IACUC APPROVAL FORM



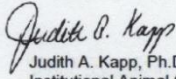
THE UNIVERSITY OF ALABAMA AT BIRMINGHAM

Institutional Animal Care and Use Committee (IACUC)

NOTICE OF APPROVAL

DATE: September 27, 2010

TO: Jiao, Kai
KAUL-768 0024
996-4198

FROM: 
Judith A. Kapp, Ph.D., Chair
Institutional Animal Care and Use Committee

SUBJECT: Title: Functions of Tgf-B/Bmp Signaling During Cardiogenesis in Mouse Embryos
Sponsor: Internal
Animal Project Number: 100907589

On September 27, 2010, the University of Alabama at Birmingham Institutional Animal Care and Use Committee (IACUC) reviewed the animal use proposed in the above referenced application. It approved the use of the following species and numbers of animals:

Species	Use Category	Number in Category
Mice	A	242

Animal use is scheduled for review one year from September 2010. Approval from the IACUC must be obtained before implementing any changes or modifications in the approved animal use.

Please keep this record for your files, and forward the attached letter to the appropriate granting agency.

Refer to Animal Protocol Number (APN) 100907589 when ordering animals or in any correspondence with the IACUC or Animal Resources Program (ARP) offices regarding this study. If you have concerns or questions regarding this notice, please call the IACUC office at 934-7692.

Institutional Animal Care and Use Committee
CH19 Suite 403
933 19th Street South
205.934.7692
FAX 205.934.1188

Mailing Address:
CH19 Suite 403
1530 3RD AVE S
BIRMINGHAM AL 35294-0019